UC Davis

UC Davis Electronic Theses and Dissertations

Title

UNDERSTANDING THE EFFECTS OF UPPER LIMB TREMOR DURING ADAPTATION TO NOVEL MOVEMENT DYNAMICS

Permalink

https://escholarship.org/uc/item/81p670n2

ISBN

9798193263227

Author

Foray, Katherine

Publication Date

2026-09-08

Peer reviewed|Thesis/dissertation

eScholarship.org Powered by the California Digital Library
University of California

Understanding the Effects of Upper Limb Tremor During Adaptation to Novel Movement Dynamics

By

KATHERINE FORAY

DISSERTATION

Submitted in partial satisfaction of the requirements for the degree of

Doctor of Philosophy

in

Neuroscience

in the

Office of Graduate Studies

of the

University of California

Davis

Approved:

Wilsaan Joiner, Chair

Joy Geng

Carina Oehrn

Matt Brown

Lee Miller

Committee in Charge
2026

Abstract

In this dissertation, we aimed to understand how to understand the specific mechanisms by which tremor effects motor adaptation. The driving hypothesis of the project was that externally-generated pathological tremor impairs the ability to distinguish errors that require corrections while internally-generated tremor (e.g. Parkinson's Disease (PD) and Essential Tremor (ET)) does not impair learning in adaptation (the ability to detect errors) but rather impairs movement execution. Previous studies focused on patients with pathological tremor suggest an overall impairment of motor adaptation despite the retention of the learned movement recalibration. Thus, we investigated the extent learning is impacted by different manifestations of tremor in two distinct motor adaptation tasks. **(1)** Our first step to accomplish this was to examine the extent externally-generated tremor affects motor adaptation to physical movement perturbations in neurologically healthy individuals. We found that increasing externally-generated tremor magnitude reduced the ability to adapt to novel movement dynamics via impairment of the fast-learning process. **(2)** Next, we applied the same physical adaptation experimental paradigm to individuals with internally-generated tremor (both pathological and physiological) to systematically quantify tremor and measure its impact on adaptation. By quantifying differences in tremor across disease symptomatology in PD and ET, we determined that increasing internally-generated tremor magnitude does not impair the ability to adapt, as reaching movements account for internal error. However, increasing internally-generated tremor magnitude appeared to impair parts of movement that rely on feedback control, such as movement stabilization and postural hold. **(3)** Finally, we determined the extent pathological tremor affects the ability to detect self-generated error during motor adaptation to both visual and physical feedback perturbations. We found that while patients with PD have more self-generated error, such as tremor, their ability to parse self-generated error from externally-generated error was intact. Furthermore, patients with PD only adapted in response to externally-generated perturbations, similar to control subjects. Through

these findings, we hope to enhance our current understanding of how varying etiologies and manifestations of pathological tremor resulting from movement disorders impacts motor learning and control. The ability to quantify the characteristics of disrupted motor learning and control, as well as tremor itself, will lay the foundation to develop more specific interventions that may potentially be applied earlier during disease progression.

Acknowledgements

I am very lucky that I have so many people to be thankful for. I would like to first thank Dr. Wil Joiner for being such a supportive, knowledgeable, and kind mentor. I am also grateful to the incredible people in the Joiner lab (Pierre, Kartik, Justin, Rose, Reshma, Jessica, Ada, Weiwei, and Katie) for being amazing friends as well as colleagues. Many thanks to Dr. Jonathan Snider at the UC Davis Movement Disorders Clinic for aiding with participant recruitment. My research was well supported by my committee members: Dr. Matt Brown, Dr. Carina Oehrn, Dr. Joy Geng, and Dr. Lee Miller. Their guidance and collaboration were very influential in the success of this dissertation. Thank you to the Neuroscience Graduate Group program coordinator, Linette Scibelli, for her counsel and administrative support. To my dear friends, Ari, Genna, Josh, Manola, Sierra, Alyssa, and Meagan, you have all played such a big role in this journey. To my Mom, Dad, Thing 1 (Nick), Thing 2 (Jack), and extended family, your love and support have meant the world to me.

This dissertation would not have existed without any of you and I would like to express my deepest gratitude.

Table of Contents

Title Page……..i

Abstract……ii

Acknowledgements……iv

Table of Contents……v

Chapter 1: Movement Tremor and Motor Learning……...1

Chapter 2: Applied motor noise affects specific learning mechanisms during short-term adaptation to novel movement dynamics…….23

Chapter 3: How Pathological Tremor Impacts Movement and Motor Adaptation…….…….76

Chapter 4: Parsing Error Source During Motor Adaptation in Parkinson's Disease……115

Chapter 5: Conclusion……..…….134

Chapter 1: Movement Tremor and Motor Learning

Everyone, at some point in their life, has been aware of their body trembling. Whether it be while performing in front of an audience or taking a picture with a cell phone, we have all experienced an involuntary, rhythmical oscillation of muscles, called physiological tremor. Although a universal experience, some individuals with neurological disorders experience tremor so severe that it interferes with their daily lives (i.e., pathological tremor) making it the most common movement disorder (Smaga, 2003). Pathological tremor is a key characteristic of many neurodegenerative diseases, such as Parkinson's Disease and Essential Tremor, both of which are hallmarked by impaired motor skills (e.g., difficulty with drawing and handwriting, inability to balance). However, despite its prevalence, the literature is currently unclear as to how or to what extent pathological tremor underlies the motor learning impairments that are observed in movement disorders. Here, we examine this issue across tremor types, disease states, and motor learning mechanisms to better understand the impact of tremor severity on goal-directed movement.

	Physiological Tremor	Pathological Tremor
Type of Movement	Involuntary, rhythmical, and oscillatory contractions of the muscles	Involuntary, rhythmical, and oscillatory contractions of the muscles
Prevalence	Typical in everyone	Associated with neurological disease states
Visibility	Usually invisible/subtle	Visible
Frequency	High Frequency (8-12 Hz)	Variable Frequency (0.5-12 Hz)
Amplitude	Low Amplitude (mm)	High Amplitude (cm)
Presence	Enhanced by stress, caffeine, low blood sugar	Persistent or progressive
Category	Movement, rest, postural hold	Movement, rest, postural hold

Figure 1. Comparison of physiological and pathological tremor

Physiological tremor

Physiological tremors are involuntary, rhythmical, and oscillatory contractions of the muscles (Lippold, 1971). This tremor is typical in all humans, occurring in skeletal muscles during movement, rest, or while holding a body segment against gravity (Marshall & Walsh, 1956). These oscillatory contractions are commonly characterized as being low amplitude and high frequency (Crawford & Zimmerman, 2011), specifically around the 8-12Hz range in young adults (Marshall, 1961; Elble & Randall, 1976; Hallett, 1998; Habib-ur-Rehman, 2000) though it can decrease to 6-7Hz in adults over 60 years (Habib-ur-Rehman, 2000; Marshall, 1961; Elble, 1998) (Figure 2 and 3). The tremor can increase in amplitude and frequency during times of anxiety and stress, during use of certain medications, and some metabolic conditions (such as low blood sugar) (Crawford & Zimmerman, 2011). For example, this type of tremor is evident when trying to raise a glass of water to one's mouth when extremely anxious; the hand shaking due to physiological tremor causes the water to ripple in the cup. Moreover, resistance-based and fatiguing tasks, specifically isometric exercise (i.e. carrying heavy groceries or performing a wall sit), eccentric loading (i.e. lowering a heavy box to the floor), and supramaximal exertion (i.e. shoveling heavy snow), consistently increase physiological tremor amplitude (Kulis et al. 2025).

There is a debate as to whether physiological tremors result from the mechanical properties of the limb (Lippold, 1971, the peripheral resonance model), or a rhythmic signal in the central nervous system (CNS) that modulates neural firing (Elble & Randall, 1976, the central oscillator model). However, current consensus appears to point towards both being at least partially accurate, with peripheral resonance driving most physiological tremor characteristics but also being modulated by a central oscillator (Raethjen et al. 2000). Therefore, due to being primarily driven by mechanical properties of the limb, physiological tremor does not typically impair activities of daily living as it fades as soon as changes in muscle mechanics, perhaps due factors such as stress or blood sugar, also diminish. It is important to note, however, that when

physiological tremor is increased, this can be considered *enhanced* physiological tremor (Bhatia et al., 2018), which is thought to be symptomatic and can require neurological treatment.

Pathological Tremor

Pathological tremor is also a visible, persistent, involuntary, rhythmical, and oscillatory contraction of a body part but is driven mainly by a central oscillator (Hallett, 2014; Bhatia et al., 2018) and interferes with activities of daily living (Jankovic & Stanley, 1980). This impaired functioning of the central oscillator in the CNS is associated with a range of neurological disorders, the variety of which can affect how pathological tremor manifests. These tremors are typically classified dependent upon whether they occur at rest (rest tremor), or during action, including while holding postures (postural tremor) or during movements (kinetic tremor). In addition, they can be categorized based on whether they are isolated or combined (with other neurological signs and symptoms) (Bhatia et al., 2018). In this dissertation, we focus specifically on Essential Tremor (ET) and Parkinson's Disease (PD):

ET, typically a bilateral, 4-12 Hz action tremor of the upper limbs (Louis, 2005), is thought to be caused by impaired functional connectivity within the cerebello-thalmo-cortical circuitry (Holtbernd & Shah, 2021). Patients with ET are known to have difficulty with fine motor control, impairing activities such as handwriting (Alty et al. 2011).

PD tremor is classically a 4-7 Hz rest tremor when the limb is not moving and fully supported against gravity that typically originates unilaterally in the upper limbs but can progress to the legs, lip/chin, and bilaterally (Gironell et al., 2018). The rest tremor is significantly reduced in amplitude or abolished at the onset of movement or when holding a posture but may re-emerge while sustaining a posture (Bhatia et al., 2018). The origin of this tremor is still under debate, but it is currently thought to be produced by impaired cerebello-thalamo-cortical circuitry as a result of depleted dopaminergic projections from the basal ganglia (Helmich et al., 2012). Later in disease

progression, PD can manifest as a kinetic tremor (Zampogna et al., 2025), tremor that occurs during voluntary movement. Both the rest and action tremors in PD affect patients' ability to write, eat, and dress themselves.

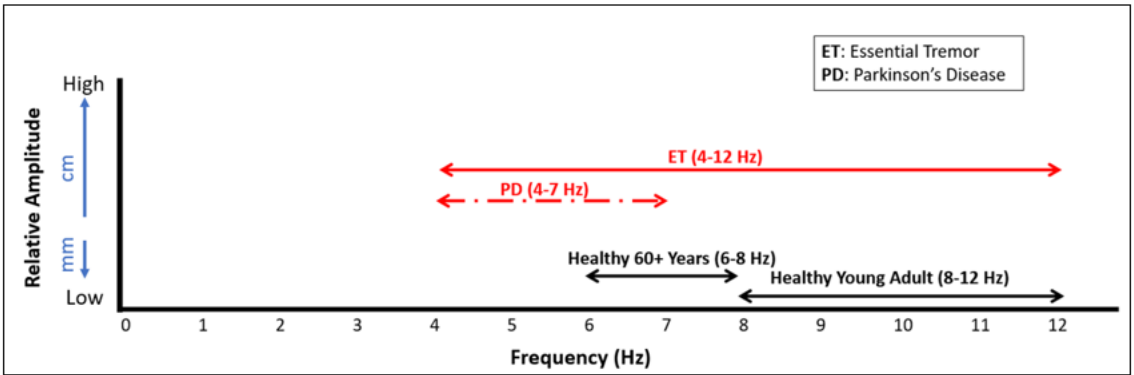

Figure 2. Relative magnitude and frequency range of pathological (Parkinson's Disease and Essential Tremor) and physiological (young and old) tremor

Motor Adaptation vs. Motor Acuity

Every day, we navigate a dynamic, unpredictable world. In the face of constantly changing sensory information, we must frequently update our movements (i.e., motor output) to achieve the goals of our motor actions. When reaching for a drink in the refrigerator, we have to account for our own movement variability (how accurate we are in aiming our hand towards the drink) as well as any external variability, such as underestimating the weight of the door resulting in it swinging back more than expected and knocking the motion of the limbs off their intended course. The literature refers to this recalibration/learning as motor adaptation, which is the process of adjusting how we execute a familiar motor action in response to sensed errors (Krakauer et al., 2019). The accuracy and precision that we execute a desired motor action with its intended outcome is referred to as motor acuity (Krakauer et al., 2019). This can be reflected by absolute improvements in error-related measures or by reductions in variability. Learning how to adjust our limb movement despite internal and external changes to grasp the drink is a form of motor adaptation, while the ability to maintain consistency in a motor action (e.g., throwing a dart at the same spot on the dart board) is a form of motor acuity.

Motor adaptation is largely driven by the movement errors encoded by our sensory system. However, sensed errors could be due to a variety of causes: incorrect sensory information, errors in motor executions, or a combination of both. Importantly, these experienced sensory errors are not always due to outside factors but can be attributed to internal sources (Osborne et al., 2005; Faisal et al. 2008), such as tremor. While it is well-documented that patients with movement disorders involving tremor have difficulties with motor learning, such as adaptation and fine motor control, it is currently unclear if this is due to the tremor itself or other factors, such as co-existing cognitive and/or motor impairments.

Essential Tremor

Tremor in ET does not impact motor adaptation

Tremor in Essential Tremor (ET) patients is of unknown origin, but growing evidence points to a deficit in the cerebellar networks (Louis, 2005). This is further supported by the successful use of cerebellar transcranial focused ultrasound to improve tremors in ET patients (Shah et al., 2025). ET typically presents as a bilateral tremor of the upper limbs during movements, which can take the form of kinetic tremors that occur as patients make voluntary reaches towards a target, such as reaching for a glass of water (Louis, 2005). This tremor can also manifest during postural holds (postural tremor), when the limb is at rest but not fully supported against gravity (Louis, 2005). Patients with ET have impaired adaptation in upper limb recalibration to physical and visual perturbations when reaching towards a target (Bindel et al., 2023; Blondiaux et al., 2023; Chen et al., 2006) and acquiring eyeblink responses to a conditioned stimulus (Kronenbuerger et al., 2007; Shill et al., 2009). The tremor itself (as measured by clinical rating or angular velocity), however, does not underlie this overall impairment (Bindel et al., 2023; Blondiaux et al., 2023; Chen et al., 2006). Movement execution, rather than anticipation, is significantly impacted in patients with ET during both upper limb movement and saccade adaptation paradigms (Bindel et al., 2023;

Blondiaux et al., 2023; Chen et al., 2006). When decomposing upper limb movement into distinct components, reaching (action) and stabilization (posture), tremor typically plays a role in lowering performance during the stabilization phase (Blondiaux et al., 2023). Previous studies largely did not differentiate between these two phases, making it difficult to determine the specific mechanisms of movement that tremor impacted during motor adaptation. Not differentiating between the two is counterintuitive, as a well-supported hypothesis demonstrates that reaching and stabilization are controlled by two different neural networks and motor pathways (Hadjosif et al., 2025, Shadmehr 2017; Jayasinghe et al., 2022). Interestingly, once the removal of a visual feedback perturbation occurs, de-adaptation remains intact (Bindel et al., 2023). In addition, any noted impairment to motor adaptation (regardless of tremor) occurs mostly in the affected upper limbs as lower limb adaptation is largely not impaired in patients with ET (Roper et al., 2019) nor functional mobility (Monaghan et al., 2024). Therefore, while there are documented upper-limb adaptation impairments in ET, this is likely not due to tremor itself but some other characteristic of the disorder.

Postural tremor, not action tremor, in ET is associated with impaired motor acuity

As noted above, ET is characterized by tremors, which increase in intensity as patients perform voluntary, goal directed movements towards a target or hold posture, both taking place during the stabilization phase of a movement. In healthy subjects, the ability to adapt movements to a visual perturbation improves with increased variability (noise) in processing sensory information during motor planning (inferred computationally from variability in intended movement), but adaptation is impaired by the accompanying increased variability in movement execution (variability in endpoint error) (van der Vliet et al., 2018). If tremor is considered a type of movement noise, this may suggest that the transition from action to postural tremor during the stabilization phase reaches a certain threshold of noise that impairs end-of-movement precision, which gives the appearance of impairment in overall motor adaptation.

Therefore, the stabilization phase of a movement is a time when the motor system must coordinate volitional muscle activity to go from dynamic movement (action) to a postural hold (Blondiaux et al., 2023). Impaired postural stability is associated with impaired motor precision, especially in tasks such as drawing and handwriting (Miyahara, 2008). Moreover, postural stability can be impacted directly by noisy muscle contractions (i.e. tremor). Dysmetria is a characteristic of ET in which patients have a difficult time coordinating the end stage of movement, resulting in overshooting or undershooting of the reach target (Casamento-Moran et al., 2020). Dysmetria in ET occurs independent of tremor (Casamento-Moran et al., 2020), which could account for the difference in stabilization performance between ET patients with reduced tremor via Deep Brain Stimulation (DBS) and their control counterparts. For example, during spiral drawing, as ET patients improve in general acuity, the degree of tremor severity (spiral shape and line smoothness) improves as well, though tremor amplitude increases (Kim et al., 2019). Thus, acuity and tremor in ET are most likely mediated by separate neural mechanisms (Kim et al., 2019, Casamento-Moran et al., 2020). Collectively, this suggests that *postural* tremor (rather than action tremor) in this case does not impact the selection of actions during motor learning but rather *coincides* with the amount of movement variability (acuity) during stabilization.

Parkinson's Disease

Tremor does not appear to impact motor learning in Parkinson's Disease

Parkinson's Disease (PD) is the result of progressive degradation of dopaminergic neurons in the substantia nigra pars compacta, resulting in disruption within the basal ganglia, movement difficulties and a characteristic resting tremor (Gironell et al., 2018). Additionally, while the destruction of dopaminergic neurons leads to most of the motor signs and impairments of PD, the disease is characterized as progressively neurodegenerative, which eventually impacts neurons beyond the basal ganglia. Previous studies have suggested motor learning is impaired in PD

(Cristini et al., 2023; Udupa et al., 2022), but the impact of tremor is unclear. Tremor severity in PD does not impair cognitive performance, including verbal and non-verbal episodic memory, attention, working memory, and executive function during declarative and procedural motor learning tasks (Domellöf et al., 2011; Vakil & Herishanu-Naaman, 1998), acoustically cued finger tapping (Stegemöller et al., 2016), punishment-based learning (Moustafa et al., 2013), nor vividness of motor imagery (Readman et al., 2023). As in ET, patients with PD rely more on external cues (e.g., auditory cues) and intentional motor planning when executing movement compared to neurologically healthy adults (Luft et al., 2020). Interestingly, ET patients require visual monitoring of their hands during finger tapping more than patients with PD and control subjects (Luft et al., 2020). In addition, patients with PD have impaired timing cues in go/no go tasks (Purzner et al., 2007), which may be related to a diminished utilization of external cues and motor planning ability. Overall, the observed behavior suggests that patients with PD have an impaired ability to rely on internal cues for motor learning and control.

As PD is a heterogeneous disorder, determining the impact of tremor in isolation of other symptoms mainly comes in the form of comparing PD subtypes, specifically Postural Instability and Gait Difficulty (PIGD-PD) compared to tremor-dominant PD (TD-PD). PIGD-PD is a subtype characterized by greater deficits in balance and movement initiation in addition to greater non-motor symptoms, such as dementia (Gong et al., 2017). TD-PD is mainly characterized by a persistent, low frequency rest and postural tremor with greater mobility and less non-motor symptoms (Gong et al., 2017). When comparing the two subgroups, it has been reported that patients with TD-PD have greater response inhibition (Tolleson et al., 2017), less difficulty transitioning from sitting to walking (Pelicioni et al., 2020), and make less motor errors in suppressing impulsive motor reactions (Wylie et al., 2012) compared to patients with PIGD-PD. However, without systematic testing of how these subtypes impact motor adaptation, it is an open question on the extent that tremor in PD plays a direct role in impairing the learning process during

motor adaptation. This is in line with the meta-analysis performed by Cristini et al., 2023, which supports the idea that motor learning impairments are independent of disease severity, which would include tremor severity. Since mild cognitive impairments and dementia can manifest in PD, in addition to explicit processes that may play a prominent role in various types of motor learning, controlling for this variable is critical to understanding the influence of tremor within any patient population, including PD.

Tremor, Task Error, and Motor Acuity

Over the training period with a movement perturbation the motor system adapts to the applied specific task requirements. For some types of perturbations, there is usually a transition from reliance on task error (explicit) to sensory prediction error (implicit) to drive learning (Krakauer et al., 2019). Thus, there is typically less reliance on task error feedback over the course of motor adaptation.

In the examples above it is clear that tremor often accompanies a large degree of task error. In fact, as motor adaptation and acuity improve over time, the reliance on task performance feedback decreases while physiological and pathological tremor decreases in severity (Feys et al., 2006; Lason et al., 2012). The relationship between tremor, motor acuity, and task error is exemplified in neurologically healthy older adults, who have greater amounts of physiological tremor compared to younger adults (Hong et al., 2008). For example, older adults are known to have impaired explicit learning during motor adaptation (Vandevoorde & Orban de Xivry, 2020), which is strongly correlated with processing task error (Krakauer et al., 2019; Taylor et al., 2014). Additionally, there is evidence that, as motor learning on a repeated task (i.e., the pursuit rotor task) increases, high amplitude tremor decreases (Lason et al., 2012), suggesting that tremor severity may be linked to task error processing in healthy individuals.

Moreover, a study focused on neurologically healthy individuals investigated how decreasing access to visual information and mobility impacted tremor; in young adults, lack of mobility was associated with increased tremor amplitude and frequency while visual (sensory) feedback had no impact (Murnaghan et al., 2017). The researchers concluded that physiological (non-pathological) tremor during postural holds might be a method of gathering sensory information from the environment to inform predictions for future movements (Murnaghan et al., 2017). Keeping in mind that physiological tremor is largely driven by peripheral mechanisms and pathological tremor is predominantly driven by a central oscillator, the role that these respective movement oscillations play in the motor system may differ. Enhanced physiological tremor is centrally neurogenic in origin (Bhatia et al., 2018), which can suggest that the transition from benign (physiological) to pathological tremor results from overactivity of the central component over the peripheral mechanisms. This is supported by evidence that the central and peripheral components of ET are closely related (Pan & Kuo, 2018), with Cao et al. (2018) putting forth further evidence that the central component of ET drives the peripheral components of ET. Following this line of reasoning, the underlying purpose of pathological tremor and physiological tremor could be similar. As lower task error leads to greater motor acuity and more successful movement outcomes, it is possible that pathological tremor may allow the motor system to gather more task-based sensory information in a disease state that impairs movement acuity.

This creates uncertainty in the causal relationship: is low motor acuity (driven by high task error) the cause of greater magnitude and frequency in tremor or does the high magnitude/frequency of tremor result in high task error and therefore lower motor acuity? Lakie et al. (1995) addressed this question by applying different temperatures (hot or cold) to the arms of amateur pistol shooters. The cooling condition decreased physiological tremors in the arm, specifically decreasing any high frequency tremors, while the heating condition increased the severity of tremor frequency. The authors found that the group with the cooling condition (less

tremor) had higher motor acuity than the unaltered control group while the group undergoing the heating condition had reduced motor acuity than both the control group and the cooled group (Lakie et al., 1995). Lakie's later review on the existing literature on physiological tremor and shooting performance (Lakie, 2010) demonstrates that, across studies, increasing the frequency and magnitude of physiological tremor results in a corresponding decrease in motor acuity. In both cases, we presume only the peripheral component of physiological tremor was changed and therefore the reason why acuity was impacted. Further research is needed to understand the extent changing the central oscillatory component of tremor (as seen in pathological tremor) has a similar effect on motor acuity or if there are other underlying factors (e.g., the peripheral oscillatory component, impaired sensory processing).

We must also consider that there is no underlying purpose for pathological tremor. While there exists a known relationship between task error and intention tremor severity, it is unclear if this is cause and effect. It is possible that as centrally-located motor learning systems minimize task error over each updated movement, so too do they learn to compensate for movement noise, such as tremor. This is especially plausible if tremors are a distinguishable type of motor noise, since motor learning primarily occurs in response to an identifiable error (Krakauer et al., 2019).

CONCLUSION

While motor adaptation asymptotes over time, motor acuity continues to increase throughout practice (Listman et al. 2021). This suggests that motor acuity and adaptation are mediated by different neural pathways. Depending on disease pathology, impairment of these pathways could result in unique deficiencies in motor learning, which may differentially affect motor learning types, such as motor adaptation or de novo (i.e. entirely new) learning of movements. Most of the experimental evidence that we have reviewed suggests that pathological tremor does not impact

motor adaptation except in cases where the adaptation is largely reliant on task error feedback, but it does have a strong association with impaired acuity.

While little is known about the neurobiological mechanisms of motor acuity, there is some evidence that it may be due to an increased signal-to-noise ratio in motor cortex neural signaling (Kargo & Nitz, 2004; Krakauer et al., 2019) in addition to improved state estimation in the cerebellum (Krakauer et al., 2019). Therefore, the deficits in task error observed in patients with pathological tremor may be partially compensated by implicit feedback learning mechanisms, such as sensory feedback error processing (Henson, 1978; Robinson et al., 2003; Krakauer et al., 2019; Wong & Shelhamer, 2011) which is primarily mediated by the cerebellum (Wolpert et al., 1998; Blakemore et al., 2001; Ishikawa et al., 2016; Johnson et al., 2019). While action tremor impairs motor acuity, it may conversely assist in motor adaptation by gathering more sensory information from the environment and maintaining that the motor system is primed for motion in patient populations with movement difficulty.

The majority of the studies discussed above typically examined movement as a whole, as opposed to different components. When a single movement can be separated into different components (e.g., reaching vs. stabilizing periods) there are subsequently differences in the influence of tremor. Characterizing tremor during each stage of movement (i.e. planning, reaching, execution, stabilization) would provide more insight into the relationship between motor tremor, adaptation, and acuity particularly as the severity of the tremor evolves throughout the time course of movement.

REFERENCES

Alty, J. E., & Kempster, P. A. (2011). A practical guide to the differential diagnosis of tremor. *Postgraduate Medical Journal*, *87*(1031), 623–629. https://doi.org/10.1136/pgmj.2009.089623

Analysis of tremor in motor learning task. (n.d.). Retrieved August 20, 2026, from https://bamsjournal.com/article/541548/en

Bhatia, K. P., Bain, P., Bajaj, N., Elble, R. J., Hallett, M., Louis, E. D., Raethjen, J., Stamelou, M., Testa, C. M., & Deuschl, G. (2018). Consensus Statement on the Classification of Tremors. From the Task Force on Tremor of the International Parkinson and Movement Disorder Society. *Movement Disorders : Official Journal of the Movement Disorder Society*, *33*(1), 75–87. https://doi.org/10.1002/mds.27121

Bindel, L., Mühlberg, C., Pfeiffer, V., Nitschke, M., Müller, A., Wegscheider, M., Rumpf, J.-J., Zeuner, K. E., Becktepe, J. S., Welzel, J., Güthe, M., Classen, J., & Tzvi, E. (2022). Visuomotor Adaptation Deficits in Patients with Essential Tremor. *The Cerebellum*. https://doi.org/10.1007/s12311-022-01474-5

Blakemore, S. J., Frith, C. D., & Wolpert, D. M. (2001). The cerebellum is involved in predicting the sensory consequences of action. *Neuroreport*, *12*(9), 1879–1884. https://doi.org/10.1097/00001756-200107030-00023

Blondiaux, F., Lebrun, L., Hanseeuw, B. J., & Crevecoeur, F. (2023). Impairments of saccadic and reaching adaptation in essential tremor are linked to movement execution. *Journal of Neurophysiology*, *130*(5), 1092–1102. https://doi.org/10.1152/jn.00165.2023

Cao, H., Thompson-Westra, J., Hallett, M., & Haubenberger, D. (2018). The response of the central and peripheral tremor component to octanoic acid in patients with essential tremor. *Clinical Neurophysiology*, *129*(7), 1467–1471. https://doi.org/10.1016/j.clinph.2018.03.016

Casamento-Moran, A., Yacoubi, B., Wilkes, B. J., Hess, C. W., Foote, K. D., Okun, M. S., Wagle Shukla, A., Vaillancourt, D. E., & Christou, E. A. (2020). Quantitative Separation of Tremor and Ataxia in Essential Tremor. *Annals of Neurology*, *88*(2), 375–387. https://doi.org/10.1002/ana.25781

Chen, H., Hua, S. E., Smith, M. A., Lenz, F. A., & Shadmehr, R. (2006). Effects of Human Cerebellar Thalamus Disruption on Adaptive Control of Reaching. *Cerebral Cortex*, *16*(10), 1462–1473. https://doi.org/10.1093/cercor/bhj087

Crawford, P., & Zimmerman, E. E. (2011). Differentiation and Diagnosis of Tremor. *American Family Physician*, *83*(6), 697–702.

Cristini, J., Parwanta, Z., De Las Heras, B., Medina-Rincon, A., Paquette, C., Doyon, J., Dagher, A., Steib, S., & Roig, M. (2023). Motor Memory Consolidation Deficits in Parkinson's Disease: A Systematic Review with Meta-Analysis. *Journal of Parkinson's Disease*, *13*(6), 865–892. https://doi.org/10.3233/JPD-230038

Domellöf, M. E., Elgh, E., & Forsgren, L. (2011). The relation between cognition and motor dysfunction in drug-naive newly diagnosed patients with Parkinson's disease. *Movement Disorders: Official Journal of the Movement Disorder Society*, *26*(12), 2183–2189. https://doi.org/10.1002/mds.23814

Elble, R. J. (2013). Tremor disorders. *Current Opinion in Neurology*, *26*(4), 413. https://doi.org/10.1097/WCO.0b013e3283632f46

Elble, R. J. (2017). Tremor. In B. Tousi & J. Cummings (Eds.), *Neuro-Geriatrics: A Clinical Manual* (pp. 311–326). Springer International Publishing. https://doi.org/10.1007/978-3-319-56484-5_20

Elble, R. J., & Randall, J. E. (1976). Motor-unit activity responsible for 8- to 12-Hz component of human physiological finger tremor. *Journal of Neurophysiology*, *39*(2), 370–383. https://doi.org/10.1152/jn.1976.39.2.370

Faisal, A. A., Selen, L. P. J., & Wolpert, D. M. (2008). Noise in the nervous system. *Nature Reviews Neuroscience*, *9*(4), Article 4. https://doi.org/10.1038/nrn2258

Feys, P., Helsen, W., Buekers, M., Ceux, T., Heremans, E., Nuttin, B., Ketelaer, P., & Liu, X. (2006). The effect of changed visual feedback on intention tremor in multiple sclerosis. *Neuroscience Letters*, *394*(1), 17–21. https://doi.org/10.1016/j.neulet.2005.10.010

Gironell, A., Pascual-Sedano, B., Aracil, I., Marín-Lahoz, J., Pagonabarraga, J., & Kulisevsky, J. (2018). Tremor Types in Parkinson Disease: A Descriptive Study Using a New Classification. *Parkinson's Disease*, *2018*(1), 4327597. https://doi.org/10.1155/2018/4327597

Gong, T., Xiang, Y., Saleh, M. G., Gao, F., Chen, W., Edden, R. A. E., & Wang, G. (2018). Inhibitory motor dysfunction in parkinson's disease subtypes. *Journal of Magnetic Resonance Imaging*, *47*(6), 1610–1615. https://doi.org/10.1002/jmri.25865

Habib-ur-Rehman, N. A. (2000). Diagnosis and Management of Tremor. *Archives of Internal Medicine*, *160*(16), 2438–2444. https://doi.org/10.1001/archinte.160.16.2438

Hadjiosif, A. M., Kita, K., Albert, S. T., Scheidt, R. A., Shadmehr, R., & Krakauer, J. W. (2025). Separating the control of moving and holding in human post-stroke arm paresis. *eLife*, *12*, RP90780. https://doi.org/10.7554/eLife.90780

Hallett, M. (1998). Overview of Human Tremor Physiology. *Movement Disorders*, *13*(S3), 43–48. https://doi.org/10.1002/mds.870131308

Helmich, R. C., Hallett, M., Deuschl, G., Toni, I., & Bloem, B. R. (2012). Cerebral causes and consequences of parkinsonian resting tremor: A tale of two circuits? *Brain*, *135*(11), 3206–3226. https://doi.org/10.1093/brain/aws023

Henson, D. B. (1978). Corrective saccades: Effects of altering visual feedback. *Vision Research*, *18*(1), 63–67. https://doi.org/10.1016/0042-6989(78)90078-0

Holtbernd, F., & Shah, N. J. (2021). Imaging the Pathophysiology of Essential Tremor—A Systematic Review. *Frontiers in Neurology*, *12*. https://doi.org/10.3389/fneur.2021.680254

Hong, S. L., James, E. G., & Newell, K. M. (2008). Coupling and irregularity in the aging motor system: Tremor and movement. *Neuroscience Letters*, *433*(2), 119–124. https://doi.org/10.1016/j.neulet.2007.12.056

Ishikawa, T., Tomatsu, S., Izawa, J., & Kakei, S. (2016). The cerebro-cerebellum: Could it be loci of forward models? *Neuroscience Research, Body Representation in the Brain*, *104*, 72–79. https://doi.org/10.1016/j.neures.2015.12.003

JANKOVIC, J., & STANLEY, F. (1980). Physiologic and Pathologic Tremors. *Annals of Internal Medicine*, *93*(3), 460–465. https://doi.org/10.7326/0003-4819-93-3-460

Jayasinghe, S. A. L., Scheidt, R. A., & Sainburg, R. L. (2022). Neural Control of Stopping and Stabilizing the Arm. *Frontiers in Integrative Neuroscience*, *16*, 835852. https://doi.org/10.3389/fnint.2022.835852

Johnson, R. E., Kording, K. P., Hargrove, L. J., & Sensinger, J. W. (2017). Adaptation to random and systematic errors: Comparison of amputee and non-amputee control interfaces with varying levels of process noise. *PLOS ONE*, *12*(3), e0170473. https://doi.org/10.1371/journal.pone.0170473

Kargo, W. J., & Nitz, D. A. (2004). Improvements in the Signal-to-Noise Ratio of Motor Cortex Cells Distinguish Early versus Late Phases of Motor Skill Learning. *Journal of Neuroscience*, *24*(24), 5560–5569. https://doi.org/10.1523/JNEUROSCI.0562-04.2004

Kim, C. Y., Luo, L., Yu, Q., Mirallave, A., Saunders-Pullman, R., Lipton, R. B., Louis, E. D., & Pullman, S. L. (2019). Repeated Spiral Drawings in Essential Tremor: A Possible Limb-Based Measure of Motor Learning. *The Cerebellum*, *18*(2), 178–187. https://doi.org/10.1007/s12311-018-0974-x

Krakauer, J. W., Hadjiosif, A. M., Xu, J., Wong, A. L., & Haith, A. M. (2019). Motor Learning. In R. Terjung (Ed.), *Comprehensive Physiology* (1st ed., pp. 613–663). Wiley. https://doi.org/10.1002/cphy.c170043

Kronenbuerger, M., Gerwig, M., Brol, B., Block, F., & Timmann, D. (2007). Eyeblink conditioning is impaired in subjects with essential tremor. *Brain: A Journal of Neurology*, *130*(Pt 6), 1538–1551. https://doi.org/10.1093/brain/awm081

Lakie, M. (2010). The influence of muscle tremor on shooting performance. *Experimental Physiology*, *95*(3), 441–450. https://doi.org/10.1113/expphysiol.2009.047555

Lakie, M., Villagra, F., Bowman, I., & Wilby, R. (1995). Shooting performance is related to forearm temperature and hand tremor size. *Journal of Sports Sciences*, *13*(4), 313–320. https://doi.org/10.1080/02640419508732245

Lippold, O. (1971). Physiological Tremor. *Scientific American*, *224*(3), 65–73.

Listman, J. B., Tsay, J. S., Kim, H. E., Mackey, W. E., & Heeger, D. J. (2021). Long-Term Motor Learning in the “Wild” With High Volume Video Game Data. *Frontiers in Human Neuroscience*, *15*. https://doi.org/10.3389/fnhum.2021.777779

Louis, E. D. (2005). Essential tremor. *The Lancet Neurology*, *4*(2), 100–110. https://doi.org/10.1016/S1474-4422(05)00991-9

Luft, F., Sharifi, S., Mugge, W., Schouten, A. C., Bour, L. J., van Rootselaar, A. F., Veltink, P. H., & Heida, T. (2020). Distinct cortical activity patterns in Parkinson's disease and essential tremor during a bimanual tapping task. *Journal of NeuroEngineering and Rehabilitation*, *17*(1), 45. https://doi.org/10.1186/s12984-020-00670-w

Marshall, J. (1961). THE EFFECT OF AGEING UPON PHYSIOLOGICAL TREMOR. *Journal of Neurology, Neurosurgery, and Psychiatry*, *24*(1), 14–17. https://doi.org/10.1136/jnnp.24.1.14

Marshall, J., & Walsh, E. G. (1956). PHYSIOLOGICAL TREMOR. *Journal of Neurology, Neurosurgery, and Psychiatry*, *19*(4), 260–267. https://doi.org/10.1136/jnnp.19.4.260

Miyahara, M., Piek, J. P., & Barrett, N. C. (2008). Effect of postural instability on drawing errors in children: A synchronized kinematic analysis of hand drawing and body motion. *Human Movement Science, Motor Control and Coordination across the Lifespan*, *27*(5), 705–713. https://doi.org/10.1016/j.humov.2008.03.001

Monaghan, P. G., Murrah, W. M., Walker, H. C., Neely, K. A., & Roper, J. A. (2024). Cognitive-motor interference in people with essential tremor. *Scientific Reports*, *14*(1), 23456. https://doi.org/10.1038/s41598-024-74310-x

Moustafa, A. A., Krishna, R., Eissa, A. M., & Hewedi, D. H. (2013). Factors underlying probabilistic and deterministic stimulus-response learning performance in medicated and unmedicated patients with Parkinson's disease. *Neuropsychology*, *27*(4), 498–510. https://doi.org/10.1037/a0032757

Murnaghan, C. D., Carpenter, M. G., Chua, R., & Inglis, J. T. (2017). Keeping still doesn't "make sense": Examining a role for movement variability by stabilizing the arm during a postural control task. *Journal of Neurophysiology*, *117*(2), 846–852. https://doi.org/10.1152/jn.01150.2015

Osborne, L. C., Lisberger, S. G., & Bialek, W. (2005). A sensory source for motor variation. *Nature*, *437*(7057), Article 7057. https://doi.org/10.1038/nature03961

Pan, M.-K., Ni, C.-L., Wu, Y.-C., Li, Y.-S., & Kuo, S.-H. (2018). Animal Models of Tremor: Relevance to Human Tremor Disorders. *Tremor and Other Hyperkinetic Movements*, *8*, 587. https://doi.org/10.7916/D89S37MV

Pelicioni, P. H. S., Pereira, M. P., Lahr, J., Rodrigues, M. M. L., & Gobbi, L. T. B. (2020). Biomechanical analysis of sit-to-walk in different Parkinson's disease subtypes. *Clinical Biomechanics (Bristol, Avon)*, *75*, 105010. https://doi.org/10.1016/j.clinbiomech.2020.105010

Purzner, J., Paradiso, G. O., Cunic, D., Saint-Cyr, J. A., Hoque, T., Lozano, A. M., Lang, A. E., Moro, E., Hodaie, M., Mazzella, F., & Chen, R. (2007). Involvement of the Basal Ganglia and Cerebellar Motor Pathways in the Preparation of Self-Initiated and Externally Triggered Movements in Humans. *Journal of Neuroscience*, *27*(22), 6029–6036. https://doi.org/10.1523/JNEUROSCI.5441-06.2007

Raethjen, J., Pawlas, F., Lindemann, M., Wenzelburger, R., & Deuschl, G. (2000). Determinants of physiologic tremor in a large normal population. *Clinical Neurophysiology*, *111*(10), 1825–1837. https://doi.org/10.1016/S1388-2457(00)00384-9

Readman, M. R., Crawford, T. J., Linkenauger, S. A., Bek, J., & Poliakoff, E. (2023). Motor imagery vividness and symptom severity in Parkinson's disease. *Journal of Neuropsychology*, *17*(1), 180–192. https://doi.org/10.1111/jnp.12293

Robinson, F. R., Noto, C. T., & Bevans, S. E. (2003). Effect of Visual Error Size on Saccade Adaptation in Monkey. *Journal of Neurophysiology*, *90*(2), 1235–1244. https://doi.org/10.1152/jn.00656.2002

Roper, J. A., Brinkerhoff, S. A., Harrison, B. R., Schmitt, A. C., Roemmich, R. T., & Hass, C. J. (2019). Persons with essential tremor can adapt to new walking patterns. *Journal of Neurophysiology*, *122*(4), 1598–1605. https://doi.org/10.1152/jn.00320.2019

Shadmehr, R. (2017). Distinct neural circuits for control of movement vs. Holding still. *Journal of Neurophysiology*, *117*(4), 1431–1460. https://doi.org/10.1152/jn.00840.2016

Shah, B. R., Tanabe, J., Jordan, J. E., Kern, D., Harward, S. C., Feltrin, F. S., O'Suilliebhain, P., Sharma, V. D., Maldjian, J. A., Boutet, A., Mattay, R., Sugrue, L. P., Narsinh, K., Hetts, S., Shah, L. M., Druzgal, J., Lehman, V. T., Lee, K., Khanpara, S., … Kaufmann, T. J. (2025). State of Practice on Transcranial MR-Guided Focused Ultrasound: A Report from the ASNR Standards and Guidelines Committee and ACR Commission on Neuroradiology Workgroup. *AJNR. American Journal of Neuroradiology*, *46*(1), 2–10. https://doi.org/10.3174/ajnr.A8405

Shill, H. A., De La Vega, F. J., Samanta, J., & Stacy, M. (2009). Motor learning in essential tremor. *Movement Disorders*, *24*(6), 926–928. https://doi.org/10.1002/mds.22479

Smaga, S. (2003). Tremor. *American Family Physician*, *68*(8), 1545–1552.

Stegemöller, E., Zaman, A., MacKinnon, C. D., Tillman, M. D., Hass, C. J., & Okun, M. S. (2016). Laterality of repetitive finger movement performance and clinical features of Parkinson's disease. *Human Movement Science*, *49*, 116–123. https://doi.org/10.1016/j.humov.2016.06.015

Taylor, J. A., Klemfuss, N. M., & Ivry, R. B. (2010). An Explicit Strategy Prevails When the Cerebellum Fails to Compute Movement Errors. *The Cerebellum*, *9*(4), 580–586. https://doi.org/10.1007/s12311-010-0201-x

Tolleson, C., Turchan, M., van Wouwe, N., Isaacs, D., Phibbs, F., & Wylie, S. (2017). Parkinson's Disease Subtypes Show Distinct Tradeoffs Between Response Initiation and Inhibition Latencies. *Journal of the International Neuropsychological Society: JINS*, *23*(8), 665–674. https://doi.org/10.1017/S1355617717000467

Udupa, K., Bhattacharya, A., Bhardwaj, S., Pal, P. K., & Chen, R. (2022). Parkinson's disease: Alterations of motor plasticity and motor learning. *Handbook of Clinical Neurology*, *184*, 135–151. https://doi.org/10.1016/B978-0-12-819410-2.00007-2

Vakil, E., & Herishanu-Naaman, S. (1998). Declarative and procedural learning in Parkinson's disease patients having tremor or bradykinesia as the predominant symptom. *Cortex; a Journal Devoted to the Study of the Nervous System and Behavior*, *34*(4), 611–620. https://doi.org/10.1016/s0010-9452(08)70518-5

Vandevoorde, K., & Orban de Xivry, J.-J. (2020). Why is the explicit component of motor adaptation limited in elderly adults? *Journal of Neurophysiology*, *124*(1), 152–167. https://doi.org/10.1152/jn.00659.2019

Vliet, R. van der, Frens, M. A., Vreede, L. de, Jonker, Z. D., Ribbers, G. M., Selles, R. W., Geest, J. N. van der, & Donchin, O. (2018). Individual Differences in Motor Noise and Adaptation Rate Are Optimally Related. *eNeuro*, *5*(4). https://doi.org/10.1523/ENEURO.0170-18.2018

Wolpert, D. M., Miall, R. C., & Kawato, M. (1998). Internal models in the cerebellum. *Trends in Cognitive Sciences*, *2*(9), 338–347. https://doi.org/10.1016/S1364-6613(98)01221-2

Wong, A. L., & Shelhamer, M. (2011). Sensorimotor adaptation error signals are derived from realistic predictions of movement outcomes. *Journal of Neurophysiology*, *105*(3), 1130–1140. https://doi.org/10.1152/jn.00394.2010

Wylie, S. A., van den Wildenberg, W., Ridderinkhof, K. R., Claassen, D. O., Wooten, G. F., & Manning, C. A. (2012). Differential susceptibility to motor impulsivity among functional subtypes of Parkinson's disease. *Journal of Neurology, Neurosurgery, and Psychiatry*, *83*(12), 1149–1154. https://doi.org/10.1136/jnnp-2012-303056

Zampogna, A., Suppa, A., Patera, M., Cavallieri, F., Bove, F., Fraix, V., Castrioto, A., Schmitt, E., Pelissier, P., Chabardes, S., Meoni, S., & Moro, E. (2025). Resting and action tremor in Parkinson's disease: Pathophysiological insights from long-term STN-DBS. *Npj Parkinson's Disease*, *11*(1), 284. https://doi.org/10.1038/s41531-025-01130-9

Chapter 2: Applied motor noise affects specific learning mechanisms during short-term adaptation to novel movement dynamics

This chapter was previously published in eNeuro under the following citation: Foray, K., Zhou, W., Fitzgerald, J., Gianferrara, P. G., & Joiner, W. M. (2025). Applied motor noise affects specific learning mechanisms during short-term adaptation to novel movement dynamics. *eneuro*, *12*(1), ENEURO-0100.

Copyright © 2024 Foray et al.

ABSTRACT

Short-term motor adaptation to novel movement dynamics has been shown to involve at least two concurrent learning processes: a slow process that responds weakly to error but retains information well, and a fast process that responds strongly to error but has poor retention. This modeling framework can explain several properties of motion-dependent motor adaptation (e.g., 24-hour retention). An important assumption of this computational framework is that learning is only based on the experienced movement error, and the effect of noise (either internally generated or externally applied) is not considered. We examined the respective error sensitivity by quantifying adaptation in three subject groups distinguished by the noise added to the motion-dependent perturbation (magnitudes of 0, 3 or 7N, at a frequency of 10 Hz, 20 subjects/group). We assessed the feedforward adaptive changes in motor output and examined the adaptation rate, retention and decay of learning. Applying a two-state modeling framework showed that the applied noise during training mainly affected the fast learning process, with the slow process largely unaffected; participants in the higher noise groups demonstrated a reduced force profile following training, but the decay rate across groups was similar, suggesting that the slow process was unimpaired across conditions. Collectively, our results provide evidence that noise significantly decreases motor adaptation, but this reduction may be due to its influence over

specific learning mechanisms. Importantly, this may have implications for how the motor system compensates for random fluctuations, especially when affected by brain disorders that result in movement tremor (e.g., Essential Tremor).

INTRODUCTION

Motor learning is a type of experience-dependent learning that involves changes in behavioral output to achieve a desired outcome (Wolpert et al. 2001; Halsband and Lange, 2006; Wolpert et al. 2011; Krakauer et al. 2019). The nervous system integrates different sources of information (e.g., externally generated sensory feedback, internally generated predictive signals, etc.) to determine the appropriate motor output to compensate for experienced errors (Mazzoni and Krakauer, 2006; Wolpert et al. 2011; Krakauer et al. 2019). Motor adaptation, a form of short-term motor learning, can occur on a trial-by-trial basis (i.e., error-based learning) to recalibrate motor output to reduce sensory prediction errors (Synofzik et al. 2006; Berniker and Kording, 2008; Synofzik et al. 2008; Shadmehr et al. 2010; Wolpert et al. 2011; Butcher et al. 2017; Izawa and Shadmehr, 2011).

Motor adaptation of arm-reaching movements (Shadmehr and Mussa-Ivaldi, 1994) is typically studied using a robotic manipulandum. Participants hold the handle of the robot and are asked to make reaching movements between targets in the presence of a dynamic, lateral force-field (FF) perturbation (Joiner and Smith, 2008; Mckenna et al. 2017; Alhussein et al. 2019; Zhou et al. 2022). These FF perturbations are usually orthogonal to the direction of the arm reaching motion and the amount of force is proportional to the motion state of the movement (e.g., movement velocity). During this perturbation, participants must adapt the temporal pattern of force to counteract the lateral force of the perturbation (Conditt et al. 1997; Conditt and Mussa-Ivaldi, 1999; Sing et al. 2009; Yousif and Diedrichsen, 2012; Sing et al. 2013; Hosseini et al. 2017; Joiner et al. 2017). Interspersed randomly throughout the task, error-clamp (EC) trials restrict movement (in the absence of the perturbation) so that participants are guided towards the target in a straight line while keeping lateral errors very small (Scheidt et al. 2000; Hwang et al. 2006; Smith et al

2006; Wagner and Smith, 2008; Sing et al. 2009; Wei and Kording, 2010; Wanda and Thoroughman, 2013). EC trials capture the applied force of the subject and provide a measure of adaptation; the temporal profile of the lateral force produced by subjects is compared to the ideal force pattern based on the measured motion state throughout the movement (e.g., movement velocity).

Retention of motor adaptation of arm reaching movements can be modeled as a multi-rate, gain-independent two-state model developed by Smith et al. (2006). This framework postulates that adaptation is the result of two concurrent learning processes: one process that responds quickly to movement errors but has poor retention (i.e., the fast process) and another that responds slowly to movement errors but retains the learning well from one trial to the next (i.e., the slow process) (Smith et al. 2006; Joiner and Smith, 2008; Shadmehr et al. 2010; Wolpert et al. 2011; Albert and Shadmehr, 2018; Sarwary et al. 2018; Coltman et al. 2019). The two-state model has been shown to account for the retention of adaptation following a 24-hour period (Joiner and Smith, 2008); at the end of training, the best predictor of retention is the slow learning process's efficiency over time as opposed to the overall adaptation level reflective of learning, as might have been expected. In a further attempt to understand which specific mechanisms during training affects the stability of adaptation, Alhussein et al. (2019) systematically examined the influence of training duration and type of exposure (gradual versus abrupt) on the short-term decay of learning. The authors found that the training duration had the strongest effect on adaptation stability, (i.e., the persistence of the adapted motor output over a period of time); the longer training durations resulted in a slower decay of adaptation, independent of the type of exposure. Using the two-state modeling framework, the authors further showed that the slow-learning process was best able to predict the stability; the less stable the slow-learning process, the faster the adaptation decayed. Thus, the studies above show that the slow learning process plays a substantial role in the long-term memory formation and stability (observed by the time course of decay) of motor adaptation.

One current limitation of the two-state model is its interpretation of the error as a perturbation originating from a single source. That is, the model assumes that the motor error that drives learning has idiosyncratic consistent characteristics. However, error can possess different characteristics, such as source, magnitude, and frequency (Faisal et al. 2008; Wolpert and Landy, 2012). While the slow-learning process is most influenced by the duration of training and evolves over time, the fast-learning process is characterized by quick responses to movement errors, which are rapid changes in the environment resulting in motor variability (Smith et al. 2006; Alhussein et al. 2019). However, it is unclear how the error sensitivity of the respective processes changes when faced with variability. That is, it is unknown to what extent the learning mechanisms adjust their response when faced with fluctuations in the experienced error. Thus, there is a need to understand the exact relationship between variability in error, or noise, and the subsequent effect on these two learning processes. By understanding the impact that different noise parameters have in adaptation, we will gain greater insight into how variability in the experienced error influences motor learning. This in turn will allow updating the current models of adaptation to reflect the compensation to real-world movement errors.

In addition to the underlying temporal and spatial characteristics, motor noise can be broadly categorized as either internally- or externally-generated (coming from a source within or separate from the organism) (Berniker and Kording, 2008; Faisal et al. 2008). Understanding this influence will assist in assessing the consequences of noise on the motor behavior in certain patient populations. For example, motor noise has been shown to impair the ability to appropriately adapt motor output when either internally-generated (McCrea and Eng, 2005; Kronenbuerger et al. 2007; Shill et al. 2009) or externally-applied (Therrien et al. 2018). This is particularly relevant to patients with pathological tremor, a type of internally-generated noise, who have impaired motor learning (McCrea and Eng, 2005; Kronenbuerger et al. 2007; Shill et al. 2009). Specifically, patients with Essential Tremor (ET) are known to have a high-frequency tremor (6-12 HZ) (Agarwal and Biagioni, 2018) that impairs their ability to adapt (Shill et al. 2009). In a study

examining visual sensory feedback noise, higher amounts of externally-generated noise during adaptation have been suggested to require compensation from explicit learning strategies (Miyamoto et al 2020), which have been thought to constitute the fast learning process of the two-state model (McDougle et al. 2015). While these studies provide initial insight into how noise impairs motor adaptation, there has not yet been direct evidence of the specific mechanisms and timescales by which these impairments occur. To better understand the precise aspects of motor learning affected by internally-generated noise, especially in disease models, we must first establish how varying characteristics of externally-generated noise with the same frequency as Essential Tremor impacts healthy participants.

The objective of this study was to assess motor adaptation in the presence of additional noise of different magnitudes. By applying the two-state model we aimed to further understand the impact of externally applied motor noise on different characteristics of motor learning (e.g., adaptation rate, retention, and decay). Through the addition of noise with the same frequency as Essential Tremor to movement error, we hoped to gain greater insight into real-world representations of movement error and contribute to the current two-state model, which currently interprets error as being non-variable. We hypothesized that as the magnitude of externally-generated noise increased, the motor adaptation rate in response to the novel movement dynamics would decrease, specifically as a result of impairment of the fast-learning process. Subsequently, due to a largely intact slow process, the specificity of impairment would result in similar retention and decay rates of adaptation across the different levels of applied noise. Ultimately, a more comprehensive understanding of error sensitivity will provide insight into how the motor system compensates for random fluctuations, especially when affected by brain disorders that result in movement tremor (e.g., Essential Tremor or Parkinson's Disease).

MATERIALS AND METHODS

Sixty right-handed participants (15 male, 44 female, and 1 unknown; aged between 18 and 30 years) without known neurological impairments were recruited at the University of California, Davis. Participants received financial compensation for their participation. All participants used their right dominant hand to complete the experiment and their handedness was measured by the Edinburgh Handedness Inventory (Oldfield, 1971). Each participant only performed a single experimental paradigm. All participants were naive to the purpose of the experiment and gave written informed consent in accordance with protocols approved by the Institutional Review Board at the University of California, Davis.

Motor adaptation was investigated through an arm-reaching paradigm (Shadmehr and Mussa-Ivaldi, 1994; Scheidt et al. 2000) (Fig. 1*).* The paradigm required participants to move a robotic arm on a planar workspace that moved a screen cursor between presented targets. The robotic arm manipulandum (KINARM End-Point Lab, BKIN Technologies) sampled motor output, including position, force, velocity, and acceleration at 1000 Hz. A horizontal screen display blocked participants from viewing their arm directly. A downward facing LCD monitor, reflected by an upward-facing mirror, allowed viewing of trial start locations and targets, marked by small circles. Participants were seated in an adjustable chair so that they could comfortably view the mirrored display.

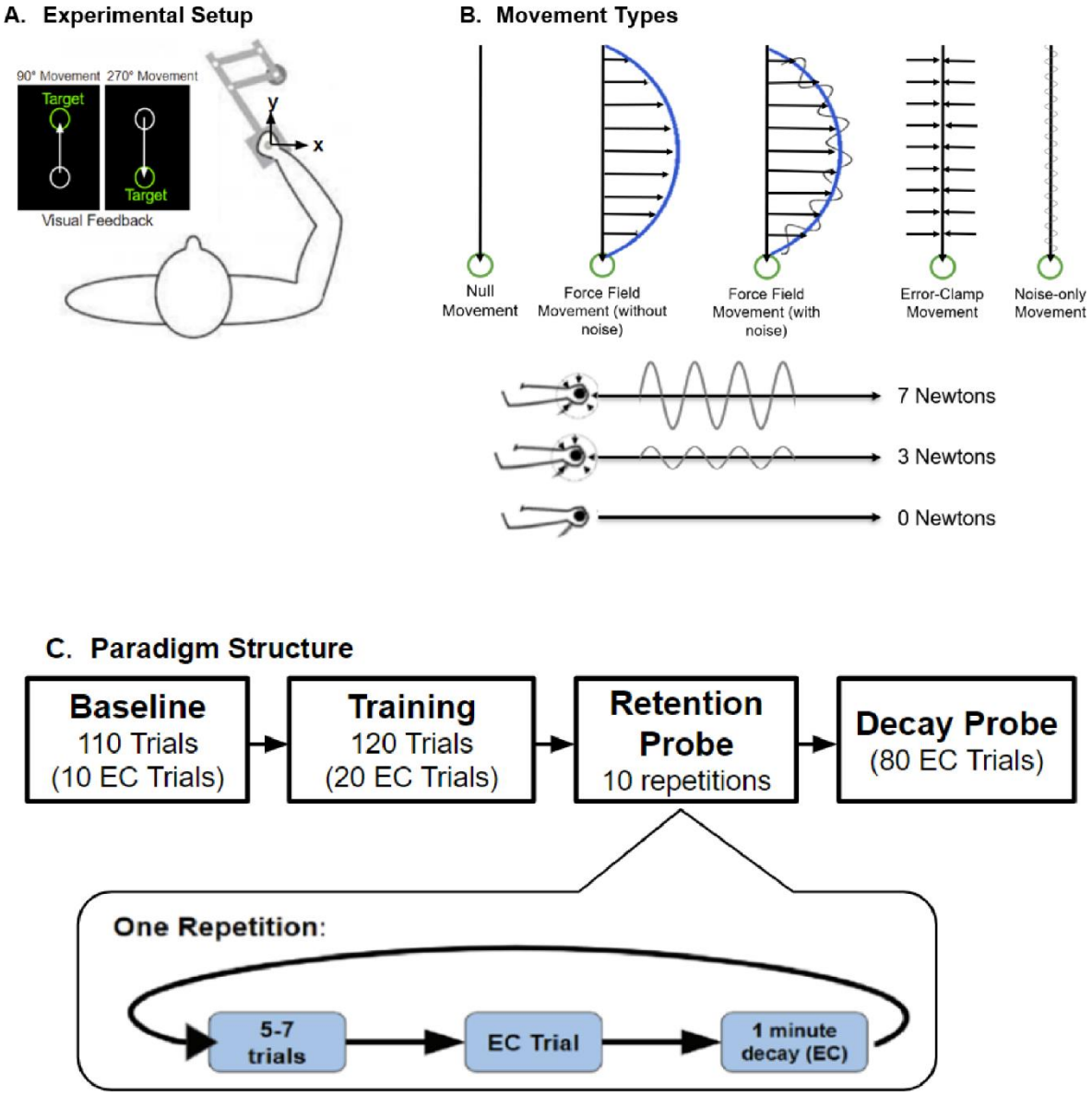

Figure 1. Experimental set-up and protocol. (A) Participants made straight-arm reaching movements between two circular targets from midline approximately 10 cm apart while holding the handle of a robotic manipulandum. Forward reaching motion was completed in the 90 degree direction while reaching back towards oneself was completed in the 270 degree direction. However, we only used arm movements completed in the 270 degree direction to compute adaptation coefficients and assess force profiles. The location of the hand was represented on the screen as a white filled

circle. (B) There were four movement types: null, noise-only, force field (without noise), force field (with noise), and error-clamp movements. Each trial consisted of one movement. Null movements were completed as a free-range movement (no resistance from the robot) without any added noise or force field perturbation. Noise-only movements were free-range movements with added noise (according to condition). During force field movements, participants experienced a velocity-dependent, lateral perturbation (horizontal small black arrows). For the 270 degree reaching motion, the force-field perturbed the participant arm reach to the right. The control condition experienced this perturbation without any added noise (Force-Field Movement (without noise)). The experimental groups experienced this perturbation with the addition of either 3N or 7N of noise (applied at 10Hz) supplied by the robot (Force-Field Movement (with noise)). This noise was generated by the sine function described in the Methods. During error-clamp trials (EC), lateral movement was constrained by clamps, constraining lateral error to less than 0.6mm. (C) Paradigm structure. Participants started off with a block consisting of null movements with occasional error-clamp trials to establish baseline performance. During the training blocks, participants experienced the force-field perturbation (with added noise in the 3N and 7N noise groups). During the retention probe block, on some of the trials, participants were asked to hold the cursor at the start target for approximately one-minute before proceeding with the reaching movement. During the decay probe block, participants were given a series of 80 error-clamp trials to assess the decay of adaptation.

Participants were instructed to make straight arm reaching movements between two circular targets 0.5 cm in diameter spaced 10 cm apart on a screen while holding the handle of the robotic manipulandum (Fig. 1A). The two targets were located 20-30 cm away from the body on the sagittal axis. Arm movement via the robotic manipulandum was represented by a white filled

circle, 3 mm in diameter on the screen. Horizontal and vertical arm movement (i.e., movement within the 2D plane that results in x and y movement directions of the cursor) was measured, and a successful movement to the target was achieved when the peak movement velocity in the y direction (towards the target) was within a range of 0.2–0.55 m/s. Additionally, participants were given both visual and auditory feedback on successful reaches. When peak movement velocity met the specific criteria, the target would turn green and make a brief auditory tone. When the reach was too slow, the target would turn yellow. If too fast, red. At the beginning of the task, participants were instructed to obtain “as many green feedback trials as possible”.

Within the task, there were four types of trials: null, force-field perturbation (FF), error-clamp, and noise-only (Fig. 1B). During null trials, participants made straight arm reaching movements between the targets without any perturbations or restrictions to movement (no noise and no force-field). During FF trials, reaching arm movements were systematically perturbed during the training period. On these trials, the robot perturbed the hand motion with forces that were proportional to the velocity of movement and perpendicular to the direction of hand motion (Equation 1). Within the FF trials, there were three groups of subjects, and each group experienced a different level of noise, (magnitudes of either 0, 3, or 7N, at a frequency of 10 Hz) in addition to the main FF perturbation. For the level of noise, we wanted to simulate the pathological tremor experienced by those with Essential Tremor. A 10 Hz frequency is within the range for that experienced by individuals with Essential Tremor. However, we were limited by the KINARM’s generation of noise magnitude (i.e., force). Using our best estimates, we wanted to capture the full range of noise magnitude that could be produced by the KINARM without causing discomfort to participants The 7N magnitude was the far end of this range while the 3N magnitude was approximately between 0N and 7N. The noise was generated by a sine function (see Equation 2) and applied along the x-axis— the axis that subjects would eventually experience the force-field perturbation.

$$\begin{bmatrix} F_x \\ F_y \end{bmatrix} = c_k \begin{bmatrix} 0 & -k \\ k & 0 \end{bmatrix} \begin{bmatrix} \dot{x} \\ \dot{y} \end{bmatrix}, k = 15 \text{ Ns/m}$$ **(Equation 1)**

Error clamp (EC) trials assessed the feedforward adaptive changes in motor output. EC trials involved restricting lateral movement, forcing participants to move the cursor in a straight line towards the target so that lateral errors were kept to a minimum. In this case, the robot motors constrained movements in a straight line toward the reach target by counteracting any motion perpendicular to the target direction. This was achieved by applying a stiff one-dimensional spring (6 kN/m) and a damper (150 Ns/m) in the axis perpendicular to the reach direction. In these trials, perpendicular displacement from a straight line to the reach target was held to less than 0.6 mm and averaged about 0.2 mm in magnitude. Importantly, the force-field (and added noise) was not applied on these error-clamp trials. Thus, there wouldn't be any rapid feedback correction on these error-clamp trials. The error-clamp trials provide the force profiles shown in Figures 2 and 4 (The force the robot must apply in order to ensure the subject moved in a straight line).

During noise-only trials, participants made straight arm reaching movements between the targets while the robot applied the amount of noise consistent with their condition (magnitudes of either 0, 3, or 7N, at a frequency of 10 Hz).

$$Noise = m \cdot sin(2 \cdot \pi \cdot f \cdot t)\ ,\ f = 10Hz, m = 0, 3\ or\ 7N$$ **(Equation 2)**

Experimental Paradigm

The task began with a familiarization period, where participants of all groups had null (no added noise or FF) movement trials. One group (0N noise) served as the control group. Two groups experienced noise with an amplitude of 3 or 7N (except for during the familiarization period). This was followed by baseline trials. For the control group, the baseline block contained 100 null trials randomly dispersed with 10 EC trials (110 trials total). For the two noise groups, the

baseline consisted of 50 noise-only trials and 60 null trials (no noise) randomly dispersed with 10 EC trials (120 trials total). Immediately following baseline, participants were exposed to a training block. As described above, we divided participants into three groups based on the amplitude of the noise experienced during the training period. Each participant only experienced one type of training and the training period consisted of 100 FF trials interspersed randomly with 20 EC trials (120 trials total). For every 5 FF trials, there was 1 EC trial randomly dispersed. In addition to the FF perturbation, the robot applied the magnitude of noise that corresponded to the condition of each participant.

The retention block (Fig. 1C) immediately followed the training period. During this block participants experienced 5-7 trials of the FF perturbation (with the added noise based on the subject group) followed by an EC trial. This EC trial was followed by a delay period of one minute during which participants were asked to hold the cursor at the start location. Based on prior work, we hypothesized that during this delay, the fast process would rapidly decay so that the subsequent error-clamped movement on the trial following the delay would reflect the amount of slow learning process retained over the period without movement. This sequence (5-7 FF trials, 1 EC trial, a one-minute delay, and 1 EC trial) was repeated 10 times within the retention block. Finally, following the retention block there was a decay block, which consisted of 80 consecutive EC trials. This allowed a measure of the decay of adaptation towards baseline.

Quantification of Adaptation

To quantify adaptation throughout the task, we use the lateral force profiles measured throughout the EC trials. For our analyses, we only calculated adaptation and the applied force profiles for reaches in the direction towards the body (270-degrees). Since we only perturbed arm-reaching movement during the 270-degree movements, we wanted to analyze only that direction for changes in participant force profile. For each FF trial, there is an ideal temporal pattern of compensatory force to fully compensate for the lateral perturbation. This ideal compensatory force

is directly proportional to the velocity profile of movement on that trial, so the ideal force profile for each FF trial is unique. Force profiles are the temporal pattern of applied force (N) which is measured continuously throughout a single reaching movement. The force profiles on individual trials were centered on the peak velocity with a temporal window of 1,200 ms (±600 ms, where 0 ms is the moment when the movement reaches peak velocity). This provides an alignment of all movements in the same temporal window. Force profiles were aligned to the peak velocity because the force-field perturbation applied by the robot is based on the movement velocity. Thus, plotting the ideal force pattern (based on the actual movement velocity on that trial) with the actual applied force on that trial provides a straightforward comparison of the two profiles. We calculated the participants' ability to adapt to the perturbations by linearly regressing the baseline-subtracted actual force profile applied by participants to the ideal compensatory force profile for each EC trial. The baseline subtractions are subtracting the average force profile, determined over the same 1,200 ms window, obtained during the EC trials during the baseline period from the force profile on the EC trials experienced during training. Determining the regression slope involved utilizing a least squares estimate to minimize the model fit error, and the slope was used as the measure to quantify adaptation (i.e., the adaptation coefficient, AC). It is this slope of the linear regression between the baseline-subtracted actual force and the ideal force (based on the movement velocity on that trial) that is the scalar AC—a measure of how well the applied force matches the ideal force based on the movement velocity. If the actual compensatory force was equal to the ideal compensatory force, then the AC =1. If they are exact opposites, AC = -1. If they are unrelated to one another, $AC = 0$.

Baseline Analyses

To better understand how the groups performed before exposure to the perturbation condition, we quantified the variability of null movements during the baseline period. In this case

variability refers to the angular deviation from the straight-line path at the point of maximum lateral movement deviation.

Computational Modeling

To determine the effect of the applied noise on specific learning mechanisms we used the multi-rate gain-independent two-state model from Smith et al. (2006). The equations for adaptation to error (perturbation) are shown below.

Two-State Model (Smith et al. 2006):

$$x_f[n+1] = A_f \cdot x_f[n] + B_f \cdot e[n] \quad \textbf{(Equation 3)}$$

$$x_s[n+1] = A_s \cdot x_s[n] + B_s \cdot e[n] \quad \textbf{(Equation 4)}$$

$$B_f >> B_s, A_s >> A_f, x[n] = x_f[n] + x_s[n]$$

$x_f[n]$, $x_s[n]$: Net motor output on trial n

A_f, A_s : Retention factors

B_f, B_s : Learning rates

$e[n]$: Error on trial n

FF Trials:

$$e[n] = f[n] - x[n] \quad \textbf{(Equation 5)}$$

EC Trials:

$$f[n] = x[n] \rightarrow e[n] = 0 \quad \textbf{(Equation 6)}$$

$e(n)$: error on trial n

$f(n)$: strength of FF disturbance on trial n

$x(n)$: state of learned motor output on trial n

The two-state model postulates that adaptation is supported by two, distinct processes that operate in parallel (Equations 3 and 4). The total compensation to error ($x[n]$) is the sum of the fast ($x_f[n]$) and slow ($x_s[n]$) learning processes. The fast and slow learning processes differ in their respective learning (B_f, B_s) and retention (A_f, A_s) rates. Here, learning rates are quantified by the previously mentioned adaptation coefficients, which are averaged across participants for each trial. The fast learning process has a faster learning rate than the slow learning process ($B_f >> B_s$) but the slow learning process has a much greater retention factor ($A_s >> A_f$)**.** The net motor output on the next trial (x[n+1], A) is dependent on the amount of learning retained (retention factor) scaled by the amount of the fast or slow process (the internal state). The amount of the fast or slow process has been intrinsically normalized based on the current motor output in addition to the current learning rate (B) scaled by the amount of error on the current trial (e[n]). The net motor output on a specific trial (x_f[n], x_s[n]) refers to the AC for each learning process (fast or slow). As the ACs themselves are scalar (-1 to 1), the net motor output reflects this learning in a scalar fashion. The potential amount of learning based on presence or absence of error on the current trial, for the purposes of this study, was normalized as either $f[n] = 0$ (no perturbation) or $f[n] = 1$ (FF is present). In the FF trials, the strength of the perturbation (f[n]) minus the learned force to counteract that perturbation (x[n]) during a single trial will provide the amount of error (e[n]) that remains. Note that to determine the adaptation coefficient, we change the sign of the ideal force profile to have a direct comparison to the actual force profile. That is, the actual force should be opposite the FF, but we ensure that both are in the same direction (flip the sign) to determine how well they match. In this way, a positive coefficient represents a successful cancellation of the perturbation. Thus, in this case the error is f(n) – x(n). Additionally, x_f[n] and x_s[n] represent the respective amount of the adaptation to the force-field perturbation attributed to either process. When f[n] = 0 during EC trials, there is no potential for learning because the error is clamped to zero.

Model parameters were derived within groups (i.e., Controls, 3N, 7N) by minimizing the model fit's error relative to the collected data with the *fmincon* function in MATLAB; see Equation 7). Because our optimization function is biased towards the asymptote, we wanted our initial parameters to more closely reflect the initial rise in the adaptation coefficient ($A_f = 0.775$, $B_f = 0.06$, A_s= 0.992, $B_s = 0.02$). To accurately constrain the best-fit parameter estimates of the data, we ran a bootstrapping algorithm that sampled participant data with replacement and added a regularization term to the error function to prevent biasing effects from repeated outliers in the data (see Equation 8). This procedure was replicated 2,000 times to reliably estimate a distribution of bootstrapped parameters. Each replicate was made by sampling data from 20 randomly generated choices generated from the 20 participants in the study. We made 2,000 different bootstrap estimates and fit the model to each estimate. We used the 2.5 and 97.5 percentile values of each parameter distribution's fitted Gaussian as the 95% confidence interval limits.

Estimating plausible ranges of estimates for each of the four model parameters (A_f, B_f, A_s, B_s) happened in two steps. In Step 1, we computed the original parameter estimates based on the least-squares method. We first estimated reasonable values for each of the four model parameters by minimizing the model prediction error relative to the original data ***y*** (i.e., best model fit). Specifically, we ran the *fmincon()* function in MATLAB to extract the parameter estimates that would minimize the error function as described on Equation 7.

$$\boldsymbol{\theta_{LMSE}} = argmin\left\{\frac{\sum_{n=1}^{N}(y^{(n)}-\hat{y}^{(n)})^2}{N}\right\} \qquad \textbf{(Equation 7)}$$

where *N* refers to the total number of trials, $y^{(n)}$ refers to the original observation on trial n, and $\hat{y}^{(n)}$ refers to the model prediction on trial n.

In Step 2, we estimated plausible confidence intervals around the original parameters $\boldsymbol{\theta_{LMSE}}$. We implemented a bootstrapping strategy to estimate a reasonable confidence interval around each of the original LMSE parameters within $\boldsymbol{\theta_{LMSE}}$. This strategy consisted in sampling data

with replacement and estimating new $\widehat{\boldsymbol{\theta}}$ vectors for each bootstrap. Bootstraps were made by concatenating 20 randomly generated choices corresponding to data produced by the 20 participants in the study. We extracted 2,000 different bootstrapped parameter estimates by fitting the model to each random data concatenation. We added a regularization term to Equation 7 to penalize extreme weights due to the biasing effect of occasional repeated outliers in the sampled data. We implemented the *fmincon()* function in MATLAB to estimate each of the 2,000 bootstrapped $\hat{\theta}$ based on Equation 8.

$$\widehat{\boldsymbol{\theta}} = argmin\left\{\frac{\sum_{n=1}^{N}(y^{(n)}-\hat{y}^{(n)})^2}{N} + \lambda\sum_{s=1}^{4}\left[\frac{\widehat{\theta_s}-\theta_{LMSE_s}}{\sqrt{\theta_{LMSE_s}}}\right]^2\right\} \quad \textbf{(Equation 8)}$$

where *N* refers to the total number of trials, $y^{(n)}$ refers to the original observation on trial n, $\hat{y}^{(n)}$ refers to the model prediction on trial n, $\boldsymbol{\theta_{LMSE}}$ refers to the original model parameters from step 1, and λ refers to a regularization constant which was set to λ = 0.05. This choice of value for the hyperparameter λ was found to be a reasonably low option that optimizes the trade-off between data overfitting (yielding $\hat{\theta}$ outliers) and the overly-constrained normalization of the $\hat{\theta}$ distribution. Note, here, that for each parameter estimate *s* the choice of $\sqrt{\theta_{LMSE_s}}$ as the denominator in the regularization term ensured that all four $\widehat{\theta_s}$, lying between 0 and 1, would equally be constrained by the regularization factor λ regardless of their relative magnitude.

For the bootstrapping algorithm, we used the following bounds in the initialization of the *fmincon()* function across all conditions:

A_f: 0.25-0.75

B_f: 0.0 – 0.2

A_s: 0.93-1.0

B_s: 0.0-0.2

This method was replicated 2,000 times in each bootstrap to estimate four $\hat{\theta}$ distributions. A normal gaussian was fitted to each of these distributions to estimate each

parameter's mean and 95 % confidence interval. Specifically, we used the 2.5 and 97.5 percentile values of each parameter as the 95% confidence interval lower and upper bounds.

Code Accessibility

The code/software described in the paper is freely available online at osf.io/cktnw. The code is available as Extended Data.

Statistical Analysis

Statistical analyses were performed in MATLAB (version R2023a) on trials that met the speed, duration, and position criteria listed above. Based on these criteria, 5% of trials were discarded for the control group, 1.8% percent of trials were discarded for the 3N group, and 5.45% of trials were discarded for the 7N group. In our statistical analyses, we used both fixed (i.e. condition) and random (i.e. subjects) effects. To compare the learning rate for each noise condition, we utilized a logistic growth model (Equation 9, listed in results) using trial number and average adaptation coefficient across participants for each trial number. We then calculated the R-squared value for goodness of fit for our data. We hypothesized that the control group would have a greater maximum adaptation and would reach this asymptote at a faster rate than the 3N and 7N groups. To compare force profiles across the force windows (150ms before peak movement, peak movement, and 150ms after peak movement) and period of training (early, middle, and late training) for each noise condition, in addition to comparing average adaptation coefficient for each period of training across groups, we utilized a two-way and three-way Analysis of Variance (ANOVA). We predicted that the adaptation would be greater for the control group than the 3N and 7N conditions during middle and late training due to the 3N and 7N groups having impaired learning during early training. For the retention trials, we compared the average adaptation coefficient at the end of training and the average adaptation coefficient during the retention probe across groups with a two-way ANOVA. Due to our overall hypothesis of an unimpaired slow

learning process, we predicted that there would not be a significant difference between the end of training and retention probe performance across groups. If significant results were found, we further investigated significance between groups. Additionally, to confirm statistical equivalence across all groups for retention probe performance, we conducted Mann-Whitney U-Tests. To better compare the differences in the average amount of decay across motor noise conditions, we performed a two-phase exponential fit (Equation 10, listed in results), using trial number and average adaptation coefficient across participants for each trial number, and compared the exponential decay constants. To again address our overarching hypothesis that long-term retention, driven by the slow learning process, was not impaired by the added noise, we predicted that the rate of decay would show no statistical difference across conditions. We conducted an Akaike Information Criterion (AIC) test to determine the optimal model, specifically evaluating the appropriateness of one-phase and two-phase exponential decay models. We computed the log-likelihood from fits to the one-phase and two-phase exponential decay models by fitting the data under a t-distribution and basing the AIC on the sum of the squared errors (Akaike, 1998). The results of the goodness-of-fit assessment revealed that the two-phase exponential decay model provided the most favorable fit for our dataset. For all ANOVAs, we corrected for multiple comparisons using a Bonferroni post-hoc test. For significant interactions, we conducted post-hoc Tukey-HSD tests. Effect size (eta squared) was calculated using the hhentschke/measures-of-effect-size-toolbox in MATLAB (Hentschke, 2023). For all tests, the significance level was 0.05 and data are presented by means ± SE.

RESULTS

In this study we investigated the specific mechanisms by which increasing externally-applied motor noise magnitude affected motor adaptation. We utilized a force-field adaptation task (Shadmehr and Mussa-Ivaldi, 1994) in which three groups of participants were exposed to varying levels of noise magnitude (0, 3, or 7N, at a frequency of 10 Hz) while being simultaneously perturbed by the velocity-dependent force-field perturbation. Each group consisted of 20 individuals. Each individual only experienced one noise level within the experiment. We examined the effects of the externally-applied noise on the time course of adaptation, as well as the retention and decay of the learning.

The effect of motor noise on unperturbed and perturbed movements

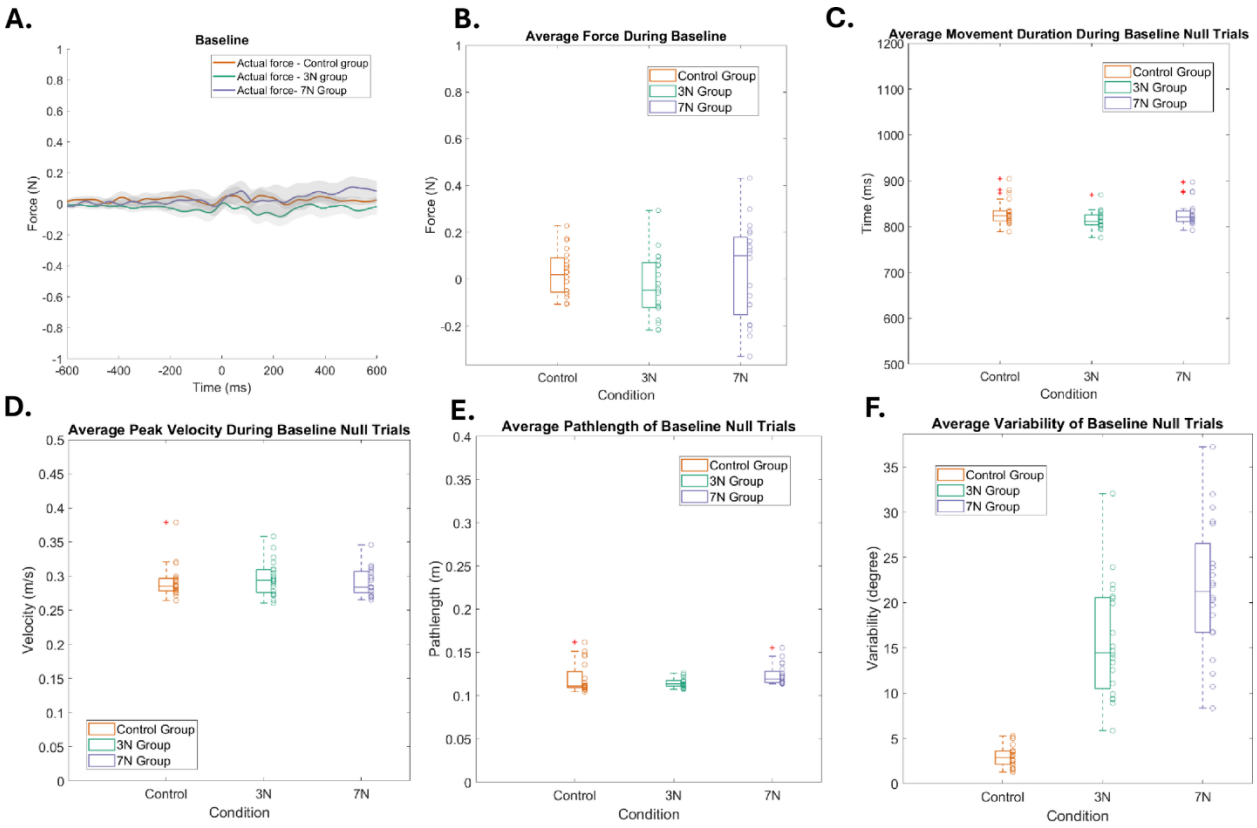

Figure 2. Comparison of baseline movements. (A) Force profiles comparison across

conditions (orange: control group with no added noise, green: 3N of added motor noise, purple: 7N of added motor noise). Force profile is the value, measured in magnitudes (N) on the y-axis, used to indicate how much lateral force was exerted during EC trials throughout a single reaching movement. Force profiles on individual trials were centered on peak velocity (peak velocity indicated as 0 ms). Box plots are shown for the average (B) force (C) movement duration, (D) peak velocity, (E) path length, (F) and variability of baseline null trials. Each unfilled circle represents the results for the average of the windowed trials. Force, movement duration, peak velocity, and path length were not significantly different across the three conditions. However, movement variability was significantly different at baseline.

To determine if the three groups differed during baseline movements (prior to any training), we examined force profiles during EC trials in addition to the movement duration, peak velocity, and path length of the null trials. Average force profiles were not significantly different across the three conditions (Fig. 2A,B; 1-way ANOVA, $F(2,59)=0.96$, $p=0.39$, $\eta^2 = 0.03$). However, movement duration (Fig. 2C; 1-way ANOVA, $F(2,59) =2.06$, $p= 0.14$, $\eta^2 = 0.68$), peak velocity (Fig. 2D; 1-way ANOVA, $F(2,59)=0.35$, $p= 0.7$, $\eta^2 =0.01$), and path length (Fig. 2E; 1-way ANOVA, $F(2,59) = 2.37$, $p=0.1$, $\eta^2 = 0.08$) of baseline null trials were not significantly different across conditions. Variability of baseline null trials was significantly different between conditions (Fig. 2F; 1-way ANOVA $F(2,59)=39.2$, $p=1.99\text{x}10^{-11}$, $\eta^2 = 0.58$), with the 7N group having greater pre-training variability followed by the 3N and 0N groups (See Methods). Thus, the added noise affected certain aspects of movement kinematics on the baseline trials. Next, we examined these effects on movement adaptation in response to a velocity-dependent force-field perturbation.

Added motor noise affects the initial rate of adaptation

Figure 3A plots the adaptation coefficient (see Methods) as a function of training trials for the three subject groups. To quantify the learning rate of each motor noise condition, we utilized a logistic growth model, shown below:

$$A_n = \frac{K}{1 + (\frac{K - A_0}{A_0})e^{-rn}} \qquad \textbf{(Equation 9)}$$

A_n: adaptation coefficient on trial n

K: Carrying capacity (maximum adaptation coefficient subjects could reach)

A_0: initial adaptation coefficient

r: growth rate for learning curve

The control group (0N of applied motor noise) achieved the greatest maximum adaptation (K_{control}= 0.60, 95% CI [0.57 0.63]) and did so at the fastest rate (r_{control}= 0.37, 95% CI [0.15 0.59], R^2 = 0.92) (Fig. 3A). The 3N group achieved a maximum adaptation of K_{3N} = 0.42, 95% CI [0.39 0.45] with a learning rate that was slower than the control group (r_{3N}= 0.26, 95% CI [0.08 0.44], R^2= 0.85). The 7N group achieved the lowest maximum adaptation (K_{7N}= 0.24, 95% CI [0.20 0.28]) with the slowest earning rate (r_{7N} = 0.07, 95% CI [0.02 0.12], R^2= 0.78). These results suggest that as motor noise magnitude increased, the ability of each group to adapt decreased ($K_{\text{control}} > K_{3N} > K_{7N}$). Additionally, increasing motor noise magnitude also affected the rate at which peak adaptation occurred, with higher magnitudes of motor noise associated with slower learning rates ($r_{\text{control}} > r_{3N} > r_{7N}$).

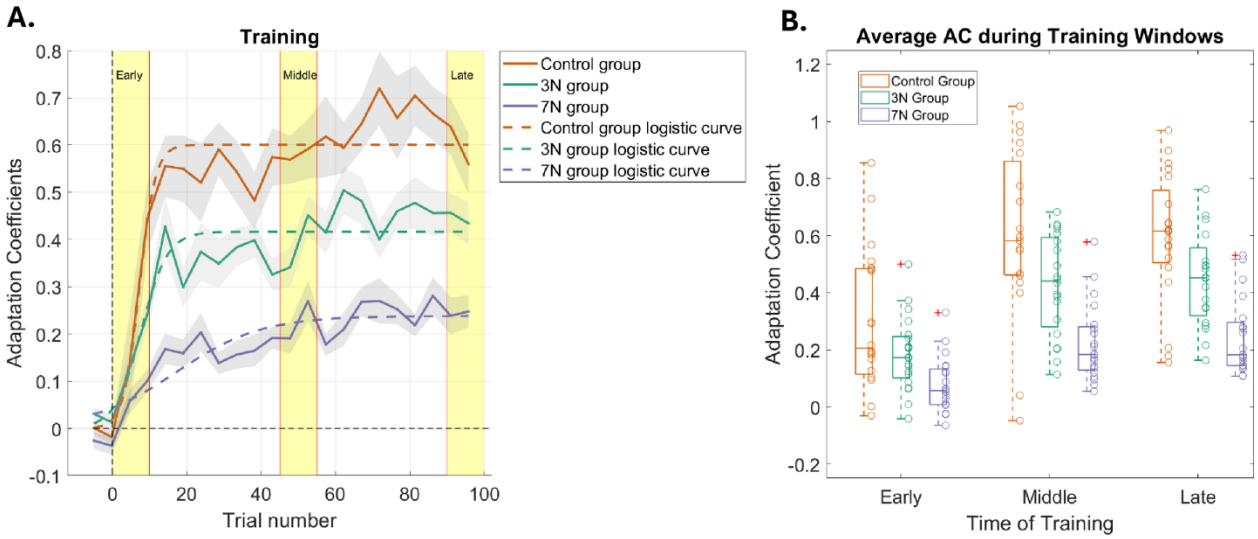

Figure 3. Learning curves during training. (A) Adaptation, quantified by the adaptation coefficient, is plotted as a function of trial number for each condition. These learning curves show that as noise increases (control: orange trace, 3N: green trace, 7N: blue trace), the ability to adapt becomes impaired. Logistic growth curve fits (dashed traces) for each condition are shown: $R^2_{control} = 0.92$, $R^2_{3N} = 0.85$, $R^2_{7N} = 0.78$. Gray shading represents SEM. Yellow regions mark the early, middle and late periods of training. (B) Box plots of the average adaptation coefficient for each condition during early, middle, and late periods of training for each group. Each unfilled circle represents the results for one subject.

To better understand how the average adaptation coefficients differed at specific time periods of training, we examined the average adaptation coefficient from the first 10% of training trials (early trials), the middle 10% (middle trials), and last 10% (late trials), (Fig. 3B). A 2-way ANOVA demonstrated that there was a significant difference in adaptation between motor noise groups ($F(2, 178) = 25.89$, $p = 1.53 \times 10^{-10}$, $\eta^2 = 0.2$) and within each motor noise group, adaptation was significantly different between three training periods (2-way ANOVA, $F(2,178) = 26.07$, $p = 1.33 \times 10^{-10}$, $\eta^2 = 0.2$). No significant interaction between the two factors was found ($F(4,178) = 1.53$, $p = 0.2$, $\eta^2 = 0.02$). The decrease in learning rate occurred early in training; in the early

training period, the control group (orange trace; adaptation coefficient (AC) of 0.24± 0.10) has a steep rise whereas the 3N (0.19 ± 0.03) and 7N (0.08 ± 0.02) groups had not adapted as well (green and purple traces, respectively). The slowed and impaired ability to adapt in early trials due to increasing motor noise magnitude is subsequently followed by lower performance overall in the middle and later trials (middle training period: control: 0.61 ± 0.07, 3N: 0.44 ± 0.04, and 7N: 0.23 ± 0.03, late training period: control: 0.6 ± 0.05, 3N: 0.44 ± 0.04, and 7N: 0.24 ± 0.03).

Added motor noise affects the temporal force profiles

We analyzed the respective force profiles within a 100ms window to identify differences between the temporal structures of adaptation (Joiner et al. 2017). This also provided information on the effect of increasing noise magnitude on adaptation reflected in the force profiles across conditions (Fig. 4). We continued to separate the training data into early, middle, and late trials, as described previously.

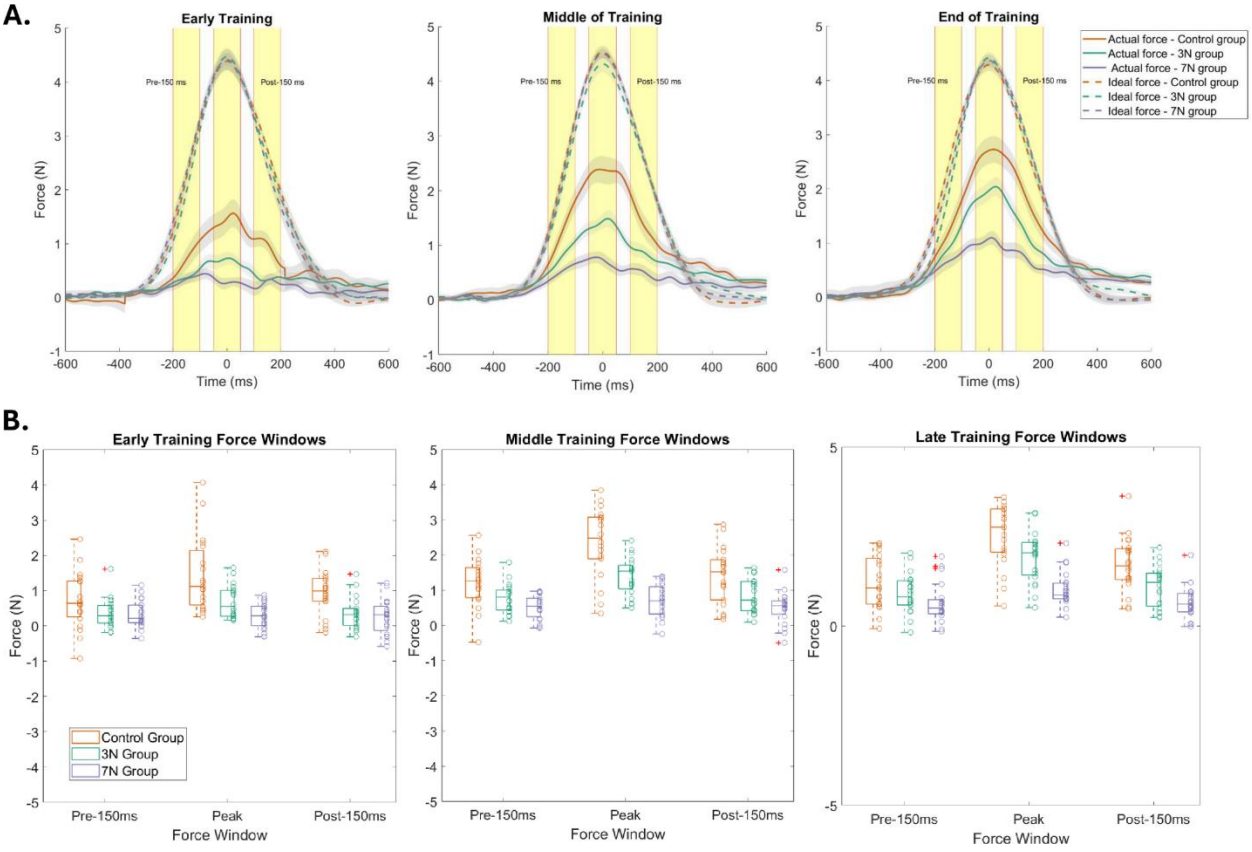

Figure 4. Temporal force profiles during training. (A) Average force-profiles for each group during early, middle, and late periods of training for the three conditions (orange: control group with no added noise, green: 3N of added motor noise, purple: 7N of added motor noise). Force profile is the value, measured in magnitudes (N) on the y-axis, of force used to counteract the FF perturbation throughout the reaching movement. Ideal force profile represents how much force would be needed to exactly counteract the FF perturbation to continue making a straight-arm reaching movement. The actual force profile indicates how much force, on average, participants used to counteract the FF perturbation. Force-profiles were split into three windows: one 100 ms window centered around 150 ms prior to peak movement velocity, one 100 ms window centered around the peak (time = 0) movement velocity, and one 100 ms window centered around 150 ms after peak movement velocity. These three time periods are represented by the three yellow regions. (B) Box plots show differences in the average force profile for each condition during the pre-150ms force window, peak force window, and post-150ms force window within early, middle, and late periods of training.

To best represent the differences between the temporal force profiles, we also separated the data to compare the applied force within a 100 ms window centered on peak velocity, 150 ms before peak velocity, and 150 ms after peak velocity for each training period (Fig. 4A). There was a significant effect of training period (3-way repeated measures ANOVA, $F(2,530) = 59.60$, $p=5.49\text{x}10^{-24}$), temporal force window (3-way ANOVA, $F(2,530)=31.98$, $p=8.21\ \text{x}10^{-14}$), and noise condition (3-way ANOVA, $F(2,530)=58.70$, $p=1.14\text{x}10^{-23}$) on average force profile. These results verify that the difference in performance, as indicated by force profile, between the three conditions is dependent on specific periods of training, namely middle and late training periods (explored in post-hoc tests). Additionally, the control group had significantly greater peak force (2.32 ± 0.16) across training windows than the 3N (1.43 ± 0.1) and 7N (0.72 ± 0.08) groups, which suggests that increasing the magnitude of artificially applied noise impairs one's ability to

accurately adapt. All three factors had significant interaction effects, which we further explored by looking at each training period (see Table 1) and conducting post-hoc tests. Post-hoc Tukey-HSD tests revealed that there was greater force exerted in the 0N middle training period (0.84 ± 0.76) than in the 3N middle training period (0.54 ± 0.43; 95% CI[0.29 1.02], $p = 8.4 \times 10^{-7}$) and in the 7N middle training period (0.32 ± 0.22; 95% CI[0.72 1.46], $p = 9.76 \times 10^{-20}$). Moreover, there was greater force exerted in the 3N middle training period than the 7N middle training period (95% CI[0.12 0.98], p=0.002). Peak force was overall significantly different between the 0N and 3N conditions (95% CI[0.37 1.23], $p = 3.28 \times 10^{-7}$), the 0N and 7N conditions (95% CI[0.92 1.79], $p = 3.31 \times 10^{-22}$), and the 3N and 7N conditions (95% CI[0.12 0.98], p=0.002). Further testing revealed that the peak force was specifically greater during the middle training period than the early training period (95% CI[-1.3 -0.89], $p = 8.86 \times 10^{-9}$) but there was no significant difference in peak force between the middle and late training period.

Table 1. Mean and Standard Error for Actual Force Throughout Training

		Early	Middle	Late
Control	Pre-150ms	0.42 ± 0.34	1.21 ± 0.16	1.21± 0.17
	Peak	1.11 ± 0.4	2.36 ± 0.23	2.65 ± 0.23
	Post-150ms	0.7 ± 0.28	1.42 ± 0.18	1.73 ± 0.17
3N	Pre-150ms	0.38 ± 0.09	0.78 ± 0.09	0.91 ± 0.12
	Peak	0.69 ± 0.10	1.40 ± 0.12	1.94 ± 0.16
	Post-150ms	0.35 ± 0.10	0.85 ± 0.11	1.10 ± 0.13
7N	Pre-150ms	0.33 ± 0.09	0.51 ± 0.08	0.65 ± 0.12
	Peak	0.29 ± 0.08	0.71 ± 0.10	1.02 ± 0.11
	Post-150ms	0.26 ± 0.10	0.49 ± 0.10	0.66 ± 0.10

Mean ± standard error of the actual force at different periods in training (early, middle and late) and at different force windows (at peak velocity, and 150 ms before and after peak velocity) within each noise condition.

During the early training period (Fig. 4, left column), there was a significant effect of noise group on average force profile (2-way ANOVA, F(2,179)=3.69, p=0.03, η^2 =0.04), but the force window did not have a significant effect (2-way ANOVA, F(2,179) = 0.94, p=0.5, η^2 =0.01). There was no significant interaction effect between the two factors (2-way ANOVA, F(4,179)= 0.89, p=0.5, η^2 =0.02). Thus, regardless of temporal force window, as the magnitude of noise increased during the early training period, the average force profile decreased (Control: 0.34 ± 0.21, 3N: 0.29 ± 0.06, and 7N: 0.17 ±0.06).

During the middle training period (Fig. 4, middle column), there was a significant effect of temporal force window (2-way ANOVA, F(2,170) = 19.56, p=2.47x10^{-8},η^2 = 0.13) and noise level (2-way ANOVA, F(2,170)=45.21, p=2.5x10^{-16}, η^2 =0.3) on the average force profile. Therefore,

noise level affected specific temporal force windows. There was a significant interaction effect between the two factors (2-way ANOVA, F(4,170) = 3.05, p= 0.02, $\eta^2 = 0.04$), which we further explored by looking at each noise level (see Table 1) and by conducting a post-hoc test. Post-hoc Tukey-HSD tests revealed that the 0N condition had a greater amount of peak force (2.35$\pm$1.02) than the 3N condition (1.4$\pm$0.54; 95% CI[0.34 1.57], p =4.64x10^{-5}) and the 7N condition (0.7$\pm$0.46; 95% CI[1.03 2.27], p=2.15x10^{-15}). Additionally, the 3N condition had a significantly greater amount of peak force than the 7N condition (95% CI[0.09 1.3], p=0.01). With this, we demonstrate that as the magnitude of noise increased during the middle training period, the average force profile decreased, and this variation was modulated throughout the force profile (see Table 1).

During the late training period (Fig. 4, right column), there was also a significant effect of both temporal force window (2-way ANOVA, F(2,179) = 32, p=1.57x10^{-12}, η^2 =0.2) and noise level (2-way ANOVA, F(2,179) = 38.76, p=1.31x10^{-14}, η^2 =0.24) on the average force profile. Thus, noise level affected specific temporal force windows. There was a significant interaction effect between the two factors (2-way ANOVA, F(4,179)=3.33, p=0.01, η^2 =0.04). Post-hoc Tukey-HSD tests revealed that the 0N condition had a greater peak force (2.65$\pm$1.03) than the 3N condition (1.94$\pm$0.7; 95% CI[0.05 1.38], p=0.02) and the 7N condition (1.02$\pm$0.5; 95% CI[0.97 2.3], p =3.81x10^{-13}). Moreover, the 3N condition had a significantly greater peak force than the 7N condition (95% CI[0.26 1.58], p=0.001). Similar to the middle of the training period, this suggests that as the magnitude of noise increased during the late training period, the average force profiled decreased and that this difference changed throughout the force profile (see Table 1).

Overall, these results support the previous finding that increasing the magnitude of externally-generated noise impairs adaptation to the force-field perturbation. Across all training windows, higher magnitudes of noise significantly reduced the force profiles, especially during peak movement velocity.

Added motor noise affects the fast learning process underlying motor adaptation

We hypothesized that increasing the externally-applied motor noise magnitude impaired adaptation by specifically affecting the fast-learning process while the slow-learning process remained largely unaffected. This can be attributed to the fast learning process, due to it having greater influence during early adaptation. Thus, the impairment of the initial steep increase in adaptation (Fig. 3) suggests that the fast-learning process is impaired by the increase in motor noise magnitude.

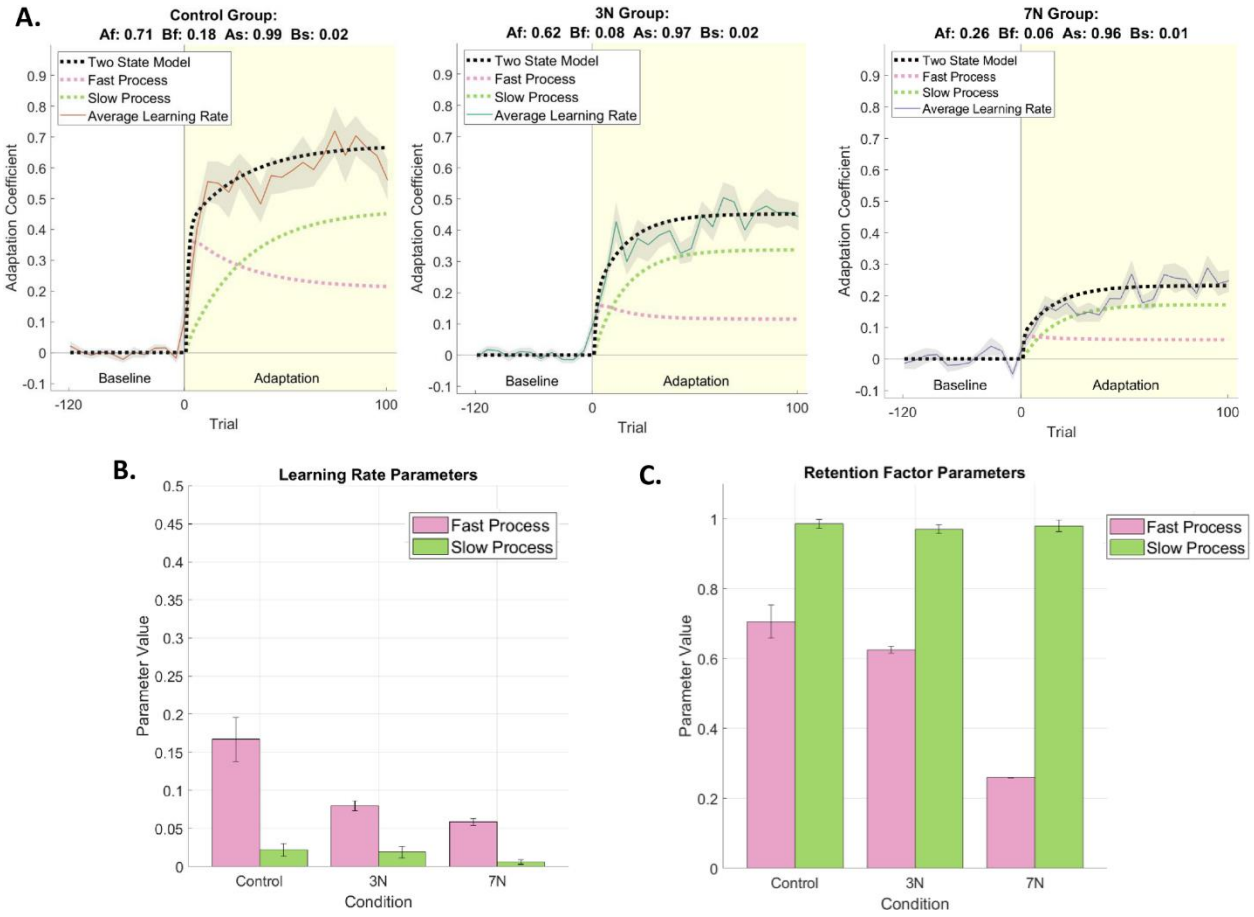

Figure 5. Two-state model results. (A) The overall adaptation (black trace), fast process (pink trace) and slow process (green trace) are shown for the three conditions (orange: control group with no added noise, green: 3N of added motor noise, purple: 7N of added motor noise).

Colored traces represent the mean adaptation coefficient and gray shading represents SEM. Best fit model coefficients are stated at the top of each graph. As noise magnitude increases, the learning rate for the fast process (B_f) decreases while the learning rate for the slow process (B_s) remains relatively unimpaired. (B) Learning rate parameters for each condition. As noise magnitude increases, the fast learning process rate decreases while the slow learning process rate remains relatively unimpaired. (C) Retention factor parameters for each condition. Retention for the fast learning process decreases as noise magnitude increases. However, retention in the slow learning process appears unaffected by the addition of motor noise. Error bars represent the 95% confidence intervals.

To test this hypothesis, we applied the two-state model to our data (Fig. 5A). In Figure 5, the overall adaptation rate for each group is represented by a solid black line (95% confidence intervals, Control [0.66 0.71], 3N[0.38 0.42], 7N[0.18 0.23]). The slow process learning rate, indicated by the dotted green line in Figure 5A, is relatively unimpaired across conditions (Parameter values for slow learning rate across groups, Control B_s:0.02, 3N B_s: 0.02, 7N B_s: 0.01; 95% confidence intervals, Control B_s[0.01 0.03], 3N B_s[0.01, 0.03], 7N B_s[0.003 0.01]) (Fig. 5B). Additionally, the retention rates for the slow process (Fig. 5C) are unchanged (Control:A_s= 0.99, 3N: A_s= 0.97, 7N: A_s= 0.96; 95% confidence intervals, Control:A_s[0.97 1.0], 3N:A_s[0.96 0.98], $7N$: A_s[0.96 1.0]. Conversely, the fast process learning rate, indicated by the dotted pink line in Figure 5A, is impaired by increasing motor noise magnitude (Control B_f: 0.18, 3N B_f: 0.08, 7N B_f: 0.06; 95% confidence intervals, Control B_f[0.14 0.2], 3N B_f[0.07 0.09], 7N B_f[0.05 0.06]). These modeling results are summarized in Figure 5B and Table 2. Thus, application of the two-state model confirms that increasing the magnitude of externally-applied motor noise impairs adaptation specifically by influencing the fast learning process (pink bars in Fig. 5) while the slow learning process remains relatively unaffected (green bars in Fig. 5).

Table 2. 95% Confidence Intervals for Two-State Model Parameters

	A_f 95% CI	A_s 95% CI	B_f 95% CI	B_s 95% CI
Control Group	**[0.66 0.75]**	**[0.97 1.0]**	**[0.14 0.20]**	**[0.01 0.03]**
3N Group	**[0.61 0.63]**	**[0.96 0.98]**	**[0.07 0.09]**	**[0.01 0.03]**
7N Group	**[0.26 0.26]**	**[0.96 0.99]**	**[0.05 0.06]**	**[0.003 0.01]**

Added motor noise does not affect short-term retention of motor adaptation

We next examined the extent to which retention was affected by increasing motor noise magnitude, as measured by the one-minute delay probe during the retention block of the experiment (see Methods). One of the benefits of applying the two-state model to our results is the predictions we can make about behavior under different conditions. A prediction of a systematically impaired fast-learning process (with the increase in noise) is that we should observe less of a decrease in overall learning over a one-minute hold period. This is due to the fast-learning process decaying with time while the slow-learning process maintains learning amounts well with the passage of time. Thus, by examining the difference in the learning amount before and immediately following the one-minute delay we can indirectly assess changes in the fast-learning process. During the one-minute delay, we expected that adaptation would rapidly decay by a set amount due to the time-dependence of the fast process. Thus, during the error-clamp trial following the delay period, we could isolate the amount of adaptation that was retained due to the (relative) time-independence of the slow process. Figure 6A shows the adaptation coefficient before and after the one-minute delay for each subject group. There was a significant difference in the amount of adaptation between the end of the re-training period and the amount of adaptation after the 1-minute delay period (2-way ANOVA, $F(1,119) = 119.23$, $p = 1.97 \times 10^{-19}$, $\eta^2 = 0.44$) that was significantly different across motor noise conditions ($F(2,119) = 12.1$, $p = 1.71 \times 10^{-5}$, $\eta^2 = 0.09$). These results suggest that there was a significant amount of decay between the end of the re-training period and the decay period and that this was true across noise

levels. There was also a significant interaction effect between these two factors (F(2, 119) = 6.32, p = 0.003, η^2 =0.05). A post-hoc Tukey-HSD test confirmed that there is no significant difference between the amount of adaptation during the one-minute delay between the control group and the 3N group (p> 0.05). However, there is a significant difference between the control group and 7N group (p=0.03) as well as the 3N group and 7N group (p=0.01). We do see that the mean difference over the one-minute hold period is in fact decreasing with noise level (0.45 ± 0.05, 0.26 ± 0.03 and 0.1 ± 0.02, for 0, 3 and 7N respectively)—there is less of the fast-learning process to decay with the increase in noise. Importantly, based on the model predictions, this difference should be minimal because the contributions of the fast-learning process at asymptotic learning should be small compared to the slow-learning process. That is, our intent was not to determine if there were significant differences between the subject groups, but rather to confirm that there is very little difference because the decay over the hold period is largely caused by the fast-learning process.

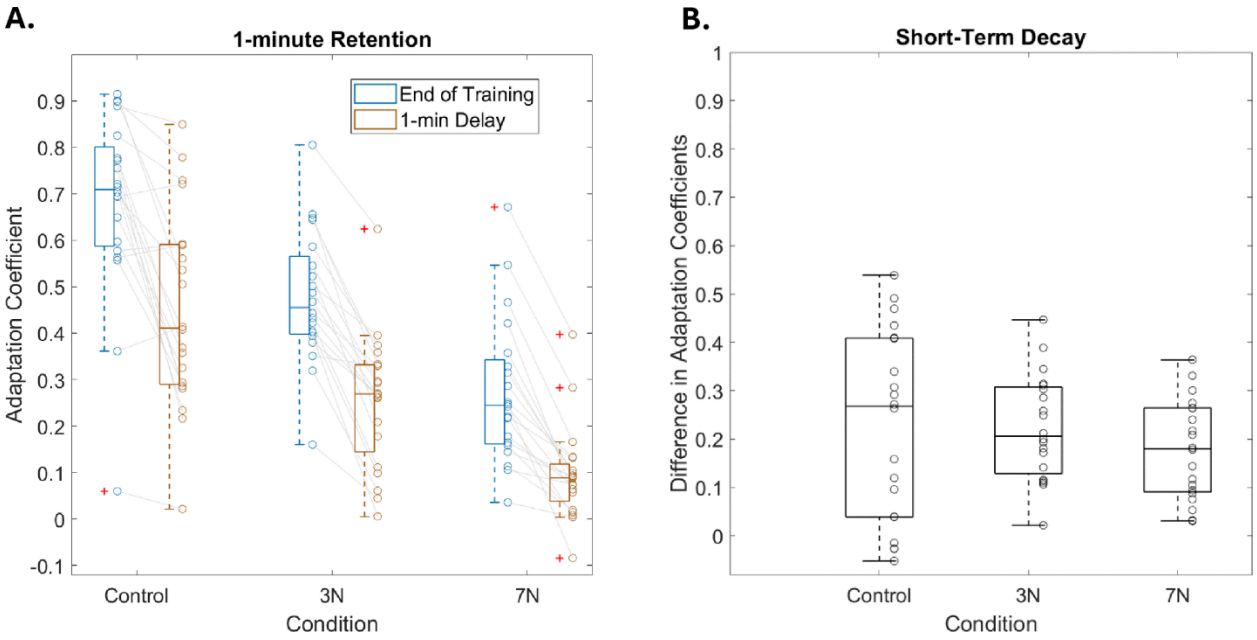

Figure 6. Retention of adaptation. During the retention probe, participants were initially re-exposed to the force-field movements, which was followed by error-clamp trials. (A) The

average adaptation coefficients on these trials (blue box plots and circles) were compared to the average adaptation coefficients on the retention trials which followed a one-minute delay period (red box plots and circles). Each unfilled circle represents the results for one subject. (B) Amount of short-term decay (the difference between the amount of adaptation at the end of training and after the 1-minute delay period) for each condition.

Next, we determined if there was a significant difference in the amount of decay across noise conditions. We were interested in the amount of decrease in learning over the one-minute delay. Since the two-state model predicted that a decrease in the overall learning over a one-minute hold period should be attributed to the fast-learning process, we plotted the difference in the adaptation coefficient before and immediately after the delay period. We wanted to determine if this decrease was roughly equivalent between groups despite there being significant differences in the level of adaptation before the delay. As reflected in Figure 6B, there was not a difference in the short-term retention of adaptation (difference before and after the one-minute delay) (control: 0.23$\pm$0.04, 3N: 0.22$\pm$0.02, 7N: 0.18$\pm$0.02). We found that the amount of reduction in the adaptation over the one-minute delay was not significantly different across conditions (one-way ANOVA, F(2,59)= 0.75, p= 0.5, η^2 =0.03). By examining the delta, we can postulate that the slow-learning process is largely unaffected; even though the learning amount before the delay is different across the three conditions, the drop over the one-minute hold is comparable, suggesting learning is decaying to the level achieved by the slow-learning process in each respective group. A Mann-Whitney U-Test showed that the control group (Mean±SE: 0.23±0.04) did not have significantly different decay from the 3N group (0.22±0.02), z = 0.07, p=0.95, nor the 7N group (0.18±0.02), z=0.83, p=0.41. Additionally, the 3N group and 7N did not have significantly different decay (Mann-Whitney U-Test, z=1.26, p=0.21). The similarities in the reduction suggest that increasing motor noise magnitude does not significantly impair the short-term retention of adaptation.

Added motor noise does not affect the decay of motor learning

In addition to retention, we also investigated the effect of motor noise on the decay of adaptation. Figure 7A shows the non-normalized decay curves, which have different starting adaptation coefficient percentages due to the previous impairment to learning based on noise condition (Fig. 3). To better compare the decay rate of each group, we normalized the decay curves (Fig. 7B). Figure 7A displays the raw adaptation coefficient and Figure 7B displays the adaptation coefficient as a percentage of the value at the end of training.

Figure 7B shows the normalized adaptation coefficient percentage over consecutive error clamp trials in the decay period (see Methods). During the decay block, participants were exposed to 80 consecutive EC trials in which lateral movement was restricted, allowing for the adapted movement to return to baseline. To best determine which exponential fit model would best capture the rate of decay, we performed an Akaike Information Criterion (AIC) test with a single-phase and a two-phase exponential model. Based on the results of the AIC, we determined that a two-phase exponential fit would best capture the rate of decay:

$$y = Ae^{bx} + Ce^{dx} \qquad \textbf{(Equation 10)}$$

This two-phase model assumes that the rate of decrease is the result of a fast ($y = Ae^{bx}$) and slow ($y = Ce^{dx}$) exponential decay, both of which are concurrent throughout the decay period (See Fig. 7D). For the fast decay process, the Control, 3N and 7N groups had similar decay rates (Control: b_{control} = -0.19, 95% CI [-0.23 -0.14], R^2 =0.98; 3N: b_{3N} = -0.32 95% CI [-0.38 -0.26], R^2 = 0.97; 7N: b_{7N} = -0.36, 95% CI [-0.45 -0.26], R^2 = 0.93), though the confidence intervals for the control group decay rates did not overlap those of the 3N or 7N groups. For the slow decay process, there were similar decay rates across groups (Control: d_{control} = -0.01, 95% CI [-0.02 -

0.005]; 3N: d_{3N} = -0.008, 95% CI [-0.01 -0.005]; 7N: d_{7N} = -0.004, 95% CI [-0.01 0.002]). Regardless of the varying levels of noise introduced, it's important to note that the 95% confidence intervals for all decay rates overlap.

To better understand how the average adaptation coefficients differed at specific time periods of decay, we examined the average adaptation coefficient as a percentage of the value at the end of training from the first 10% of decay trials (early trials), the middle 10% (middle trials), and last 10% (late trials), (Fig. 7C,D). A 2-way ANOVA demonstrated that there was not a significant difference in adaptation between motor noise groups (2-way ANOVA, F(2,35) = 0.84, p = 0.44, η^2 =0.01) but there was a significant difference in adaptation during different temporal windows during decay (F(2, 35) = 102.07, p = 2.56x10^{-13}, η^2 =0.87), as one would expect. This observation suggests that decay rates following adaptation are relatively resistant to added motor noise.

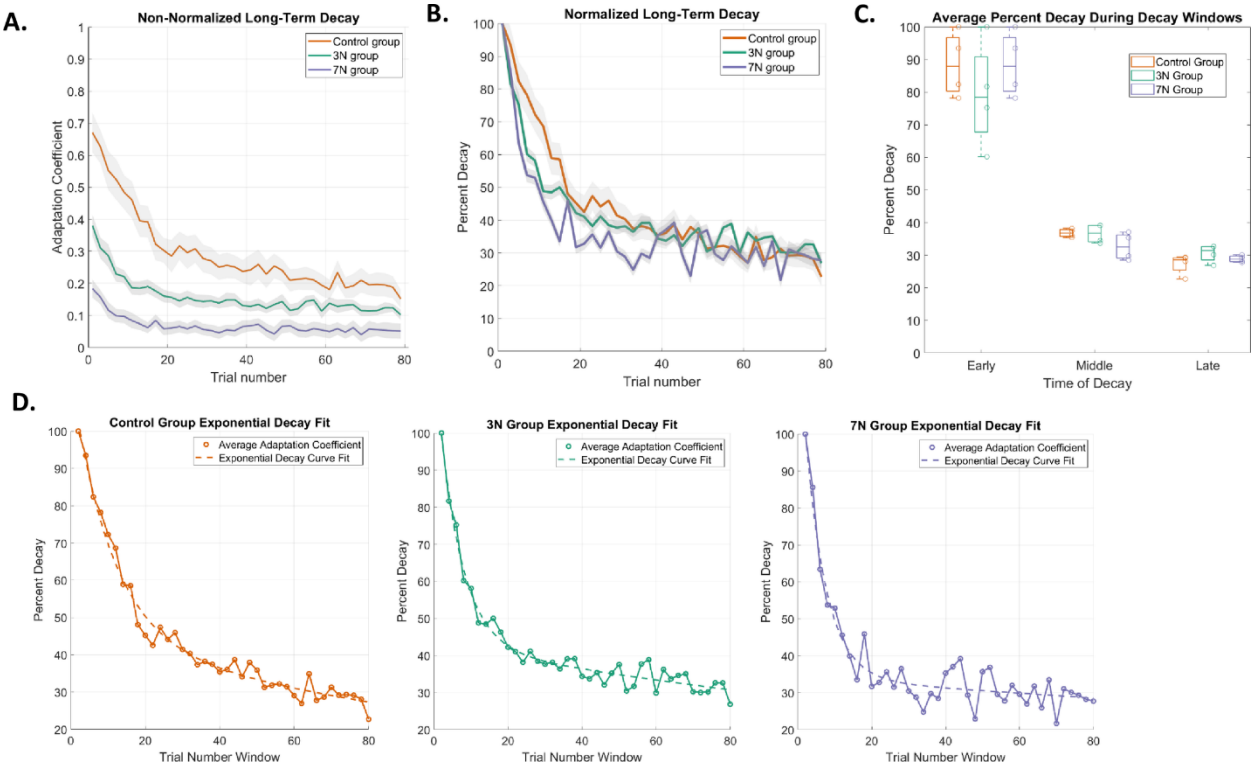

Figure 7. Decay of adaptation. (A) Non-normalized decay of adaptation, quantified by the raw adaptation coefficient, is plotted as a function of trial number for each condition (control: orange

trace, 3N: green trace, 7N: blue trace) during the decay probe block. Colored traces represent the mean adaptation coefficient and gray shading represents SEM. (B) The normalized decay curves, quantified by the adaptation coefficient as a percentage of the value at the end of training, demonstrate that decay rates are similar across groups. The curves were normalized by dividing the average adaptation coefficient of each trial by the average adaptation coefficient for each subject during the first trial of the decay period. (C) Box plots of the average adaptation coefficient for each condition during early, middle, and late periods of decay for each group. Each unfilled circle represents the results for one subject. (D) Two-phase exponential decay fit, $Ae^{bx} + Ce^{dx}$, for each condition is shown: Control: $70.91e^{-0.18x} + 44.08e^{-0.01x}$($R^2_{control}$ = 0.98);3N: $78.61e^{-0.32x} + 42.8e^{-0.009x}$ (R^2_{3N} = 0.97); 7N: $96.38e^{-0.36x} + 34.17e^{-0.004x}$ (R^2_{7N} = 0.93). Adaptation coefficient is shown as a percentage of the value at the end of training.

DISCUSSION

In this study, we sought to understand the underlying mechanisms and timescales by which externally-applied motor noise impairs the initial motor adaptation, and the retention and decay of the learning. We hypothesized that this noise impacts the learning rate specifically through the fast learning process of the two-state modeling framework used to capture short-term motor adaptation. To test this, we utilized an established motor adaptation paradigm in which participants made arm reaching movements between two targets and had to adapt to lateral perturbations (a velocity-dependent force-field) in addition to externally-applied motor noise. The participants were divided into three separate groups, in which artificial motor noise was applied at either 3N or 7N, compared to a control group that did not experience the motor noise. We found that as the magnitude of motor noise increased, the overall learning rate decreased. Applying the two-state model revealed that this overall decrease in adaptation could be explained by impairments to the fast learning process while the slow learning process remained relatively unimpaired. In addition, the applied motor noise had little effect on the retention and decay of adaptation—behavioral aspects that mainly involve the slow learning process.

Motor noise affects different processes underlying adaptation

The slow learning process has been shown to be largely responsible for both the overall decay and 24-hour retention of motor adaptation (Smith et al. 2006; Joiner and Smith, 2008; Wolpert et al. 2011; Albert and Shadmehr, 2018; Sarwary et al. 2018; Alhussein et al. 2019). Thus, based on our hypothesis that noise impacts the learning rate specifically through the fast learning process, we expected to observe no significant differences in the retention of adaptation across levels of motor noise magnitude. While initial findings appeared to suggest that retention was impacted by the motor noise (Fig. 6A), similarities in the overall reduction of adaptation over the one-minute delay revealed that the retention was relatively unaffected by increasing motor noise magnitude (Fig. 6B). Observing no significant differences in the reduction of adaptation between

conditions was also confirmed by the two-state model; the slow-learning process (the main component of long-term retention of learning (Joiner and Smith, 2008) was not modulated by motor noise magnitude (Fig. 5).

The fast learning process has previously been shown to quickly respond to movement errors (Smith et al. 2006; Joiner and Smith, 2008; Shadmehr and Mussa-Ivaldi, 2010; Wolpert et al. 2011; Albert and Shadmehr, 2018; Sarwary et al. 2018; Coltman et al. 2019). In theory the more variability in the error, the more impairment there will be in determining the appropriate recalibration of the motor output due to increased uncertainty. Our results suggest that it is the fast learning process that is impaired by the noise added to the force-field perturbation. This increase in uncertainty of the movement disruption may be captured by predictive models, such as the impaired learning rate parameter captured in the two-state model (Figure 5). Increasing uncertainty can impair the ability of predictive models to capture learning. Increasing noise, a source of uncertainty, lowers the signal-to-noise ratio, which may influence the model to learn less from the error and more from the noise, which we see with the impaired learning curves of the 3N and 7N groups (Figure 3). With noise distracting the modeling process from accurately learning from the error signal, or in the current case, the lateral perturbation, we impair subsequent state estimations from being able to accurately predict and adapt to the error. Thus, resulting in poorer sensorimotor adaptation over the course of trials. We see this reflected in Figure 3 adaptation coefficient learning curves demonstrating poorer adaptation for high noise groups. As the fast process must quickly respond to changes in sensory information, such as a change in force between the previous and current trial, the model's extraction of fast process learning parameters might learn more from the noise, rather than the lateral perturbation, because the model doesn't distinguish between these sources of error when making estimations. This could ultimately make it difficult to accurately estimate the current state and lead to impaired learning (the suboptimal behavior as we observe here for the 3N and 7N groups).

The current two-state model treats error as a constant, though real-world motor errors are often “noisy” and have diverse characteristics (e.g., temporal, spatial, etc.). Our results demonstrate that increasing the magnitude of motor noise, or rather manipulating a specific characteristic of the noise, impairs motor adaptation by impacting the fast process’s temporal sensitivity to the error while the slow learning process remains relatively intact. When faced with noisy error, the fast learning process’s contribution may be reduced. Perhaps, this can be due to the fast process having noise-induced gain control and, as an effect, diminishes the slow process. It is clear that early in the learning curve (where the fast process contributes the most to overall adaptation) the initial steep, immediate increase in the learning rate is most reduced as the magnitude of motor noise increases (Fig. 3). According to the feedforward model described in Wolpert et al. (1994), increasing the noise, or uncertainty, of the sensory input will result in a decrease in relying on sensory information to predict optimal motor output. This instead leads to a reliance on the feedforward prediction. As shown in Figure 5, by increasing the noise level of the robotic manipulandum, there is a decrease in the fast-learning process, which compared to the slow process, is relatively more sensitive to changes in incoming sensory information. Thus, our study provides an initial step into utilizing the two-state framework to understand how underlying mechanisms of adaptation are impacted by noisy motor errors. Overall, our study provides an initial step into utilizing the two-state framework to understand how underlying mechanisms of adaptation are impacted by noisy motor errors. In doing so, we set the foundation to update the two-state model framework’s treatment of error as a constant to its more realistic “noisy” presence.

While previous studies (Smith et al. 2006; Joiner and Smith, 2008) have demonstrated the predictive power of the two-state model, there is currently no biological basis for the fast and slow learning processes. McDougle et al. (2015) sought to better understand what mechanisms constitute the fast and slow learning processes and proposed that implicit learning may be closely associated with the slow learning process and explicit learning may approximate the fast learning

process. Both the fast learning process and explicit learning occur during the early phase of motor learning. Doyon and Ungerleider (2002) proposed that cortico-striatal and cortico-cerebellar circuits have increased functional activity during the early phase of motor learning, which has been supported by both behavioral and clinical studies (Doyon and Benali, 2005). Indeed, early phases of motor learning, particularly explicit learning through trial-and-error, have been found to be associated with regions of the dorsolateral prefrontal cortex, as well as the cerebellum (Halsband and Lange, 2006). This aligns with previous studies of motor adaptation; online motor corrections and error feedback is largely attributed to contributions from the cerebellum (Wolpert et al. 1998; Bastian, 2006; Tseng et al. 2007; Schlerf et al. 2012; Popa and Ebner, 2018; Tzvi et al. 2022). Regions of the brain that filter noise to allow for goal-directed adaptation appear to overlap, as prefrontal cortex-basal ganglia-thalamic pathways have been demonstrated to help select between relevant and non-relevant stimuli (Wimmer et al. 2015; Marton et al. 2018; Nakajima et al. 2019; Waschke et al. 2021; Synch et al. 2022). Additionally, the cerebellum has been suggested to play the role of an adaptive filter during online error correction during movement, which involves sorting through sensorimotor noise (Fujita, 1982; Medina and Lisberger, 2007; Requarth and Sawtell, 2011). Thus, the overlap between the brain regions involved in early motor learning and those responsible for filtering sensorimotor noise may play a role in the current results. Specifically, the application of motor noise impairs the fast learning process, which has the most influence during the early phase of adaptation to the velocity-dependent force field. Our behavioral results suggesting that increasing noise specifically impairs the fast learning process implicates that perhaps this could be due to interference with the cortico-striatal (Doyon and Ungerleider, 2002; Doyon and Benali, 2005; Wimmer et al. 2015; Marton et al. 2018; Nakajima et al. 2019; Waschke et al. 2021; Synch et al. 2022) and cortico-cerebellar (Fujita, 1982; Wolpert et al. 1998; Bastian, 2006; Halsband and Lange 2006; Medina and Lisberger, 2007; Tseng et al. 2007; Requarth and Sawtell, 2011; Schlerf et al. 2012; Popa and Ebner, 2018; Tzvi et al. 2022) circuitry during the initial phase of adaptation. However, these

theories are likely a broad interpretation of a complicated network. Further studies examining these relationships are needed to better understand what neural networks are responsible for these different learning processes and the extent these neural mechanisms are also involved in compensating for different noise sources and characteristics.

Implications for impaired learning in different clinical populations

Tremor—the involuntary, rhythmical movement of the body (Deuschl et al. 2001; Elble, 2017)—is a type of noise that is present during both the preparation of movement as well as its execution. Externally-generated tremor is induced when a source outside the organism causes involuntary shaking movements of any part of the body (e.g., an electric toothbrush). Conversely, internally-generated tremor is induced when a source from within the organism results in involuntary, oscillatory movements (e.g., the pathological tremor observed in Essential Tremor, ET). Tremor is an example of noise that can be directly measured in terms of its source, magnitude, and frequency. Similar to other examples of noise, tremor has been shown to impair motor learning and control (Lakie et al. 1995; Kronenbuerger et al. 2007; Shill et al. 2009; Lakir, 2010; Hanajima et al. 2016; Alty et al. 2017; Lopez-de-Ipina et al. 2021; Bindel et al. 2022). For example, Shill et al. (2009) utilized a classical eyeblink conditioning paradigm to compare healthy control participants with ET patients. During the first block of the task, they found that motor learning was impaired by 55.6% in ET patients compared to controls and this impairment was sustained throughout the entirety of the task. While it is established that tremor-dominant movement disorders have impaired motor learning, the characteristics of tremor and their impact on the underlying components of motor learning, including adaptation, are not well quantified. However, the literature shows that ET frequency ranges between 5-10 Hz accompanied by large amplitudes (Louis, 2005; Jankovic, 2008), which we used to inform our noise characteristics. To better understand how variability in internally-generated error, such as tremor, impacts patients with movement disorders, we first had to establish how variability in error impacts healthy

subjects. This study provides a foundation for understanding how increasing the magnitude of tremor impacts specific underlying mechanisms of motor learning in healthy subjects, demonstrating that varying specific characteristics of noise, such as magnitude of tremor and tremor source, affects motor learning by impairing the fast learning process. If internally-generated tremor in disease models plays a role in impairing motor learning, we would expect that it would do so through similar means.

Internally-generated tremor, such as the pathological tremor seen in movement disorders, has also been shown to impair motor adaptation. Patients with Essential Tremor (ET), a neurological condition hallmarked by persistent tremor, are known to have impaired motor adaptation and skill acquisition. Challenges in balance, movement, and postural stability (Rao et al. 2006; Heldman et al. 2011) can lead to difficulties in self-agency and daily living (Lorenz et al. 2006; Anderson et al. 2007). The observed deficits in ET have been suggested to be attributed to the cortico-thalamo-cortical loop in addition to the cerebello-thalamo-cortical pathway (Fasano et al. 2010). The disruption of brain circuits involved in ET are located primarily in the cerebellar cortex (Welton et al. 2021), which is known to govern balance and movement control (Morton and Bastian, 2004). As previously mentioned, increased activity in the cortex, thalamus, and cerebellum is implicated in the early phases of motor learning (and, by association, possibly the fast learning process) as well as the selection of relevant information from sensory noise. It is possible that the same neural mechanisms that are disrupted in ET also contribute to the fast learning process impairment during adaptation to externally-generated noise. Deep brain stimulation of the thalamus, which relays sensorimotor information from the cerebral cortex to other motor regions within the brain, has been shown to reduce deficits, such as postural stability and tremor severity in ET patients (Wong et al. 2020). In a study by Bindel et al. (2022), initial motor learning was impaired in ET patients compared to healthy controls, but de-adaptation rates between the two groups were similar, suggesting that retention is unimpaired in ET motor learning. These results are aligned with the current findings that motor noise mainly affects the fast learning processes.

A major responsibility of the motor system is determining the source of movement errors to correctly recalibrate motor output (Scheidt et al. 2001; Joiner and Shelhamer, 2006; Berniker and Kording, 2008; Wei and Kording, 2009; Dam et al. 2013; Berniker et al. 2014; Kong et al. 2017). For example, when failing to push open a heavy door, the motor system must determine where the error originated. Is this due to the door itself (is it heavier than assumed?) or is this due to not pushing hard enough (is the exerted force less than assumed?). The motor system relies heavily on integrating information from multiple sensory systems to determine the error source (Ernst, 2006; Kording et al. 2007). It is thought that this is accomplished through reliance on the temporal characteristics of sensory changes to determine if error should be attributed to internal-generated or externally-based sources. In general, if sensory changes occur gradually over time, the source of error is attributed to the self (Fercho and Baugh, 2014). However, if sensory changes occur quickly, the source of error is often attributed to the external environment (Fercho and Baugh, 2014). After determining the error's source, the motor learning system can adapt/recalibrate motor output to achieve a desired outcome. Thus, if the door remains hard to open after several tries (over time), one might adjust how hard they are pushing on it.

Based on this difference in credit assignment, it is possible that the addition of the externally-applied motor noise may interfere with error attribution in a different way than internally-generated tremor. Further research is needed in these tremor-dominant movement disorder populations to compare the impact of internally-generated tremor in patients versus externally-applied motor noise in healthy control. Developing a more comprehensive understanding of the precise aspects of motor learning that are impaired in different movement disorder populations will assist in identifying possible treatment strategies and clinical assessments for specific motor learning deficits (Doyon, 2008; Nieuwboer et al. 2009).

Possible Limitations

With higher levels of motor noise, such as in the 7N condition, participants must use greater amounts of force to correct their reaching movement. Over time, this use of force may lead to fatigue. In our study, participants were given the opportunity to rest in between experiment blocks, which has been shown to decrease the impact of fatigue on performance (Verhoeven and Newell, 2018). There is also an immediate separation of learning rate performance early on during the training blocks between groups. If fatigue was the sole factor in explaining our results, it is likely we would largely see the largest difference and/or a decrease in learning rate during the later trials during training. The observation that this was not the case suggests that it is unlikely that fatigue significantly contributed to the observed differences between groups.

Additionally, based on our experiments, we can conclude that the applied noise impaired the ability to learn the required temporal pattern of force, but we cannot determine directly if this was the result of co-contraction. During FF trials, it is likely participants co-contracted to counteract the lateral perturbation (Franklin et al. 2003; Milner and Franklin, 2005). However, we relied on measurements from subsequent EC trials (which did not contain the lateral perturbation) to quantify the ability to adapt to previous FF trials. It is unclear if participants continued this co-contraction during EC trials without the presence of the perturbation, as muscle activation patterns tend to differ in changing environments (Osu et al. 2003). As the purpose of our current study was to determine the extent participants compensated to the standard movement perturbation (i.e., the force-field (FF) perturbation) with added levels of applied noise, we aim to investigate this possibility in future experiments.

In our study, we used the applied motor noise to examine the possible effects of externally-generated tremor on motor learning. However, it is difficult to extrapolate these findings directly to other noise sources (e.g., internally-generated tremor due to brain disorders). Thus, even though it provides valuable insight into how the nervous system handles increasing noise during adaptation to error, we should note that the externally-applied motor noise in the current study may have limitations in the generality to patient populations. For example, it is currently unclear

how physiologically relevant 3N and 7N of noise magnitude compares to pathologic tremor (Elble, 1986; Calzetti et al. 1987; Elble et al. 2006; Deuschl et al. 2022). Though, through our findings, we can now understand that when magnitude of noise increases, ability to adapt decreases, which can then be tested in the context of ET. The frequency (10Hz), which was standard across conditions, is most closely related to the tremor frequency experienced by patients with ET, whose tremor tends to range from 5-10 Hz (Louis, 2005; Jankovic, 2008). Overall, we aimed to model the general manifestation of a single characteristic of pathological tremor, which is typically described as high amplitude (Elble, 1986; Calzetti et al. 1987). Through this experiment, we provide preliminary evidence that increasing the magnitude of externally-generated tremor affects motor adaptation specifically by impairing the fast-learning process. Future studies will aim to investigate how changing other characteristics of tremor, such as frequency and source, influence specific underlying characteristics of motor learning and control.

REFERENCES

Agarwal, S., & Biagioni, M. C. (2018). Essential tremor.

Akaike, H. (1998). Information theory and an extension of the maximum likelihood principle. In Selected papers of hirotugu akaike (pp. 199-213). New York, NY: Springer New York.

Albert, S. T., & Shadmehr, R. (2018). Estimating properties of the fast and slow adaptive processes during sensorimotor adaptation. *Journal of neurophysiology*, *119*(4), 1367-1393.

Alhussein, L., Hosseini, E. A., Nguyen, K. P., Smith, M. A., & Joiner, W. M. (2019). Dissociating effects of error size, training duration, and amount of adaptation on the ability to retain motor memories. *Journal of Neurophysiology*, *122*(5), 2027-2042.

Alty, J., Cosgrove, J., Thorpe, D., & Kempster, P. (2017). How to use pen and paper tasks to aid tremor diagnosis in the clinic. *Practical Neurology*, *17*(6), 456-463.

Anderson, K. E., Gruber-Baldini, A. L., Vaughan, C. G., Reich, S. G., Fishman, P. S., Weiner, W. J., & Shulman, L. M. (2007). Impact of psychogenic movement disorders versus Parkinson's on disability, quality of life, and psychopathology. *Movement disorders: official journal of the Movement Disorder Society*, *22*(15), 2204-2209.

Bastian, A. J. (2006). Learning to predict the future: the cerebellum adapts feedforward movement control. *Current opinion in neurobiology*, *16*(6), 645-649.

Berniker, M., & Kording, K. (2008). Estimating the sources of motor errors for adaptation and generalization. *Nature neuroscience*, *11*(12), 1454-1461.

Berniker, M., Mirzaei, H., & Kording, K. P. (2014). The effects of training breadth on motor generalization. *Journal of neurophysiology*, *112*(11), 2791-2798.

Bindel, L., Mühlberg, C., Pfeiffer, V., Nitschke, M., Müller, A., Wegscheider, M., ... & Tzvi, E. (2023). Visuomotor adaptation deficits in patients with essential tremor. *The Cerebellum*, *22*(5), 925-937.

Butcher, P. A., Ivry, R. B., Kuo, S. H., Rydz, D., Krakauer, J. W., & Taylor, J. A. (2017). The cerebellum does more than sensory prediction error-based learning in sensorimotor adaptation tasks. *Journal of neurophysiology*, *118*(3), 1622-1636.

Calzetti, S., Baratti, M. A. R. I. O., Gresty, M., & Findley, L. E. S. L. I. E. (1987). Frequency/amplitude characteristics of postural tremor of the hands in a population of patients with bilateral essential tremor: implications for the classification and mechanism of essential tremor. *Journal of Neurology, Neurosurgery & Psychiatry*, *50*(5), 561-567.

Coltman, S. K., Cashaback, J. G., & Gribble, P. L. (2019). Both fast and slow learning processes contribute to savings following sensorimotor adaptation. *Journal of neurophysiology*, *121*(4), 1575-1583.

Conditt, M. A., Gandolfo, F., & Mussa-Ivaldi, F. A. (1997). The motor system does not learn the dynamics of the arm by rote memorization of past experience. *Journal of Neurophysiology*, *78*(1), 554-560.

Conditt, M. A., & Mussa-Ivaldi, F. A. (1999). Central representation of time during motor learning. *Proceedings of the National Academy of Sciences*, *96*(20), 11625-11630.

Dam, G., Kording, K., & Wei, K. (2013). Credit assignment during movement reinforcement learning. *PLoS One*, *8*(2), e55352.

Deuschl, G., Becktepe, J. S., Dirkx, M., Haubenberger, D., Hassan, A., Helmich, R. C., ... & Elble, R. J. (2022). The clinical and electrophysiological investigation of tremor. *Clinical Neurophysiology*, *136*, 93-129.

Deuschl, G., Raethjen, J., Lindemann, M., & Krack, P. (2001). The pathophysiology of tremor. *Muscle & Nerve: Official Journal of the American Association of Electrodiagnostic Medicine*, *24*(6), 716-735.

Doyon, J., & Benali, H. (2005). Reorganization and plasticity in the adult brain during learning of motor skills. *Current opinion in neurobiology*, *15*(2), 161-167.

Doyon, J., & Ungerleider, L. G. (2002). Functional anatomy of motor skill learning.

Doyon, J. (2008). Motor sequence learning and movement disorders. *Current opinion in neurology*, *21*(4), 478-483.

Elble, R. J., Pullman, S. L., Matsumoto, J. Y., Raethjen, J., Deuschl, G., & Tintner, R. (2006). Tremor amplitude is logarithmically related to 4-and 5-point tremor rating scales. *Brain*, *129*(10), 2660-2666.

Elble, R. J. (1986). Physiologic and essential tremor. *Neurology*, *36*(2), 225-225.

Elble, R. J. (2017). *Tremor* (pp. 311-326). Springer International Publishing.

Ernst, M. O. (2006). A Bayesian View on Multimodal Integration Cue. *Human body perception from the inside out*, 105.

Faisal, A. A., Selen, L. P., & Wolpert, D. M. (2008). Noise in the nervous system. *Nature reviews neuroscience*, *9*(4), 292-303.

Fasano, A., Herzog, J., Raethjen, J., Rose, F. E., Muthuraman, M., Volkmann, J., ... & Deuschl, G. (2010). Gait ataxia in essential tremor is differentially modulated by thalamic stimulation. *Brain*, *133*(12), 3635-3648.

Fercho, K., & Baugh, L. A. (2014). It's too quick to blame myself—the effects of fast and slow rates of change on credit assignment during object lifting. *Frontiers in human neuroscience*, *8*, 554.

Franklin, D. W., Osu, R., Burdet, E., Kawato, M., & Milner, T. E. (2003). Adaptation to stable and unstable dynamics achieved by combined impedance control and inverse dynamics model. Journal of neurophysiology, 90(5), 3270-3282.

Fujita, M. (1982). Simulation of adaptive modification of the vestibulo-ocular reflex with an adaptive filter model of the cerebellum. *Biological cybernetics*, *45*, 207-214.

Halsband, U., & Lange, R. K. (2006). Motor learning in man: a review of functional and clinical studies. *Journal of Physiology-Paris*, *99*(4-6), 414-424.

Hanajima, R., Tsutsumi, R., Shirota, Y., Shimizu, T., Tanaka, N., & Ugawa, Y. (2016). Cerebellar dysfunction in essential tremor. *Movement Disorders*, *31*(8), 1230-1234.

Heldman, D. A., Jankovic, J., Vaillancourt, D. E., Prodoehl, J., Elble, R. J., & Giuffrida, J. P. (2011). Essential tremor quantification during activities of daily living. *Parkinsonism & related disorders*, *17*(7), 537-542.

Hentschke,H.(2023).hhentschke/measures-of-effect-size-toolbox (https://github.com/hhentschke/measures-of-effect-size-toolbox), GitHub.

Hosseini, E. A., Nguyen, K. P., & Joiner, W. M. (2017). The decay of motor adaptation to novel movement dynamics reveals an asymmetry in the stability of motion state-dependent learning. *PLoS computational biology*, *13*(5), e1005492.

Hwang, E. J., Smith, M. A., & Shadmehr, R. (2006). Adaptation and generalization in acceleration-dependent force fields. *Experimental brain research*, *169*, 496-506.

Izawa, J., & Shadmehr, R. (2011). Learning from sensory and reward prediction errors during motor adaptation. *PLoS computational biology*, *7*(3), e1002012.

Jankovic, J. (2008). Parkinson's disease: clinical features and diagnosis. *Journal of neurology, neurosurgery & psychiatry*, *79*(4), 368-376.

Joiner, W. M., & Shelhamer, M. (2006). Responses to noisy periodic stimuli reveal properties of a neural predictor. *Journal of neurophysiology*, *96*(4), 2121-2126.

Joiner, W. M., Sing, G. C., & Smith, M. A. (2017). Temporal specificity of the initial adaptive response in motor adaptation. *PLoS computational biology*, *13*(7), e1005438.

Joiner, W. M., & Smith, M. A. (2008). Long-term retention explained by a model of short-term learning in the adaptive control of reaching. *Journal of neurophysiology*, *100*(5), 2948-2955.

Kong, G., Zhou, Z., Wang, Q., Kording, K., & Wei, K. (2017). Credit assignment between body and object probed by an object transportation task. *Scientific reports*, *7*(1), 13415.

Krakauer, J. W., Hadjiosif, A. M., Xu, J., Wong, A. L., & Haith, A. M. (2019). Motor learning. *Compr Physiol*, *9*(2), 613-663.

Kronenbuerger, M., Gerwig, M., Brol, B., Block, F., & Timmann, D. (2007). Eyeblink conditioning is impaired in subjects with essential tremor. *Brain*, *130*(6), 1538-1551.

Körding, K. P., Beierholm, U., Ma, W. J., Quartz, S., Tenenbaum, J. B., & Shams, L. (2007). Causal inference in multisensory perception. *PLoS one*, *2*(9), e943.

Lakie, M., Villagra, F., Bowman, I., & Wilby, R. (1995). Shooting performance is related to forearm temperature and hand tremor size. *Journal of sports sciences*, *13*(4), 313-320.

Lakie, M. (2010). The influence of muscle tremor on shooting performance. *Experimental physiology*, *95*(3), 441-450.

Lopez-de-Ipina, K., Solé-Casals, J., Sánchez-Méndez, J. I., Romero-Garcia, R., Fernandez, E., Requejo, C., ... & Suckling, J. (2021). Analysis of fine motor skills in essential tremor: combining neuroimaging and handwriting biomarkers for early management. *Frontiers in Human Neuroscience*, *15*, 648573.

Lorenz, D., Schwieger, D., Moises, H., & Deuschl, G. (2006). Quality of life and personality in essential tremor patients. *Movement disorders: official journal of the Movement Disorder Society*, *21*(8), 1114-1118.

Louis, E. D. (2005). Essential tremor. *The Lancet Neurology*, *4*(2), 100-110.

Marton, T. F., Seifikar, H., Luongo, F. J., Lee, A. T., & Sohal, V. S. (2018). Roles of prefrontal cortex and mediodorsal thalamus in task engagement and behavioral flexibility. *Journal of Neuroscience*, *38*(10), 2569-2578.

Mazzoni, P., & Krakauer, J. W. (2006). An implicit plan overrides an explicit strategy during visuomotor adaptation. *Journal of neuroscience*, *26*(14), 3642-3645.

McCrea, P. H., & Eng, J. J. (2005). Consequences of increased neuromotor noise for reaching movements in persons with stroke. *Experimental brain research*, *162*, 70-77.

McDougle, S. D., Bond, K. M., & Taylor, J. A. (2015). Explicit and implicit processes constitute the fast and slow processes of sensorimotor learning. *Journal of Neuroscience*, *35*(26), 9568-9579.

McKenna, E., Bray, L. C. J., Zhou, W., & Joiner, W. M. (2017). The absence or temporal offset of visual feedback does not influence adaptation to novel movement dynamics. *Journal of Neurophysiology*, *118*(4), 2483-2498.

Medina, J. F., & Lisberger, S. G. (2007). Variation, signal, and noise in cerebellar sensory–motor processing for smooth-pursuit eye movements. *Journal of Neuroscience*, *27*(25), 6832-6842.

Milner, T. E., & Franklin, D. W. (2005). Impedance control and internal model use during the initial stage of adaptation to novel dynamics in humans. The Journal of physiology, 567(2), 651-664.

Miyamoto, Y. R., Wang, S., & Smith, M. A. (2020). Implicit adaptation compensates for erratic explicit strategy in human motor learning. *Nature neuroscience*, *23*(3), 443-455.

Morton, S. M., & Bastian, A. J. (2004). Cerebellar control of balance and locomotion. *The neuroscientist*, *10*(3), 247-259.

Nakajima, M., Schmitt, L. I., & Halassa, M. M. (2019). Prefrontal cortex regulates sensory filtering through a basal ganglia-to-thalamus pathway. *Neuron*, *103*(3), 445-458.

Nguyen, K. P., Zhou, W., McKenna, E., Colucci-Chang, K., Bray, L. C. J., Hosseini, E. A., ... & Joiner, W. M. (2019). The 24-h savings of adaptation to novel movement dynamics initially reflects the recall of previous performance. *Journal of Neurophysiology*, *122*(3), 933-946.

Nieuwboer, A., Rochester, L., Müncks, L., & Swinnen, S. P. (2009). Motor learning in Parkinson's disease: limitations and potential for rehabilitation. *Parkinsonism & related disorders*, *15*, S53-S58.

Oldfield, R. C. (1971). The assessment and analysis of handedness: the Edinburgh inventory. *Neuropsychologia*, *9*(1), 97-113.

Osu, R., Burdet, E., Franklin, D. W., Milner, T. E., & Kawato, M. (2003). Different mechanisms involved in adaptation to stable and unstable dynamics. Journal of Neurophysiology.

Popa, L. S., & Ebner, T. J. (2019). Cerebellum, predictions and errors. *Frontiers in cellular neuroscience*, *12*, 524.

Rao, S. S., Hofmann, L. A., & Shakil, A. (2006). Parkinson's disease: diagnosis and treatment. *American family physician*, *74*(12), 2046-2054.

Requarth, T., & Sawtell, N. B. (2011). Neural mechanisms for filtering self-generated sensory signals in cerebellum-like circuits. *Current opinion in neurobiology*, *21*(4), 602-608.

Sarwary, A. M., Wischnewski, M., Schutter, D. J., Selen, L. P., & Medendorp, W. P. (2018). Corticospinal correlates of fast and slow adaptive processes in motor learning. *Journal of neurophysiology*, *120*(4), 2011-2019.

Scheidt, R. A., Dingwell, J. B., & Mussa-Ivaldi, F. A. (2001). Learning to move amid uncertainty. *Journal of neurophysiology*, *86*(2), 971-985.

Scheidt, R. A., Reinkensmeyer, D. J., Conditt, M. A., Rymer, W. Z., & Mussa-Ivaldi, F. A. (2000). Persistence of motor adaptation during constrained, multi-joint, arm movements. *Journal of neurophysiology*, *84*(2), 853-862.

Schlerf, J., Ivry, R. B., & Diedrichsen, J. (2012). Encoding of sensory prediction errors in the human cerebellum. *Journal of Neuroscience*, *32*(14), 4913-4922.

Shadmehr, R., & Mussa-Ivaldi, F. A. (1994). Adaptive representation of dynamics during learning of a motor task. *Journal of neuroscience*, *14*(5), 3208-3224.

Shadmehr, R., Smith, M. A., & Krakauer, J. W. (2010). Error correction, sensory prediction, and adaptation in motor control. *Annual review of neuroscience*, *33*, 89-108.

Shill, H. A., De La Vega, F. J., Samanta, J., & Stacy, M. (2009). Motor learning in essential tremor. *Movement disorders: official journal of the Movement Disorder Society*, *24*(6), 926-928.

Sing, G. C., Joiner, W. M., Nanayakkara, T., Brayanov, J. B., & Smith, M. A. (2009). Primitives for motor adaptation reflect correlated neural tuning to position and velocity. *Neuron*, *64*(4), 575-589.

Sing, G. C., Orozco, S. P., & Smith, M. A. (2013). Limb motion dictates how motor learning arises from arbitrary environmental dynamics. *Journal of neurophysiology*, *109*(10), 2466-2482.

Smith, M. A., Ghazizadeh, A., & Shadmehr, R. (2006). Interacting adaptive processes with different timescales underlie short-term motor learning. *PLoS biology*, *4*(6), e179.

Sych, Y., Fomins, A., Novelli, L., & Helmchen, F. (2022). Dynamic reorganization of the cortico-basal ganglia-thalamo-cortical network during task learning. *Cell Reports*, *40*(12).

Synofzik, M., Lindner, A., & Thier, P. (2008). The cerebellum updates predictions about the visual consequences of one's behavior. *Current Biology*, *18*(11), 814-818.

Synofzik, M., Thier, P., & Lindner, A. (2006). Internalizing agency of self-action: perception of one's own hand movements depends on an adaptable prediction about the sensory action outcome. *Journal of neurophysiology*, *96*(3), 1592-1601.

Therrien, A. S., Wolpert, D. M., & Bastian, A. J. (2018). Increasing motor noise impairs reinforcement learning in healthy individuals. *eneuro*, *5*(3).

Tseng, Y. W., Diedrichsen, J., Krakauer, J. W., Shadmehr, R., & Bastian, A. J. (2007). Sensory prediction errors drive cerebellum-dependent adaptation of reaching. *Journal of neurophysiology*, *98*(1), 54-62.

Tzvi, E., Loens, S., & Donchin, O. (2022). Mini-review: the role of the cerebellum in visuomotor adaptation. *The Cerebellum*, *21*(2), 306-313.

Wagner, M. J., & Smith, M. A. (2008). Shared internal models for feedforward and feedback control. *Journal of Neuroscience*, *28*(42), 10663-10673.

Wanda, P. A., Li, G., & Thoroughman, K. A. (2013). State dependence of adaptation of force output following movement observation. *Journal of neurophysiology*, *110*(5), 1246-1256.

Waschke, L., Kloosterman, N. A., Obleser, J., & Garrett, D. D. (2021). Behavior needs neural variability. *Neuron*, *109*(5), 751-766.

Wei, K., & Kording, K. (2009). Relevance of error: what drives motor adaptation?. *Journal of neurophysiology*, *101*(2), 655-664.

Wei, K., & Körding, K. (2010). Uncertainty of feedback and state estimation determines the speed of motor adaptation. *Frontiers in computational neuroscience*, *4*, 1151.

Welton, T., Cardoso, F., Carr, J. A., Chan, L. L., Deuschl, G., Jankovic, J., & Tan, E. K. (2021). Essential tremor. *Nature Reviews Disease Primers*, *7*(1), 83.

Wimmer, R. D., Schmitt, L. I., Davidson, T. J., Nakajima, M., Deisseroth, K., & Halassa, M. M. (2015). Thalamic control of sensory selection in divided attention. *Nature*, *526*(7575), 705-709.

Wolpert, D. M., Diedrichsen, J., & Flanagan, J. R. (2011). Principles of sensorimotor learning. *Nature reviews neuroscience*, *12*(12), 739-751.

Verhoeven, F. M., & Newell, K. M. (2018). Unifying practice schedules in the timescales of motor learning and performance. *Human movement science*, *59*, 153-169.

Wolpert, D. M., Ghahramani, Z., & Jordan, M. (1994). Forward dynamic models in human motor control: Psychophysical evidence. *Advances in neural information processing systems*, *7*.

Wolpert, D. M., Ghahramani, Z., & Flanagan, J. R. (2001). Perspectives and problems in motor learning. *Trends in cognitive sciences*, *5*(11), 487-494.

Wolpert, D. M., & Landy, M. S. (2012). Motor control is decision-making. *Current opinion in neurobiology*, *22*(6), 996-1003.

Wolpert, D. M., Miall, R. C., & Kawato, M. (1998). Internal models in the cerebellum. *Trends in cognitive sciences*, *2*(9), 338-347.

Wong, J. K., Hess, C. W., Almeida, L., Middlebrooks, E. H., Christou, E. A., Patrick, E. E., ... & Okun, M. S. (2020). Deep brain stimulation in essential tremor: targets, technology, and a comprehensive review of clinical outcomes. *Expert review of neurotherapeutics*, *20*(4), 319-331.

Yousif, N., & Diedrichsen, J. (2012). Structural learning in feedforward and feedback control. *Journal of neurophysiology*, *108*(9), 2373-2382.

Zhou, W., Kruse, E. A., Brower, R., North, R., & Joiner, W. M. (2022). Motion state-dependent motor learning based on explicit visual feedback is quickly recalled, but is less stable than adaptation to physical perturbations. *Journal of Neurophysiology*, *128*(4), 854-871.

Chapter 3: How Pathological Tremor Impacts Movement and Motor Adaptation

INTRODUCTION

Tremors are involuntary, rhythmical, and oscillatory muscle contractions (Lippold, 1971). In all healthy individuals, these appear as high frequency (8-12Hz) and low amplitude oscillations when moving, at rest, or holding a body part still against gravity (Marshall & Walsh, 1956; Crawford & Zimmerman, 2011). While normally undetectable to the naked eye, these oscillations, called physiological tremor, may be detected as frequency and amplitude temporarily increase due to certain medications, anxiety, or low blood sugar (Crawford & Zimmerman, 2011). Once these causes are removed, however, so too does the visibility of physiological tremor. When high frequency and/or high amplitude tremor becomes persistent or progressive, it can interfere with daily living and is named pathological tremor (Jankovic & Stanley, 1980). These tremors are typically classified upon whether they occur at rest (rest tremor), or during action, including while holding postures (postural tremor) or during movements (action/kinetic tremor) (Bhatia et al., 2017) and they exist as key symptoms in many common movement disorders.

The two most common adult movement disorders, Essential Tremor (ET) and Parkinson's Disease (PD) (O'Shead & Shih, 2023), list pathological tremor as a hallmark symptom. ET is believed to be caused by impaired functional connectivity within the cerebello-thalmo-cortical circuitry (Holtbernd & Shah, 2021). Tremor in ET presents as a bilateral, upper limb oscillation that increases in magnitude and frequency (4-12 Hz) during postural holds (when the limb is at rest but being held unsupported against gravity) and while making voluntary goal directed reaching movements (e.g., placing a key into a lock, Louis, 2005). Rest tremor in PD typically begins as a unilateral, upper limb tremor that increases in magnitude and frequency (4-7 Hz) when the affected limb is at rest and fully supported against gravity (e.g., resting hands in one's lap when sitting, Gironell et al., 2018).

In addition to tremor, patients with ET and PD are known to have impaired motor adaptation and control. Patients with ET have impaired adaptation to physical and visual feedback

perturbations while making upper limb reaching movements towards visual targets (Bindel et al., 2022; Blondiaux et al., 2023; Chen et al., 2006) and during fine motor control (e.g., handwriting, Alty et al. 2011). When an arm reach is viewed as an entire movement as opposed to certain phases, tremor (as measured by clinical scoring or accelerometry data) does not appear to underlie these impairments (Bindel et al., 2022; Blondiaux et al., 2023; Chen et al., 2006). However, Blondieux et al. (2023) examined single arm reaches during two distinct phases: reaching (action) and stabilization. When assessing these two phases individually, they found that cerebellar deficits associated with ET typically played a role in lowering performance during the movement execution phase (Blondiaux et al., 2023). Thus, impaired motor adaptation in ET appears not to be due to an inability to learn but rather due to a disturbance in motor execution (Blondiaux et al., 2023). In addition, final stabilization was impaired because movement execution was noisy (Blondiaux et al., 2023). Previous studies in the ET motor learning largely did not differentiate between these two phases, making it difficult to determine the specific mechanisms of movement that tremor (noisy movement execution) impacted during motor adaptation. One drawback from this study, however, is that tremor was quantified using clinical scoring separately from the arm reaching task. Thus, the relationship between online tremor and reaching movement was inferred.

Similarly, patients with PD have been shown to have impaired visuomotor adaptation (Mongeon et al., 2013), but it is unclear whether tremor underlies this impairment. Other studies on motor learning in PD have demonstrated that tremor severity does not impair cognitive performance, including verbal and non-verbal episodic memory, attention, working memory, and executive function during declarative and procedural motor learning tasks (Domellöf et al., 2011; Vakil & Herishanu-Naaman, 1998), acoustically cued finger tapping (Stegemöller et al., 2016), punishment-based learning (Moustafa et al., 2013), nor vividness of motor imagery (Readman et al., 2023).

The majority of these studies relied on correlating clinical tremor scores to task performance, collected separately from performance on the actual task. This creates a disconnect between assessing tremor from learning as the correlations do not reveal how tremor is impacting the specific mechanisms of learning. Based on our previous study (Foray et al. 2025) increasing the magnitude of externally-generated tremor in healthy subjects impaired the ability to adapt to a physical movement perturbation. One would expect to see this same impaired learning in patients with pathological tremor, but this has not been directly observed in previous patient studies. Thus, without a real-time quantification of tremor during different stages of upper limb movement, we have little insight into the extent specific characteristics of tremor (e.g., frequency and magnitude) impact motor adaptation and control.

Due to differences in underlying pathology and manifestation, tremor in PD and ET may have distinct effects on different stages of movement. For example, later in disease progression, tremor in PD uniquely manifests during rest and postural holds while ET is characteristically an action tremor (Botzel et al., 2014). There is strong evidence that upper limb movement and postural hold are controlled by two related, but distinct motor pathways (Hadjosif et al., 2025, Shadmehr 2017). By assessing how tremor (self-generated, sensorimotor noise) during maintenance of an upper limb sensory state (PD postural hold tremor) and tremor during changes of an upper limb sensory state (ET action tremor), we hope to gain insight into how tremor impacts movement reach and hold. Moreover, there may be separate but connected neural mechanisms involved in the reaching and stabilization of upper limb movements (Jayasinghe et al., 2022). This is complemented by Blondiaux et al.'s (2023) findings of cerebellar deficits in ET impairing movement execution and, subsequently, movement stabilization. To better understand how tremor impacts motor learning and control, we set out to quantify tremor during distinct stages of movement: reaching, stabilization, and postural hold.

To achieve these goals, we utilized a common arm reaching movement paradigm (Shadmehr and Mussa-Ivaldi, 1994), in which participants are asked to hold the handle of a robotic

manipulandum and make reaching movements between targets in the presence of a dynamic, lateral force-field (FF) perturbation (Joiner and Smith, 2008; Mckenna et al., 2017; Alhussein et al., 2019; Zhou et al., 2022). During this perturbation, participants must adapt the temporal pattern of force to counteract the lateral force of the perturbation (Conditt et al., 1997; Conditt and Mussa-Ivaldi, 1999; Sing et al., 2009, 2013; Yousif and Diedrichsen, 2012; Hosseini et al., 2017; Joiner et al., 2017). Interspersed randomly throughout the task, error-clamp (EC) guide participant movement toward the target in a straight line while keeping lateral errors very small (Scheidt et al., 2000; Hwang et al., 2006; Smith et al., 2006; Wagner and Smith, 2008; Sing et al., 2009; Wei and Körding, 2010; Wanda et al., 2013). EC trials capture the applied force of the subject and provide a measure of adaptation.

The handle of the robotic manipulandum contains a force sensor that captures fluctuations in subject limb movement during movement and at rest. We utilize this force data to measure tremor throughout the arm reaching task. In doing so, we are able to systematically and continuously quantify tremor during different types of movement dynamics (i.e. reaching, stabilization, and postural hold) while assessing its impact on subjects' ability to adapt.

METHODS

Table 1. Participant Demographics.

	Control	PD	ET
N =	20	21	10
Age (Mean ± SD)	70.8 ± 9.8	70.1 ± 9.6	56.9 ± 22.7
Sex at Birth	17F/3M	10F/11M	5F/5M
Handedness	19R/1L	19R/2L	6R/4L
UPDRS III (Mean ± SD)	NaN	23.7 ± 10.8	5.75 ± 1.9
MoCA (Mean ± SD)	NaN	25.2 ± 3.3	NaN
MMSE (Mean ± SD)	NaN	28.5 ± 1.8	NaN
On DA Medication	NaN	19 ON	NaN

21 patients diagnosed with Parkinson's Disease (11M/10F, 70.1 ± 9.6 years), 10 patients diagnosed with Essential Tremor (5M/5F, 56.9 ± 22.7 years), and 20 age-matched control individuals without any known neurological impairment (3M/17F, 70.8 ± 9.8) took part in this study (Table 1). We kept track of participant medication use and dosage. Clinical evaluations, such as motor scores, were performed by a neurologist at the University of California Movement Disorders Clinic. Participants provided written, informed consent in accordance with protocols approved by the Institutional Review Board at the University of California, Davis and were financially compensated for their part in the study. All participants (PD: 19R/2L, ET: 6R/4L, Control: 19R/1L) used their right hand to complete the experiment, even if it was not their dominant hand (as determined by the Edinburgh Handedness Inventory). There were no differences in performance between handedness groups. Each participant performed the paradigm only once and was naive to the purpose of the experiment.

Motor adaptation was assessed through a commonly used arm reaching paradigm (Shadmehr and Mussa-Ivaldi, 1994; Scheidt et al., 2000; Figure. 1). Participants were asked to grasp the

handle of a robotic manipulandum on a planar workspace that moved a cursor on a screen between presented targets. The manipulandum (KINARM End-Point Lab, BKIN Technologies) sampled motor output, including position, force, velocity, and acceleration at 1,000 Hz. Participants could not directly view their hand position, as it was hidden from sight by a horizontal, upward-facing mirror. A small white cursor, representing hand position, was presented on the screen in addition to targets, which were open red circles. Participants were seated in front of this set-up in a chair adjusted to allow for comfortable viewing of the task.

During the task, participants were asked to use the robotic manipulandum to move the cursor (a white, filled circle 3mm in diameter) in a straight line between the start and end targets, which were approximately 0.5cm in diameter, spaced 10 cm apart on the screen, and 20-30cm away from the body on the sagittal axis. A trial consisted of a single arm reach between the start target and end target. Although participants made point to point movements, we only assessed trials where the arm reached towards the body. A “successful” trial occurred when a movement’s peak velocity in the vertical direction (towards the end target) was within a range of 0.15-0.55 m/s. If a trial was successful, the end target would turn green and make a short “beep” sound. If a trial was not successful due to the peak velocity falling below 0.15 m/s, the end target would turn yellow with no sound. If a trial was not successful due to the peak velocity falling above 0.55 m/s, the end target would turn red with no sound. While receiving instructions for the task, participants were told to obtain “as many green feedback trials as possible”.

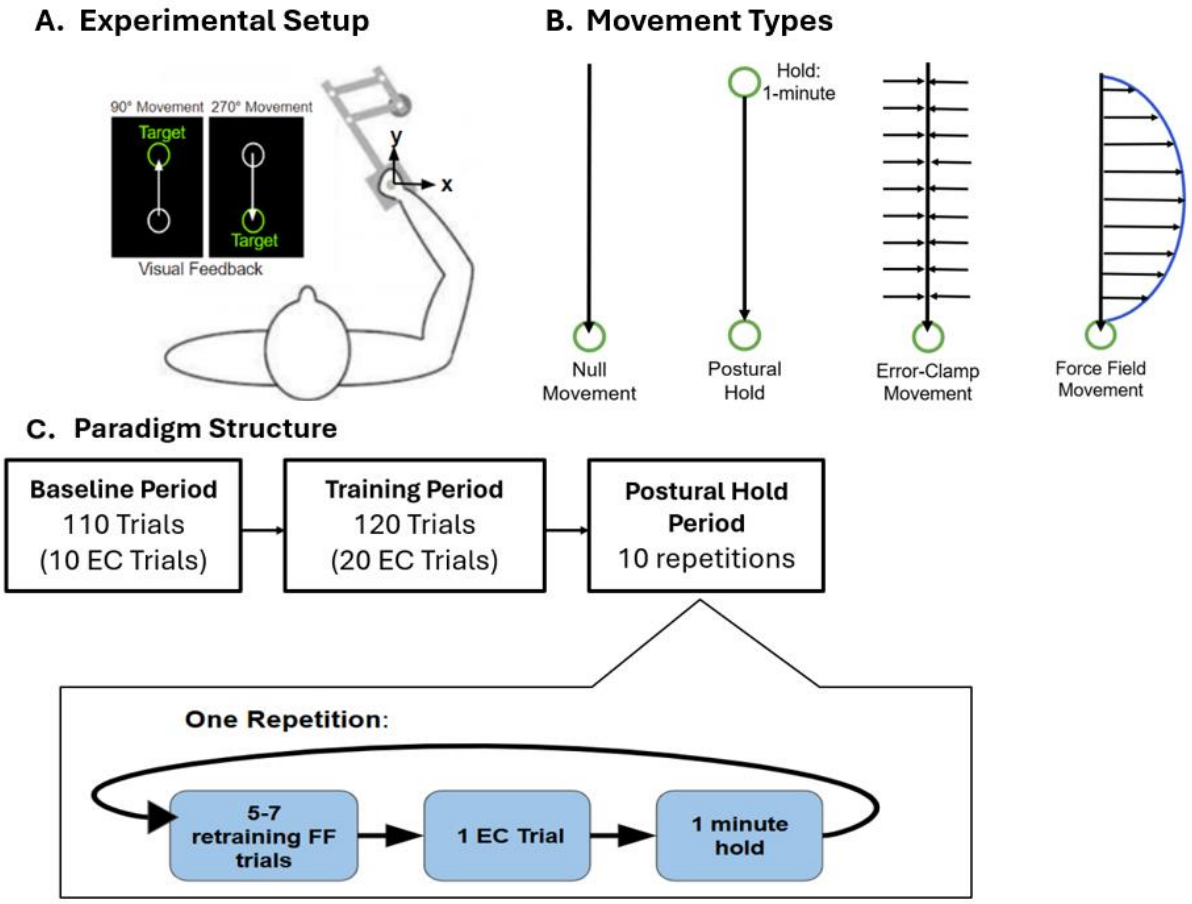

Figure 1. Experimental Set up. **A**, Participants made straight arm reaching movements between two circular targets from midline ~10 cm apart while holding the handle of a robotic manipulandum. Forward reaching motion was completed in the 90° direction while reaching back toward oneself was completed in the 270° direction. However, we only used arm movements completed in the 270° direction to compute adaptation coefficients and assess force profiles. The location of the hand was represented on the screen as a white filled circle. **B**, There were four movement types: null, force field, error-clamp, and delay probe movements. Each trial consisted of one movement. Null movements were completed as a free-range movement (no resistance from the robot) without any force field perturbation. During force field movements, participants experienced a velocity-dependent, lateral perturbation (horizontal small black arrows). For the 270° reaching motion, the force-field perturbed the participant arm to the right. Postural hold trials required participants to hold the cursor at the start target for one minute before proceeding with the reaching movement. During error-clamp trials (EC), lateral movement was constrained by clamps, constraining lateral

error to <0.6 mm. **C**, Paradigm structure. Participants started off with a period consisting of null movements with occasional error-clamp trials to establish baseline performance. In the training period, participant arm reach was laterally perturbed by a velocity-dependent force field (FF). During the postural hold period, on some of the trials, participants were asked to hold the cursor at the start target for ~1 min before proceeding with an error-clamped reaching movement.

In the task, there were four trial types: null, postural hold, error-clamp (EC), and force-field (FF) perturbation (Figure 1B). Null trials allowed participants to make straight arm reaching movements between the targets without any perturbations or restrictions to movement. Postural hold trials required participants to hold the cursor at the start target for approximately 1-minute before proceeding to the end target. During this 1-minute postural hold, participant hand position was restricted to the inside area of the start target (approximately 0.5cm in diameter) by the robot manipulandum. On EC trials the robotic manipulandum constrained lateral movement, reducing lateral error to less than 0.6mm. Robot motors restricted hand movement in a straight line towards the end target, counteracting any motion perpendicular to the end target direction. This was achieved by applying a stiff one-dimensional spring (6 kN/m) and a damper (150 Ns/m) in the axis perpendicular to the reach direction. In these trials, perpendicular displacement from a straight line to the reach target was held to less than 0.6 mm and averaged approximately 0.2 mm in magnitude. Figure 2 demonstrates the force profiles measured by the EC trials. Ideal force profiles show the exact amount of force needed to perfectly counteract the FF perturbation and maintain a straight line movement. Actual force profiles are the amount of force subjects used during the trial and also the movement signal used to extract and quantify tremor.

During the training period of the task, FF trials systematically perturbed reaching arm movements with forces proportional to movement velocity (k) and perpendicular to the direction of the hand motion on both the x (F_x)and y (F_y) axis. (Eq.1).

$$\begin{bmatrix} F_x \\ F_y \end{bmatrix} = c_k \begin{bmatrix} 0 & -k \\ k & 0 \end{bmatrix} \begin{bmatrix} \dot{x} \\ \dot{y} \end{bmatrix}, k = 15 \text{ Ns/m}$$ **(Equation 1)**

F_x: Forces applied in x direction

F_y: Forces applied in y direction

k: how strong perturbation should be based on velocity

$\dot{x}$: hand velocity in x direction

$\dot{y}$: hand velocity in y direction

Feedforward adaptive changes in motor output in response to the FF trials were assessed through EC trials, which were devoid of any force field. During postural hold trials, robot motors also restricted hand position to the inside area of the start target by applying the same one-dimensional spring and damper in a 360° border around the start target, allowing measurement of the amount of force used to maintain a stable position.

Participants were instructed on the task during a brief familiarization period, consisting of 110 null movement trials and 10 EC trials (no added FF). Once participants were familiar with the task, they were exposed to a baseline period, consisting of 110 total trials, 100 of which are null trials randomly interspersed with 10 EC trials. Following the baseline period, participants were exposed to the training period. During the training period, participants received 120 trials total, consisting of 100 FF trials dispersed pseudo-randomly with 20 EC trials (1 EC trial for every 5 FF trials). After the training period, participants underwent a postural hold period, where they experienced 5-7 trials of the FF perturbation followed by an EC trial. Immediately after the EC trial, participants engaged in a postural hold lasting 1 minute. The postural hold required participants to hold the cursor at the start location. The pattern of 5-6 FF trials, 1 EC trial, 1-minute postural hold, and 1 EC trial was repeated 10 times.

To measure adaptation throughout the task, we examined the lateral force profiles measured during the EC trials (Wagner & Smith, 2008; Joiner & Smith, 2008; Gonzalez Castro et al., 2011; Joiner et al., 2013). Since we only perturbed arm reaching movements during the 270°

movements (reaches towards the body), we only calculated adaptation and applied force profiles for reaches in that direction (Gonzalez Castro et al., 2011; Nguyen et al., 2019; Foray et al., 2025). The ideal compensatory force is the temporal pattern of force needed to counteract the FF lateral perturbation that would have been experienced on that trial based on the movement velocity profile (equation 1). To align all movements in the same temporal window, each trial's force profile was centered on the peak velocity with a temporal window of 1,200 ms (±600 ms, where 0 ms is the moment when the movement reaches peak velocity; Nguyen et al., 2019; Foray et al., 2025). Aligning the trials in this manner also allowed a comparison of the ideal force pattern, which is based on the actual movement velocity of a trial, to the actual amount of force used by participants on that. We then performed a linear regression of the baseline-subtracted actual force profile to the ideal force profile for each EC trial. The baseline subtraction was based on the average force profile, determined over the same 1,200 ms window, obtained during the EC trials during the baseline period. The adaptation coefficient (AC) for a trial, our primary metric for measuring adaptation to the FF perturbation, is the slope of the linear regression between the baseline-subtracted actual force and the ideal force (Joiner & Smith, 2008; Joiner et al., 2013; Nguyen et al., 2019). Thus, the AC is a measure of how well the actual force matches the ideal force based on the movement velocity. If the actual compensatory force was equal to the ideal compensatory force, then the AC = 1. If they are exact opposites, AC = −1. If they are unrelated to one another, AC = 0.

Tremor Extraction: SSA and Binning

We also utilized the actual force profiles to quantify upper limb tremor during different stages of movement. We based our extraction of tremor from the force profiles by applying the analysis steps constructed by Lin et al., 2020, which originally extracted and quantified tremor with acceleration data recorded from a motor task. During movement reach, differences in movement duration (Figure 3) had the potential to artificially inflate total force, so we normalized our measure by dividing by trial length.

We made use of the Singular Spectrum Analysis (SSA), a non parametric time series analysis that is useful for identifying the underlying trend of a signal with a short time window (Hassani, 2007; Golyandina et al., 2020). This is important because reaching and stabilization movement windows provide only 500-800ms of force information, which is not enough data for most signal extraction methods. It is also useful for extracting cycles with small and large periods, thereby denoising a signal (and detecting varying magnitudes and frequencies of tremor during movement). SSA is composed of two steps: deconstruction and recomposition. Deconstruction consists of an embedding method in which a time series of length N is transformed into a series of lagged vectors using a sliding window of length L, creating a trajectory matrix. The trajectory matrix is then put through singular value decomposition (SVD), which outputs a set of eigentriplets that represent the independent components of the time series. Reconstruction consists of grouping the eigentriplets based on their specific characteristics (i.e. separating slow-moving trends from high-frequency noise) followed by diagonal averaging (Hankelization), which results in each component of the time series being reconstructed independently.

For each EC trial during the training and postural hold periods, we input the raw force profile from each movement window (Reaching, Stabilization, Postural Hold) into the embedding operation of the deconstruction stage. For each trial, we used the length of the signal to determine the length of N. To determine the sliding window length (L), we divided N by 2 and rounded to the nearest whole number. This allowed us to capture both trend and tremor components because both have distinct temporal correlational structures. Components of periods less than L appear as oscillatory (tremor) reconstructive components. Components of periods greater than L appear as slow trends. Since the L parameter controls the time scale SSA can detect, we wanted to ensure that it could capture as many different oscillatory components as possible while still being able to capture voluntary movement trends. We were able to best achieve this by rounding the nyquist frequency to the nearest whole number.

Following the protocol of Lin et al., 2020, we then input each reconstruction component (RC) output from the SSA into a fast fourier transform (FFT), which identifies the various periodic variations in the RC in the frequency domain. Next, we categorized each RC into one of three bins: trend, tremor, and noise. An RC was categorized as trend if its frequency range below 2Hz comprised a majority of its total magnitude (as determined by the FFT) and it met a smoothness criterion where the difference in standard deviation values between each point of the RC is less than 0.1. An RC was categorized as tremor if its smoothness criterion was greater than 0.1 and its frequency range of 3-25Hz comprised a majority of its total magnitude (as determined by the FFT). All other RCs not labeled as trend or tremor were categorized as non-tremor noise. Once binned, all RCs sharing a common bin were added together to reconstruct a single time series representing the trend, tremor, and noise underlying the original force signal for each trial.

Once the tremor signal was extracted from a trial, we computed the total area under the curve (AUC) to determine the total amount of tremor force present during the trial. To ensure both positive and negative deflections contributed to the overall area, we took the absolute value of each signal before computing the AUC. This allowed us to compare the amount of tremor force generated on each trial and compare average tremor force during different stages of movement across individuals and groups (See Figures 4C and 5C). Separately, we input the extracted tremor signal into an FFT. To convert the frequency-domain representation (Y) of the FFT output into tremor magnitude, we obtained the absolute value of Y. Then, to normalize Y so that the magnitude was independent of the number of samples, we divided by the signal length. Finally, we binned the tremor magnitude for every frequency in increments of 1 Hz (0-1Hz, 1-2Hz, 2-3Hz, etc) and determined the average of each bin. This allowed a direct comparison of the frequency and magnitude of tremor for every trial across individuals and groups (see Figures 4B, 5B, and 7B).

Statistical Analysis

All statistical analyses were performed in MATLAB (version R2023a) on trials that met the speed, duration, and position criteria listed above. To compare average adaptation coefficient, average perpendicular displacement, average movement duration, and average peak velocity for each period of training across groups, we utilized a two-way analysis of variance (ANOVA). If significant results were found, we further investigated significance between groups. We compared each group's average tremor force with an independent t-test. We used a one-way ANOVA to compare endpoint error variability and total tremor force between groups. For all ANOVAs and t-tests, we corrected for multiple comparisons using Holm-Bonferroni's post hoc test. For significant interactions, we conducted post hoc Tukey-HSD tests. Effect size (eta squared) was calculated using the hhentschke/measures-of-effect-size-toolbox in MATLAB (Hentschke, 2023). For all tests, the significance level was 0.05 and data are presented by means ± SEM.

RESULTS

Despite differences in average tremor magnitude during movement reach, there are no learning differences between groups

Figure 2A plots the adaptation coefficient (see Materials and Methods) as a function of training trials for the three subject groups. Overall, we did not observe any significant learning differences between the three groups. To better understand how the average adaptation coefficients possibly differed at specific time periods of training, we examined the average adaptation coefficient from the first 10% of training trials (early trials), the middle 10% (middle trials), and last 10% (late trials; Figure 2B). A two-way ANOVA demonstrated that there was no significant difference in adaptation between the three groups ($F_{(2,148)} = 0.15$; $p = 0.86$, $\eta^2 = 9.65$ x 10^-4), but within each group, adaptation was significantly different between the three training periods ($F_{(2,148)} = 76.16$; $p < 0.0001$; $\eta^2 = 0.49$). No significant interaction between the two factors was found ($F_{(4,148)} = 0.6$; $p = 0.66$; $\eta^2 = 0.008$). Average force profiles during each training period

further demonstrates no significant differences in the amount of force used during movement reach between groups (Figure 2C).

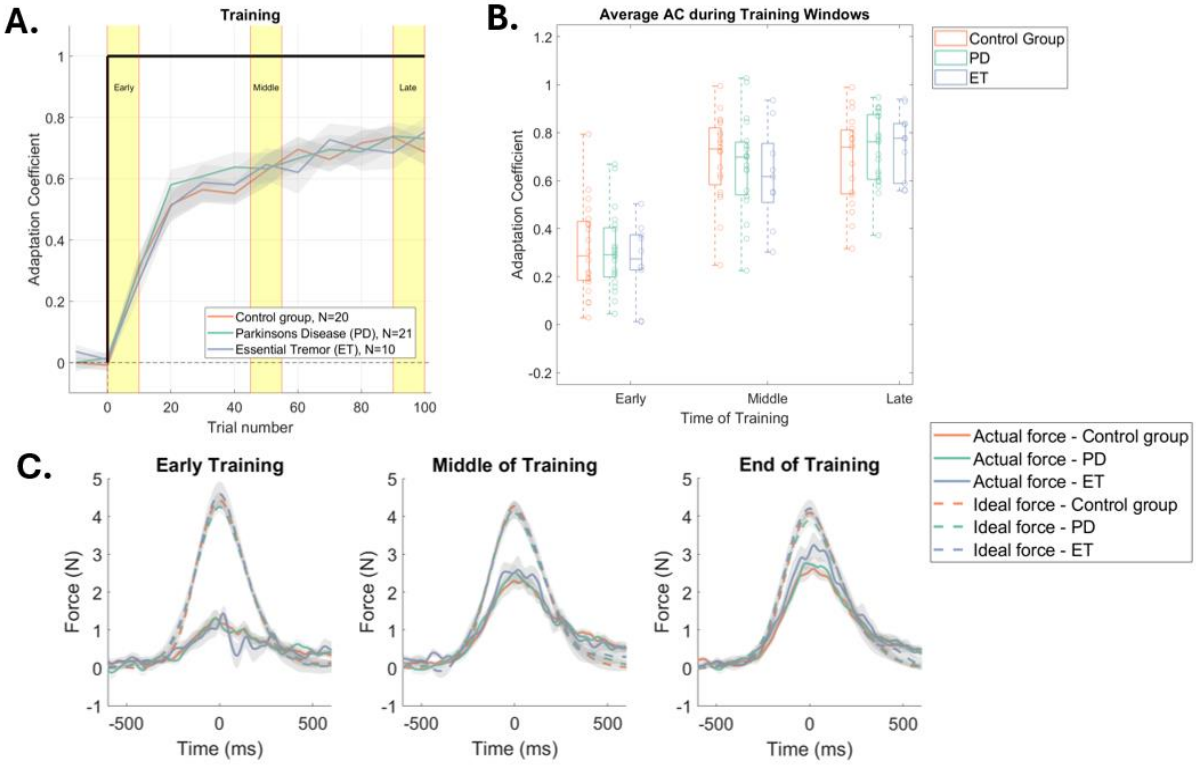

Figure 2. Adaptation. **A.** Adaptation, quantified by the adaptation coefficient, is plotted as a function of trial number for each group. These learning curves show that there are no differences in the ability to adapt between groups (control, orange trace; Parkinson's Disease, green trace; Essential Tremor, purple trace). Adaptation coefficients were split into three windows: early trials (first 10% of training trials), middle trials (the middle 10%), and late trials (the last 10%), which are represented by the three yellow regions. **B.** Box plots show differences in average adaptation coefficients. **C**. Average force profiles for each group during early, middle, and late periods of training for the three groups. Force profile is the value, measured in magnitudes (N) on the y-axis, of force used to counteract the FF perturbation throughout the reaching movement. Ideal force profile (dashed line) represents how much force would be needed to exactly counteract the FF perturbation to continue making a straight arm reaching movement. The actual force profile (solid line) indicates how much force, on average, participants used to counteract the FF perturbation.

To identify if reaching movement between groups differed aside from tremor, we examined perpendicular displacement, movement duration, and average peak velocity between the three training periods: early, middle and late; Figure 2B). To best determine how movement variability differed between groups (without using force measurements), we calculated perpendicular displacement as the shortest distance between the participant's hand position at peak velocity and the ideal straight-line path during FF trials in the training period. The ideal movement path was defined as the straight line between the start target and end target. As Figure 3A demonstrates, there was no overall significant difference in perpendicular displacement between the three groups during training. In Figure 3B, we show perpendicular displacement during early, middle, and late training periods. A two-way ANOVA demonstrated that there was no significant difference in perpendicular displacement between the three groups ($F_{(2,152)} = 0.44$, $p = 0.64$, $\eta^2 = 0.004$ but, within each group, perpendicular displacement was significantly different between the three training periods ($F_{(2,152)} = 36.99$; $p < 0.0001$, $\eta^2 = 0.32$. No significant interaction between the two factors was found ($F_{(4,152)} = 0.2$; $p = 0.94$, $\eta^2 = 0.004$).

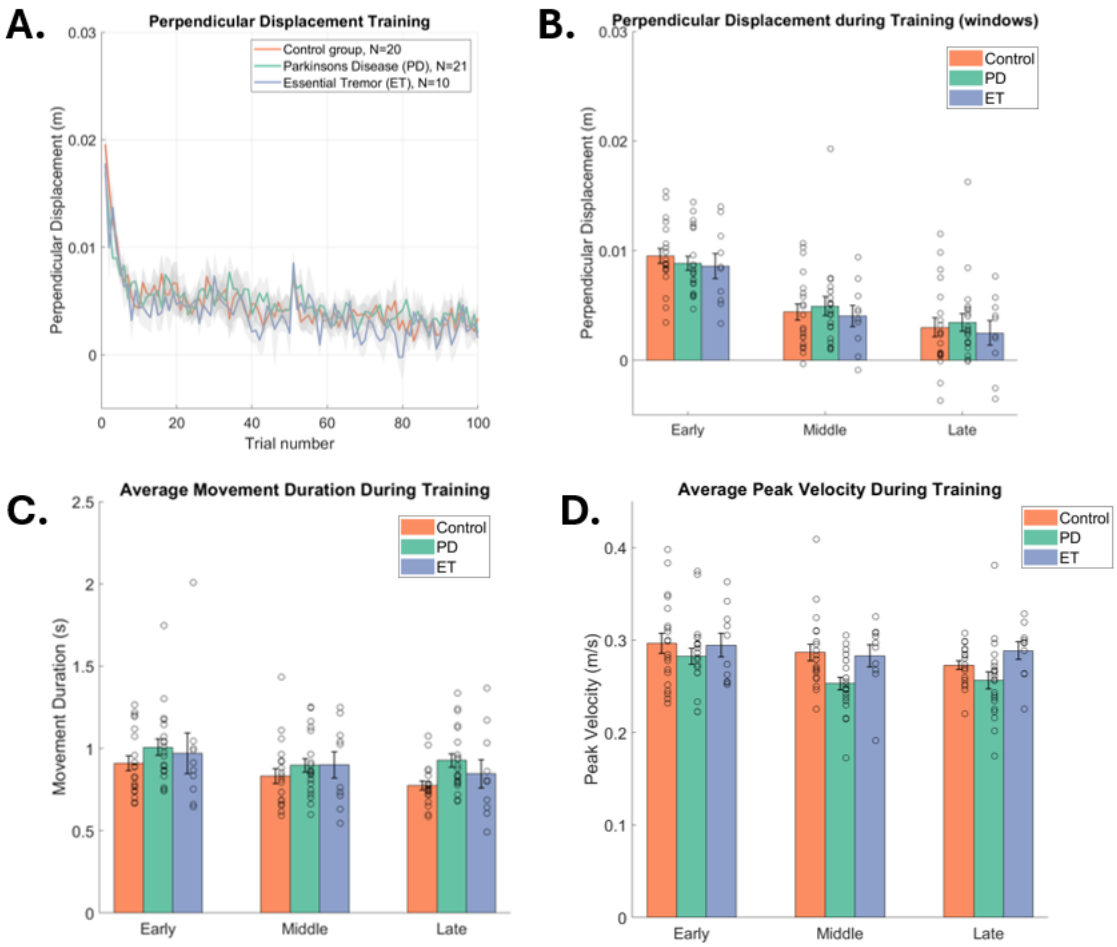

Figure 3. Underlying Movement Differences. To identify if reaching movement between groups differed aside from tremor, we examined **A,** perpendicular displacement, **C.** movement duration, and **D.** average peak velocity across training windows (early, middle, and late).

A characteristic feature of PD is bradykinesia, or slowness of movement. In Figure 3C, we investigated differences in movement duration between groups during early, middle, and late training. We found that there was a significant difference in movement duration between the three groups ($F_{(2,152)} = 3.59$; $p = 0.03$; $\eta^2 = 0.05$) and within each group, movement duration was different across training periods ($F_{(2,152)} = 3.37$; $p = 0.03$; $\eta^2 = 0.04$). However, there were no interaction effects between the two factors ($F_{(4,152)} = 0.24$; $p = 0.91$; $\eta^2 = 0.006$). On average, patients with PD had longer reaching movements compared to control subjects and patients with ET (Table 2).

Due to this longer reach time, we normalized all force profiles by dividing each trial by its movement duration before extracting tremor to prevent artificial inflation of total tremor force.

	Control	PD	ET
Early Training	0.91 ± 0.01	1.01 ± 0.008	0.97 ± 0.01
Middle Training	0.83 ± 0.009	0.89 ± 0.006	0.89 ± 0.01
Late Training	0.77 ± 0.004	0.93 ± 0.009	0.84 ± 0.009

Table 2. Movement Duration Comparison of movement duration across groups during different periods of training. Values are in seconds and Mean ± SEM

To assess if these differences in movement duration were due to actual movement speed between patients, we also examined the peak velocity in each group during different periods of training (Figure 3D). A two-way ANOVA found that peak velocity was significantly different between the three groups ($F_{(2,152)}$ = 6.67; p = 0.001; η^2 = 0.08) and, within each group, peak velocity was different across training periods ($F_{(2,152)}$ = 3.38; p = 0.03; η^2 = 0.04). There were no interaction effects ($F_{(4,152)}$ = 0.67; p =0.61; η^2 =0.01). We found that the primary difference resided in patients with PD having significantly slower average peak velocities during early, middle, and late training trials compared to patients with ET and control subjects.

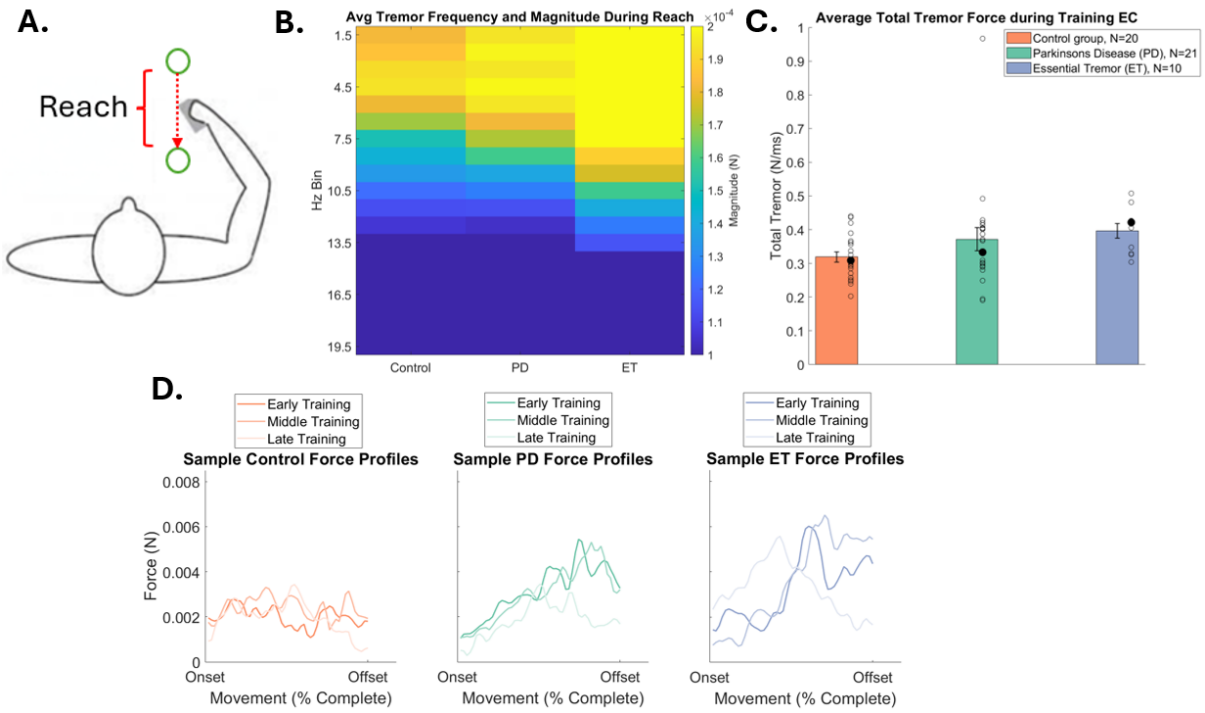

Figure 4. Movement Reach. **A.** The window of movement that defines movement reach is the first time the white cursor leaves the start target and the first time the cursor crosses the threshold of the end target. **B.** Heatmap demonstrates the average magnitude for each frequency bin across groups. **Bar** graphs (SEM error bars) demonstrate differences in total tremor magnitude during training for each group. During movement reach, we see that patients with ET have a significantly higher tremor magnitude compared to patients with PD and control subjects. **D.** Sample participant force profiles demonstrate the average difference in raw force profile before tremor extraction during reaching movement throughout different periods of training. Participants were chosen based on their data falling within the average range from figure 4C.

Having established underlying variabilities in reaching movement, we then assessed how tremor differed between each group. Figure 4B demonstrates that, during movement reach, patients with ET exhibited the greatest amount of movement tremor magnitude (Peak Magnitude, Average Corresponding Frequency: 2.91×10^{-4} N, 4.5 Hz) compared to control subjects (2.11×10^{-4} N, 4.5 Hz) and patients with PD (2.2×10^{-4} N, 2.5 Hz), as measured by the force profiles (see

Methods). In Figure 4C, we averaged the total area under the temporal force profile throughout training trials for each group. An independent t-test demonstrated a significant difference between patients with ET (Mean ± SEM, 0.3966 ± 0.022) and control subjects (0.32 ± 0.01), $t(28) = -2.9$, $p = 0.007$. Patients with PD (0.37 ± 0.03), meanwhile, did not have any significant differences between control subjects, $t(39) = -1.36$, $p = 0.17$, nor patients with ET, $t(29) = -0.48$, $p = 0.63$. Figure 4C depicts sample participants from each group (selected based on proximity to the average range of the respective group in Figure 4C), emphasizing that patients with ET typically exhibit higher magnitudes of tremor during movement reach throughout the training period. Importantly, as adaptation to the FF perturbation occurs during the reaching movement, we observe that increased tremor magnitude does not appear to impact motor adaptation (shown in Figure 2A). That is all groups show similar learning curves despite the stated differences in movement tremor.

During movement stabilization, ET patients have increased tremor magnitude and increased end movement variability

The window of movement that we used to define movement stabilization is the first time the cursor crosses the boundary of the end target to the end of movement reach (hard coded in the paradigm; as also defined in Blondieux et al., 2023), resulting in a 500ms window of stabilization for every trial. However, to account for movement remaining at the end of reach movement and movement out of the target to begin the next trial, we excluded 50ms from both the beginning and end of this window, leaving us with a 400 ms window. Figure 5B demonstrates that, during movement stabilization, patients with ET exhibit the greatest amount of stabilization tremor magnitude (Peak Magnitude, Average Corresponding Frequency: 2.45×10^{-4} N, 15.5 Hz) compared to control subjects (1.46×10^{-4} N, 4.5 Hz) and patients with PD (1.81×10^{-4} N, 4.5 Hz), as measured by the force profile. In Figure 5C, we averaged the total area under the temporal force profile during stabilization throughout the training trials for each group. An independent t-test demonstrated a significant difference in stabilization tremor between patients with ET (Mean ±

SEM, 0.2 ± 0.02) and control subjects (0.14 ± 0.01), t(28) = -2.65, p = 0.01. Patients with PD (0.16 ± 0.02), meanwhile, did not have any significant differences in stabilization tremor between control subjects, t(39) = -1.01, p = 0.32 , nor patients with ET, t(29) = -0.99, p = 0.33. Figure 5C depicts sample participants from each group (selected based on proximity to the average range of the respective group in Figure 5C), emphasizing that patients with ET typically exhibit higher magnitudes of tremor during movement stabilization throughout the training period. With this, we demonstrate that increased tremor magnitude does not impair reaching movement but may impair movement stabilization. That is, patients with ET have significantly greater tremor force magnitude during movement stabilization, generating noise that has the potential to interfere with endpoint acuity.

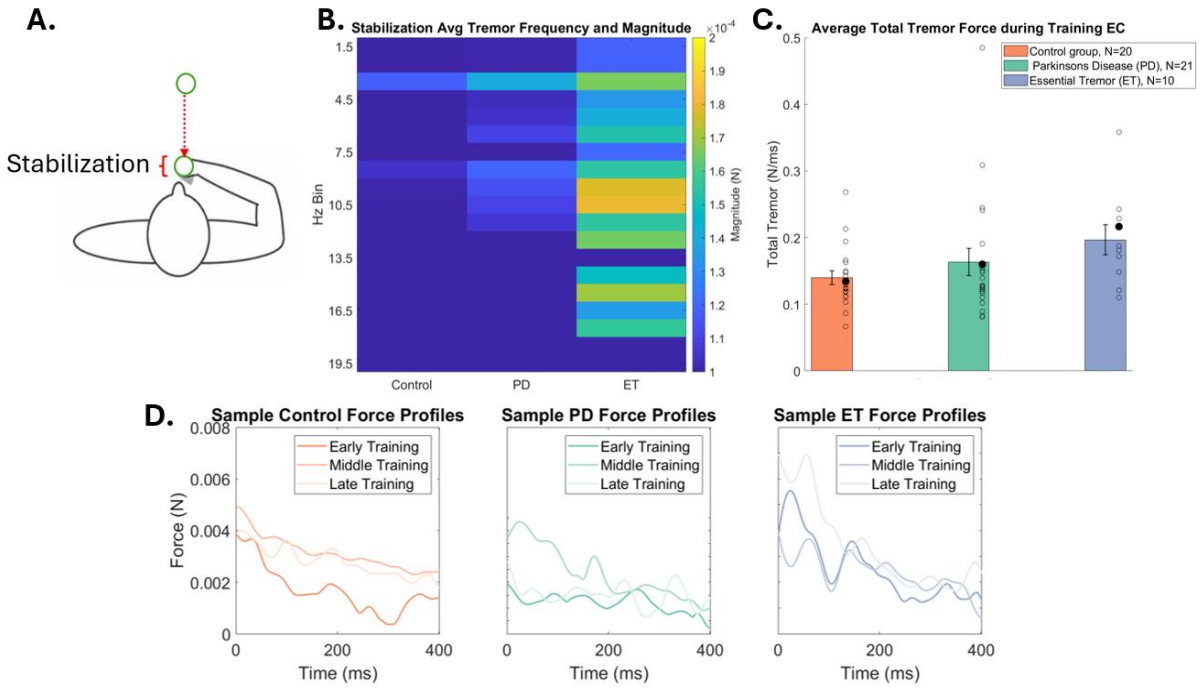

Figure 5. Stabilization. A. The window of movement that defines movement stabilization is the first time the cursor crosses the threshold of the end target to the end of movement reach (as also defined in Blondieux et al., 2023), resulting in a 500ms window of stabilization for every trial. However, to account for movement remaining at the end of reach movement and movement out of the target to begin the next trial, we got rid of 50ms from both the beginning and end of this window, leaving us with a 400 ms window. **B.** Heatmap demonstrates the

average magnitude for each frequency bin across groups **C.** Bar graphs (SEM error bars) demonstrate differences in average total tremor magnitude during training between groups. We see that, during stabilization, patients with ET have significantly greater tremor magnitudes. **C.** Sample participant force profiles demonstrate the average difference in raw force profile before tremor extraction during movement stabilization throughout different periods of training. Participants were chosen based on their data falling within the average range from figure 5C.

To assess differences in motor acuity, we looked at trial by trial endpoint precision through variable error endpoint measures, as described in McKenna et al., 2017. Movement endpoint was defined as the x- and y-positions of the subject's hand location when the movement speed was less than 0.05 m/s for at least 50 ms for the first time. Endpoint precision was measured through variable error, which was determined by the standard deviation of these displacements, calculated as the difference between movement endpoint and mean movement endpoint location. Figure 6A demonstrates that patients with ET (Mean ± SEM, 0.11 ± 0.003) had the greatest variance in end of movement precision compared to both control subjects (0.007 ± 0.0004), and patients with PD (0.007 ± 0.0005),One-way ANOVA: $F_{(2,50)} = 4.18$, $p = 0.02$. Thus, a greater tremor magnitude, as demonstrated in Figure 5B and C, is associated with greater difficulty in end of movement precision, a type of acuity.

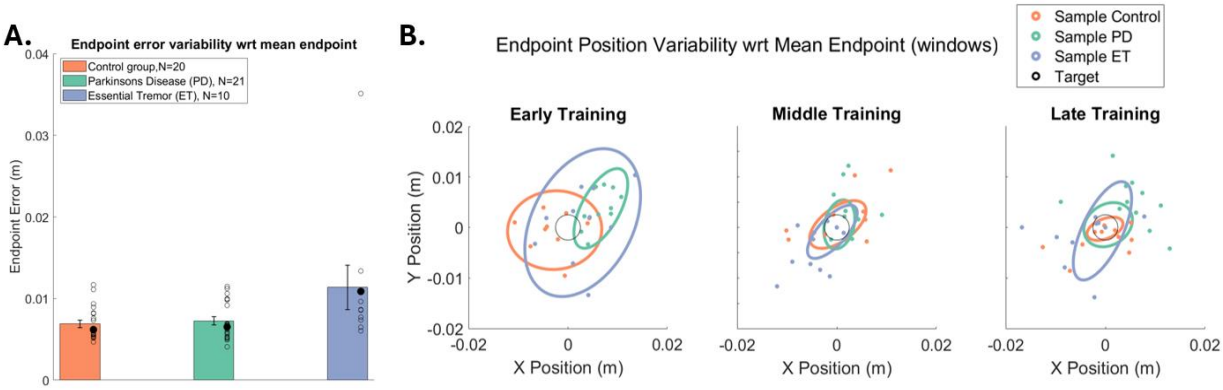

Figure 6. Endpoint Variability. A. Precision: bar graphs show how variable endpoint error (difference between endpoint error in a single trial and the mean endpoint error) differs between groups. **B.** Ellipses (2 standard deviation intervals) represent the distribution of variable endpoint error in sample participants (control: orange; PD: green; ET: purple) and trials as it relates to the target (black circle) during early, middle and late training periods. Participants were chosen based on their data falling within the average range from figure 6A.

Next, we examined the relationship between tremor magnitude and variable error in ET. A Spearman's correlation indicated an insignificant positive relationship between average tremor magnitude and endpoint variable error in patients with ET ($r_s(18) = 0.39$, $p = 0.26$). As we do not see a strong or significant relationship between tremor magnitude in ET and end-of-movement precision, we must also consider other factors for increased endpoint variability. Dysmetria is another characteristic of ET in which patients are known to overshoot or undershoot an intended target. Tremor and dysmetria are unrelated (Casamento-Moran et al., 2021), and we could not distinguish between them at this time. Therefore, our available evidence suggests that greater tremor magnitude during the end of movement is associated with reduced acuity, but is not likely the cause.

Patients with PD have increased tremor magnitude and decreased stability during postural hold

As shown in Figure 7B, during postural hold, patients with PD exhibited the largest postural tremor magnitude (Peak Magnitude, Average Corresponding Frequency: 0.0081 N, 4.5Hz) compared to patients with ET (0.0054 N ± 3.5 Hz) and control subjects (0.004 N ± 3.5 Hz). This increased tremor magnitude resulted in greater difficulty for PD patients to maintain postural hold compared to the control group, as evidenced by the significantly larger amount of total force required to remain at the target (Mean ± SEM; PD: 2.19 ± 0.29; Control: 1.36 ± 0.21),$F_{(2,50)} = 3.18$, $p= 0.05$. . Patients with ET (1.44 ± 0.26) did not have a significantly larger tremor magnitude during postural

hold and therefore did not display any greater difficulty maintaining postural hold compared to the control group. With this, we demonstrate that increased tremor magnitude present during postural hold results in increased effort to maintain a stable state in the upper limb.

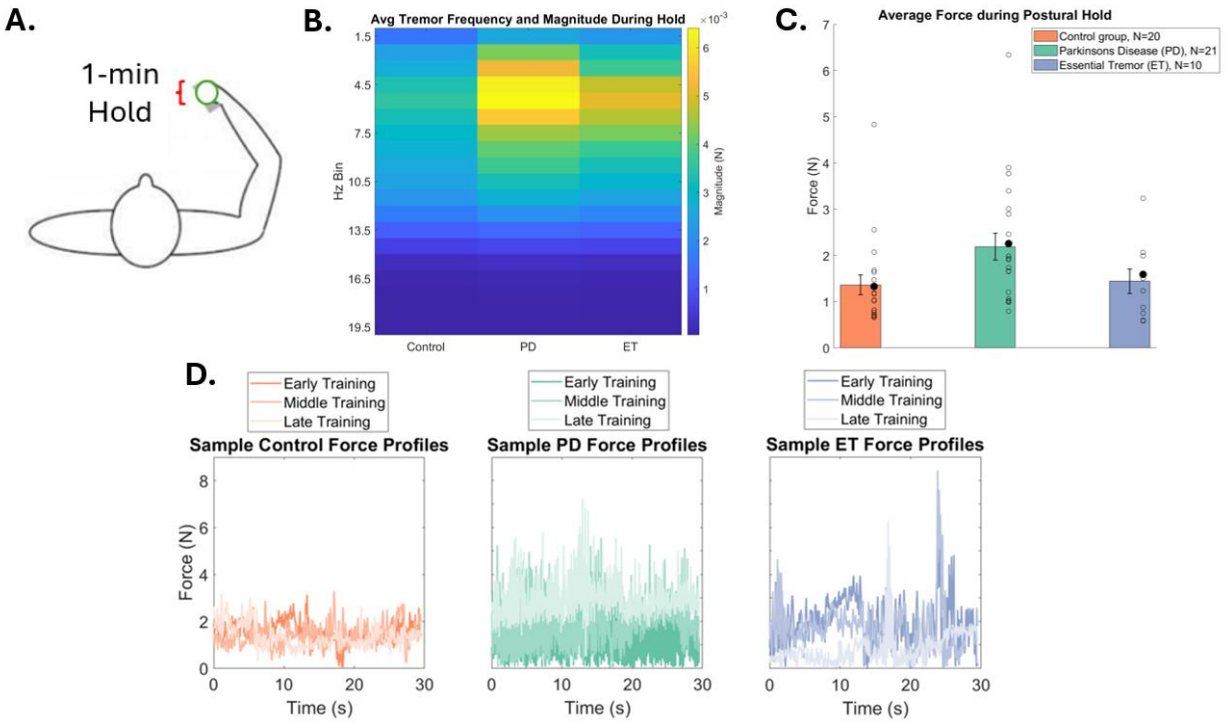

Figure 7. Postural Hold. A. Postural hold is defined as the 1-minute period during which participants are asked to hold the cursor at a target. B. A heatmap demonstrates differences in average tremor frequency (y-axis) and magnitude (heat bar) between groups during postural hold. C. Bar plots (SEM error bars) compare the total average amount of force used by each group to maintain postural hold. D. Sample participant force profiles demonstrate the average difference in raw force profile before tremor extraction during postural hold. Participants were chosen based on their data falling within the average range from figure 7C.

DISCUSSION

Pathological tremor does not impair motor adaptation to physical perturbations, regardless of magnitude

The motor learning literature for both Parkinson's Disease (PD) and Essential Tremor (ET) has demonstrated that pathological tremor does not underlie noted impairments in motor

adaptation. This is consistent with our study results, which found that there were no adaptive learning differences between patient groups with pathological tremor and control subjects regardless of pathological tremor magnitude or frequency.

As shown in Figure 2, we observed no significant difference in force profiles between participant groups during adaptation to lateral force-field perturbations. However, due to ET characteristically being an action tremor, we did see a significantly higher average tremor magnitude during the reaching movement as expected. Despite ET patients having a higher average tremor magnitude during the reaching movement (Figure 4 B, C), these patients performed similar to control subjects. This is surprising because tremor magnitude is noted to be the most disruptive to patients with pathological tremor. Thus, we can assume that increased tremor magnitude does not significantly impact the amount of force used to adapt to the lateral FF perturbation. Aside from differences in tremor manifestations during reaching movement, the three groups only differed based on movement speed, which we account for in our analyses (Figure 3).

We see no difference in total force profiles between participants during movement (Figure 4). Therefore, tremor does not significantly impact the temporal pattern of applied force during the reaching movement, specifically during the adaptation to a lateral force field perturbations. This explains why reaching movement adaptation was unimpaired across groups, regardless of tremor manifestation. On first glance, our results are not aligned with the findings of Blondieaux et al (2023), which found that ET patients had impaired upper limb adaptation to a force field perturbation. However, Blondieaux et al. demonstrated that this reduced ability to adapt was not due to learning differences (an ability to detect errors), but rather impairments in movement execution. Specifically, they detected greater movement variability, poorer movement precision, and increased endpoint scatter, all which do not directly reflect motor adaptation. Differences in how we measured learning is most likely the explanation for our differences in findings. Blondieaux measured adaptation via reach angle, which measures deviations in hand position,

while we relied on direct temporal force measures. This may also explain why differences in adaptation have been observed in individuals with PD when assessed using a visuomotor rotation paradigm that similarly relies on deviations in hand position, but were not observed in our study.We were still able to conclude that there were no learning differences between groups, but rather movement differences in tremor, movement duration, and peak velocity, which are movement execution differences rather than learning differences, just as Blondieaux found.

Increased tremor magnitude in ET co-occurs with impaired end of movement stability and acuity

Movement stabilization is a transition from movement (change in sensory state) to hold (maintenance of sensory state) (Shadmehr, 2017) and is associated with a deceleration of movement (Hadjiosif et al., 2025). Our results suggest that a significantly greater magnitude of tremor in patients with ET (Figure 4) co-occurs with impaired movement endpoint stability and acuity (Figure 5). This finding is consistent with Blondieaux et al (2023), which found greater variability in endpoint scatter (i.e. less movement endpoint precision), due to the noisiness of the reaching movement. Indeed, in our own data we see that patients with ET have significantly greater magnitudes of tremor during reaching and stabilization of movement (Figure 4) as well as impaired endpoint variability reflecting deficits in movement precision (Figure 5). Because both individuals with PD and control participants exhibited relatively low tremor-related movement variability during reaching and movement stabilization, their ability to stabilize their movements was largely preserved.

Impaired movement stabilization in patients with ET cannot be definitively attributed to increased tremor magnitude during movement reach and stabilization. Current evidence suggests that ET is caused by impaired functional connectivity within the cerebello-thalmo-cortical circuitry (Nicoletti et al., 2020). Dysfunction of the cerebellum can cause a number of ataxic movements that would explain impaired movement endpoint acuity, including dysmetria (i.e., a lack of coordination that manifests as overshooting or undershooting an intended target). Tremor and dysmetria are most likely controlled by different pathways and dysmetria is not affected by

movement tremor (Casamento-Moran et al., 2021). Since it is difficult to determine if impaired movement endpoint stability is due to dysmetria or tremor, we can only note that significantly greater tremor magnitude in patients with ET during movement stabilization was associated with reduced movement endpoint precision. Patients with PD and healthy controls who did not have this high magnitude tremor did not exhibit similar impairments in precision.

Movement reach and movement stabilization are believed to be controlled by two different pathways, or controllers, linked by a downstream neural integrator (Jayasinghe et al., 2022). Evidence from stroke patients demonstrates that, even when movement reach is impaired, there is an intact relationship between movement reach and movement stabilization, suggesting that the neural integrator is downstream of the reaching controllers (Jayasinghe et al., 2022). As the holding controller is also downstream of the reaching controller, the holding controller is impacted by the outputs of the reaching controller. Our findings support this as the increased tremor magnitude seen in patients with ET persists from the reaching stage of movement (as seen in Figure 4) into the stabilization phase (as seen in Figure 5) and may contribute to difficulties with stabilization (as seen in Figure 6).

Increased tremor magnitude in PD impairs postural hold

Movement hold is the maintenance of a specific sensory state (Shadmehr, 2017). In the case of the current study, participants were asked to hold the handle of a robotic manipulandum without any limb support for a full minute. As PD characteristically is a rest tremor that can re-emerge while sustaining a posture (Dirkx et al., 2018), we expected to see an increase in tremor magnitude in patients with PD when holding upper limb posture compared to healthy controls and patients with ET. We found that patients with PD had a significantly greater tremor magnitude, which resulted in the need to use a greater amount of force to maintain upper limb postural hold. Just as with movement stabilization, movement hold is hypothesized to be controlled by a separate pathway than movement reach and is most likely located downstream of the reaching controller (Shadmehr, 2017; Hadjiosif et al., 2025). Within this line of thinking, resting postural

force states should not have a significant effect on the control of active reaching movements (Hadjiosif et al., 2025). As reaching movement in patients with PD was unimpaired within our data, this provides further support for the idea that the hold controller is functionally distinct and downstream of the reach controller. If reaching and holding relied on the same controller, increased tremor present during the hold period would be expected to impair the reaching movement as well. Instead, we found that increased tremor magnitude only results in performance impairments in postural hold, not movement reach. This suggests that the processes underlying movement reach remain intact despite the presence of sensorimotor noise (tremor) while the mechanisms required to maintain postural hold are impaired by this increased tremor. Therefore, the selective effects of tremor on different phases on movement provides further evidence on a functionally distinct reaching and holding controller.

Additionally, we find that patients with ET who had significantly higher tremor magnitudes during movement reach and stabilization did not have the same difficulty during postural hold. Within the hypothesis, the holding controller should be impacted by the outputs of the reaching controller (Jaysinghe et al., 2022). However, within patients with ET, the higher tremor magnitudes present during movement reach only impact end of movement stabilization, though not hold. This pattern suggests that tremor-related variability during reaching may interfere with the transition from active movement to a stable final posture, rather than disrupting the mechanisms responsible for maintaining that posture once it has been established. If stabilization is thought of as the transition from reaching to hold, then we can assume that the neural integrator is impaired by reaching tremor, but reaching tremor does not impact the hold controller itself. Therefore, increased tremor magnitude during movement reach may impair the integration of sensory and motor information required to accurately terminate the movement and establish the desired posture without disrupting maintenance of the postural hold.

Implications of our findings for patients with movement disorders

We have systematically shown how tremor manifests across two different movement disorders (PD and ET) during different stages of movement (Stabilization, Reaching and Postural Hold). We provide additional support for the hypothesis that movement reach and movement hold are controlled by two different but connected neural mechanisms and find that the hold controller is most clearly impaired by increased tremor magnitude. We provide additional evidence that while motor adaptation is not impaired in patients with PD and ET, movement precision is.

Identifying which specific underlying mechanisms of movement and motor adaptation are impaired by movement disorder symptoms is vital to develop targeted treatments. For example, Bryant et al., (2018) tested a hand resistance exercise regime as an intervention for impaired handwriting in PD and ET patients. However, after 6 weeks, no improvements in either group were found. To best understand how to better tailor treatment to improve motor impairment in movement disorders, such as handwriting, we must first understand the precise neural mechanisms that are impaired. To better perform this research, we must also have a systematic and continuous method of measuring motor learning and motor symptoms, such as tremor.

The current gold standard for diagnosing and measuring pathological tremor in a clinical setting is a pen-and-paper physical assessment performed by a neurologist specializing in movement disorders (Mahendran et al., 2022; di Biase et al., 2017). Rating a tremor based on its severity and impact on daily living is typically categorized by standardized, ordinal scales. For PD tremor, the most commonly used assessment is Part III of the Movement Disorder Society-Unified Parkinson's Disease Rating Scale (MDS-UPDRS) (Schwarz et al., 2011). For ET, the most widely used is the Essential Tremor Rating Assessment Scale (TETRAS) (Elble, 2016; Ondo et al., 2017). Both of these scales rate the magnitude of the tremor on a 5-point scale from no tremor (score of 0) to severe (score of 4, MDS-UPDRS: >10cm and TETRAS: >20cm) (Elble et al., 2017; Guo et al., 2022; Pasquini et al., 2023).

In research, as well as some clinical settings, tremor is typically measured by combining the aforementioned rating scales with wearable sensors and electrophysiological tools (Hess &

Pullman, 2012). This allows investigators to quantify the frequency and tremor magnitude. Although electromyography (EMG) is considered the gold standard for this type of quantification (Vescio et al., 2021), other common tools include accelerometry and digitized spiral analysis (Hess & Pullman, 2012; Longardner et al., 2019; Paredes-Acuna et al., 2024). These methods can be utilized to measure tremor during movement and rest but have key limitations. EMG measures electrical signals of muscle contraction, not the physical amplitude or frequency of the tremor itself, making measurement of action/kinetic tremors difficult and often requiring combined use with accelerometers (Paredes-Acuna et al., 2024). Accelerometers themselves, while useful for movement-based measurements (Paredes-Acuna et al., 2024), are prone to noise such as gravitational artifacts, where the device cannot distinguish between movement of the limb and effects due to gravity (Elble, 2005). Digitized spiral analysis is useful for action/kinetic tremor in task-based measurements (Paredes-Acuna et al., 2024), such as writing and drawing. However, it is of little utility in measuring postural or resting tremor, as it requires active movement of the limb (Paredes-Acuna et al., 2024). Additionally, there are no standardized collection and analysis protocols for tremor quantification using any of these devices (Wang et al., 2025). Because of this, there has yet to be an all-inclusive, systematic quantification of tremor during different types and stages of movement. In our study, we utilized force sensors in conjunction with a commonly used arm reaching paradigm to continuously measure tremor during different stages of movement and motor adaptation. Our utilization of SSA and FFT allowed us to separate movement tremor (involuntary, oscillatory movement) from intentional movement (voluntary, non-oscillatory movement). In doing so, we are able to provide online tremor quantification simultaneously with motor adaptation and control, providing clearer insights into the underlying mechanisms affected by tremor.

Overall, our findings reveal that tremor impacts postural hold, but not movement reach. Greater tremor magnitude increases the demands placed on the postural control system by producing larger deviations from the desired body position and requiring more frequent or greater

corrective adjustments. Consequently, tremor may compromise balance by increasing the effort required to maintain postural stability. As PD and ET have different tremor presentations and pathologies (Vuong et al., 2026), understanding how tremor manifestation differentially affects specific aspects of movement could allow us to develop therapeutic strategies that improve movement and stabilize posture, allowing patients to retain agency and quality of life for longer.

Limitations

We would like to acknowledge some limitations to our findings, which have influenced our results. Almost all of our patients with PD were actively on dopaminergic medication throughout the experiment, which could have impacted tremor presentation and movement. Additionally, although PD is a heterogeneous disorder, we did not separate participants based on subtype. Finally, our ET group was, on average, younger than the PD group which is reasonable given the differences in average disease onset but may influence the differences we see between groups in addition to the tremor.

REFERENCES

Alhussein, L., Hosseini, E. A., Nguyen, K. P., Smith, M. A., & Joiner, W. M. (2019). Dissociating effects of error size, training duration, and amount of adaptation on the ability to retain motor memories. *Journal of Neurophysiology*, *122*(5), 2027–2042. https://doi.org/10.1152/jn.00387.2018

Alty, J. E., & Kempster, P. A. (2011). A practical guide to the differential diagnosis of tremor. *Postgraduate Medical Journal*, *87*(1031), 623–629. https://doi.org/10.1136/pgmj.2009.089623

Bhatia, K. P., Bain, P., Bajaj, N., Elble, R. J., Hallett, M., Louis, E. D., Raethjen, J., Stamelou, M., Testa, C. M., & Deuschl, G. (2018). Consensus Statement on the Classification of Tremors. From the Task Force on Tremor of the International Parkinson and Movement Disorder Society. *Movement Disorders : Official Journal of the Movement Disorder Society*, *33*(1), 75–87. https://doi.org/10.1002/mds.27121

Bindel, L., Mühlberg, C., Pfeiffer, V., Nitschke, M., Müller, A., Wegscheider, M., Rumpf, J.-J., Zeuner, K. E., Becktepe, J. S., Welzel, J., Güthe, M., Classen, J., & Tzvi, E. (2022). Visuomotor Adaptation Deficits in Patients with Essential Tremor. *The Cerebellum*. https://doi.org/10.1007/s12311-022-01474-5

Blondiaux, F., Lebrun, L., Hanseeuw, B. J., & Crevecoeur, F. (2023). Impairments of saccadic and reaching adaptation in essential tremor are linked to movement execution. *Journal of Neurophysiology*, *130*(5), 1092–1102. https://doi.org/10.1152/jn.00165.2023

Bötzel, K., Tronnier, V., & Gasser, T. (2014). The Differential Diagnosis and Treatment of Tremor. *Deutsches Ärzteblatt International*, *111*(13), 225–236. https://doi.org/10.3238/arztebl.2014.0225

Bryant, M. S., Workman, C. D., Jamal, F., Meng, H., & Jackson, G. R. (2018). Feasibility study: Effect of hand resistance exercise on handwriting in Parkinson's disease and essential tremor. *Journal of Hand Therapy*, *31*(1), 29–34. https://doi.org/10.1016/j.jht.2017.01.002

Casamento-Moran, A., Yacoubi, B., Wilkes, B. J., Hess, C. W., Foote, K. D., Okun, M. S., Wagle Shukla, A., Vaillancourt, D. E., & Christou, E. A. (2020). Quantitative Separation of Tremor and

Ataxia in Essential Tremor. *Annals of Neurology*, *88*(2), 375–387. https://doi.org/10.1002/ana.25781

Chen, H., Hua, S. E., Smith, M. A., Lenz, F. A., & Shadmehr, R. (2006). Effects of Human Cerebellar Thalamus Disruption on Adaptive Control of Reaching. *Cerebral Cortex*, *16*(10), 1462–1473. https://doi.org/10.1093/cercor/bhj087

Conditt, M. A., Gandolfo, F., & Mussa-Ivaldi, F. A. (1997). The Motor System Does Not Learn the Dynamics of the Arm by Rote Memorization of Past Experience. *Journal of Neurophysiology*, *78*(1), 554–560. https://doi.org/10.1152/jn.1997.78.1.554

Conditt, M. A., & Mussa-Ivaldi, F. A. (1999). Central representation of time during motor learning. *Proceedings of the National Academy of Sciences*, *96*(20), 11625–11630. https://doi.org/10.1073/pnas.96.20.11625

Crawford, P., & Zimmerman, E. E. (2011). Differentiation and Diagnosis of Tremor. *American Family Physician*, *83*(6), 697–702.

Dirkx, M. F., Zach, H., Bloem, B. R., Hallett, M., & Helmich, R. C. (2018). The nature of postural tremor in Parkinson disease. *Neurology*, *90*(13), e1095–e1103. https://doi.org/10.1212/WNL.0000000000005215

Domellöf, M. E., Elgh, E., & Forsgren, L. (2011). The relation between cognition and motor dysfunction in drug-naive newly diagnosed patients with Parkinson's disease. *Movement Disorders: Official Journal of the Movement Disorder Society*, *26*(12), 2183–2189. https://doi.org/10.1002/mds.23814

Elble, R., Comella, C., Fahn, S., Hallett, M., Jankovic, J., Juncos, J. L., LeWitt, P., Lyons, K., Ondo, W., Pahwa, R., Sethi, K., Stover, N., Tarsy, D., Testa, C., Tintner, R., Watts, R., & Zesiewicz, T. (2012). Reliability of a new scale for essential tremor. *Movement Disorders : Official Journal of the Movement Disorder Society*, *27*(12), 1567–1569. https://doi.org/10.1002/mds.25162

Elble, R. J. (1996). Central Mechanisms of Tremor. *Journal of Clinical Neurophysiology*, *13*(2), 133.

Elble, R. J. (2005). Gravitational artifact in accelerometric measurements of tremor. *Clinical Neurophysiology*, *116*(7), 1638–1643. https://doi.org/10.1016/j.clinph.2005.03.014

Elble, R. J. (2017). Tremor. In B. Tousi & J. Cummings (Eds.), *Neuro-Geriatrics: A Clinical Manual* (pp. 311–326). Springer International Publishing. https://doi.org/10.1007/978-3-319-56484-5_20

Foray, K., Zhou, W., Fitzgerald, J., Gianferrara, P. G., & Joiner, W. M. (2025). Applied Motor Noise Affects Specific Learning Mechanisms during Short-Term Adaptation to Novel Movement Dynamics. *eNeuro*, *12*(1). https://doi.org/10.1523/ENEURO.0100-24.2024

Gironell, A., Pascual-Sedano, B., Aracil, I., Marín-Lahoz, J., Pagonabarraga, J., & Kulisevsky, J. (2018). Tremor Types in Parkinson Disease: A Descriptive Study Using a New Classification. *Parkinson's Disease*, *2018*(1), 4327597. https://doi.org/10.1155/2018/4327597

Golyandina, N., & Zhigljavsky, A. (2020). Basic SSA. In N. Golyandina & A. Zhigljavsky (Eds.), *Singular Spectrum Analysis for Time Series* (pp. 21–90). Springer. https://doi.org/10.1007/978-3-662-62436-4_2

Gonzalez Castro, L. N., Hadjiosif, A. M., Hemphill, M. A., & Smith, M. A. (2014). Environmental Consistency Determines the Rate of Motor Adaptation. *Current Biology*, *24*(10), 1050–1061. https://doi.org/10.1016/j.cub.2014.03.049

Guo, Y., Stebbins, G. T., Mestre, T. A., Goetz, C. G., & Luo, S. (2022). Movement Disorder Society Unified Parkinson's Disease Rating Scale Motor Examination Retains Its 2-Domain Profile in Both On and Off States. *Movement Disorders Clinical Practice*, *9*(8), 1149–1151. https://doi.org/10.1002/mdc3.13566

Hadjiosif, A. M., Kita, K., Albert, S. T., Scheidt, R. A., Shadmehr, R., & Krakauer, J. W. (2025). Separating the control of moving and holding in human post-stroke arm paresis. *eLife*, *12*, RP90780. https://doi.org/10.7554/eLife.90780

Hassani, H. (2007, April 1). *Singular Spectrum Analysis: Methodology and Comparison* [MPRA Paper]. Cardiff University and Central Bank of the Islamic Republic of Iran. https://mpra.ub.uni-muenchen.de/4991/

Hentschke, H. (2026). *Hhentschke/measures-of-effect-size-toolbox* [Matlab]. https://github.com/hhentschke/measures-of-effect-size-toolbox (Original work published 2017)

Hess, C. W., & Pullman, S. L. (2012). Tremor: Clinical phenomenology and assessment techniques. *Tremor and Other Hyperkinetic Movements*, *2*, tre-02-65-365-1. https://doi.org/10.7916/D8WM1C41

Holtbernd, F., & Shah, N. J. (2021). Imaging the Pathophysiology of Essential Tremor—A Systematic Review. *Frontiers in Neurology*, *12*. https://doi.org/10.3389/fneur.2021.680254

Hosseini, E. A., Nguyen, K. P., & Joiner, W. M. (2017). The decay of motor adaptation to novel movement dynamics reveals an asymmetry in the stability of motion state-dependent learning. *PLOS Computational Biology*, *13*(5), e1005492. https://doi.org/10.1371/journal.pcbi.1005492

Hwang, E. J., Smith, M. A., & Shadmehr, R. (2006). Adaptation and generalization in acceleration-dependent force fields. *Experimental Brain Research*, *169*(4), 496–506. https://doi.org/10.1007/s00221-005-0163-2

JANKOVIC, J., & STANLEY, F. (1980). Physiologic and Pathologic Tremors. *Annals of Internal Medicine*, *93*(3), 460–465. https://doi.org/10.7326/0003-4819-93-3-460

Jayasinghe, S. A. L., Scheidt, R. A., & Sainburg, R. L. (2022). Neural Control of Stopping and Stabilizing the Arm. *Frontiers in Integrative Neuroscience*, *16*, 835852. https://doi.org/10.3389/fnint.2022.835852

Joiner, W. M., Brayanov, J. B., & Smith, M. A. (2013). The training schedule affects the stability, not the magnitude, of the interlimb transfer of learned dynamics. *Journal of Neurophysiology*, *110*(4), 984–998. https://doi.org/10.1152/jn.01072.2012

Joiner, W. M., Sing, G. C., & Smith, M. A. (2017). Temporal specificity of the initial adaptive response in motor adaptation. *PLOS Computational Biology*, *13*(7), e1005438. https://doi.org/10.1371/journal.pcbi.1005438

Joiner, W. M., & Smith, M. A. (2008). Long-Term Retention Explained by a Model of Short-Term Learning in the Adaptive Control of Reaching. *Journal of Neurophysiology*, *100*(5), 2948–2955. https://doi.org/10.1152/jn.90706.2008

Limb motion dictates how motor learning arises from arbitrary environmental dynamics | Journal of Neurophysiology | American Physiological Society. (n.d.). Retrieved August 20, 2026, from https://journals.physiology.org/doi/full/10.1152/jn.00497.2011

Lin, Y., Ling, B. W.-K., Xu, N., Lam, R. W.-K., & Ho, C. Y.-F. (2020). Effectiveness analysis of bio-electronic stimulation therapy to Parkinson's diseases via joint singular spectrum analysis and discrete fourier transform approach. *Biomedical Signal Processing and Control*, *62*, 102131. https://doi.org/10.1016/j.bspc.2020.102131

Lippold, O. (1971). Physiological Tremor. *Scientific American*, *224*(3), 65–73.

Longardner, K., Undurraga, F. V., Nahab, F. B., Hallett, M., & Haubenberger, D. (2019). How Do I Assess Tremor Using Novel Technology? *Movement Disorders Clinical Practice*, *6*(8), 733–734. https://doi.org/10.1002/mdc3.12818

Louis, E. D. (2005). Essential tremor. *The Lancet Neurology*, *4*(2), 100–110. https://doi.org/10.1016/S1474-4422(05)00991-9

Mahendran, S., Bichsel, O., Gassert, R., Baumann, C. R., Imbach, L. L., & Waldvogel, D. (2022). Differentiation of Parkinson's disease tremor and essential tremor based on a novel hand posture. *Clinical Parkinsonism & Related Disorders*, *7*, 100146. https://doi.org/10.1016/j.prdoa.2022.100146

Marshall, J., & Walsh, E. G. (1956). PHYSIOLOGICAL TREMOR. *Journal of Neurology, Neurosurgery, and Psychiatry*, *19*(4), 260–267. https://doi.org/10.1136/jnnp.19.4.260

McKenna, E., Bray, L. C. J., Zhou, W., & Joiner, W. M. (2017). The absence or temporal offset of visual feedback does not influence adaptation to novel movement dynamics. *Journal of Neurophysiology*, *118*(4), 2483–2498. https://doi.org/10.1152/jn.00636.2016

Mongeon, D., Blanchet, P., & Messier, J. (2013). Impact of Parkinson's disease and dopaminergic medication on adaptation to explicit and implicit visuomotor perturbations. *Brain and Cognition*, *81*(2), 271–282. https://doi.org/10.1016/j.bandc.2012.12.001

Moustafa, A. A., Krishna, R., Eissa, A. M., & Hewedi, D. H. (2013). Factors underlying probabilistic and deterministic stimulus-response learning performance in medicated and unmedicated patients with Parkinson's disease. *Neuropsychology*, *27*(4), 498–510. https://doi.org/10.1037/a0032757

Nguyen, K. P., Zhou, W., McKenna, E., Colucci-Chang, K., Bray, L. C. J., Hosseini, E. A., Alhussein, L., Rezazad, M., & Joiner, W. M. (2019). The 24-h savings of adaptation to novel movement dynamics initially reflects the recall of previous performance. *Journal of Neurophysiology*, *122*(3), 933–946. https://doi.org/10.1152/jn.00569.2018

Nicoletti, V., Cecchi, P., Pesaresi, I., Frosini, D., Cosottini, M., & Ceravolo, R. (2020). Cerebello-thalamo-cortical network is intrinsically altered in essential tremor: Evidence from a resting state functional MRI study. *Scientific Reports*, *10*, 16661. https://doi.org/10.1038/s41598-020-73714-9

Ondo, W., Hashem, V., LeWitt, P. A., Pahwa, R., Shih, L., Tarsy, D., Zesiewicz, T., & Elble, R. (2017). Comparison of the Fahn-Tolosa-Marin Clinical Rating Scale and the Essential Tremor Rating Assessment Scale. *Movement Disorders Clinical Practice*, *5*(1), 60–65. https://doi.org/10.1002/mdc3.12560

O'Shea, S. A., & Shih, L. C. (2023). Global Epidemiology of Movement Disorders: Rare or Underdiagnosed? *Seminars in Neurology*, *43*(1), 4–16. https://doi.org/10.1055/s-0043-1764140

Paredes-Acuna, N., Utpadel-Fischler, D., Ding, K., Thakor, N. V., & Cheng, G. (2024). Upper limb intention tremor assessment: Opportunities and challenges in wearable technology. *Journal of Neuroengineering and Rehabilitation*, *21*(1), 8. https://doi.org/10.1186/s12984-023-01302-9

Pasquini, J., Deuschl, G., Pecori, A., Salvadori, S., Ceravolo, R., & Pavese, N. (2023). The Clinical Profile of Tremor in Parkinson's Disease. *Movement Disorders Clinical Practice*, *10*(10), 1496–1506. https://doi.org/10.1002/mdc3.13845

Readman, M. R., Crawford, T. J., Linkenauger, S. A., Bek, J., & Poliakoff, E. (2023). Motor imagery vividness and symptom severity in Parkinson's disease. *Journal of Neuropsychology*, *17*(1), 180–192. https://doi.org/10.1111/jnp.12293

Scheidt, R. A., Reinkensmeyer, D. J., Conditt, M. A., Rymer, W. Z., & Mussa-Ivaldi, F. A. (2000). Persistence of Motor Adaptation During Constrained, Multi-Joint, Arm Movements. *Journal of Neurophysiology*, *84*(2), 853–862. https://doi.org/10.1152/jn.2000.84.2.853

Schwarz, J., Odin, P., Buhmann, C., Csoti, I., Jost, W., Wüllner, U., & Storch, A. (2011). Depression in Parkinson's disease. *Journal of Neurology*, *258*(Suppl 2), S336-338. https://doi.org/10.1007/s00415-011-6048-3

Shadmehr, R. (2017). Distinct neural circuits for control of movement vs. Holding still. *Journal of Neurophysiology*, *117*(4), 1431–1460. https://doi.org/10.1152/jn.00840.2016

Shadmehr, R., & Mussa-Ivaldi, F. A. (1994). Adaptive representation of dynamics during learning of a motor task. *Journal of Neuroscience*, *14*(5), 3208–3224. https://doi.org/10.1523/JNEUROSCI.14-05-03208.1994

Sing, G. C., Joiner, W. M., Nanayakkara, T., Brayanov, J. B., & Smith, M. A. (2009). Primitives for Motor Adaptation Reflect Correlated Neural Tuning to Position and Velocity. *Neuron*, *64*(4), 575–589. https://doi.org/10.1016/j.neuron.2009.10.001

Smith, M. A., Ghazizadeh, A., & Shadmehr, R. (2006). Interacting Adaptive Processes with Different Timescales Underlie Short-Term Motor Learning. *PLOS Biology*, *4*(6), e179. https://doi.org/10.1371/journal.pbio.0040179

Stegemöller, E., Zaman, A., MacKinnon, C. D., Tillman, M. D., Hass, C. J., & Okun, M. S. (2016). Laterality of repetitive finger movement performance and clinical features of Parkinson's disease. *Human Movement Science*, *49*, 116–123. https://doi.org/10.1016/j.humov.2016.06.015

The Essential Tremor Rating Assessment Scale. (2016). *Journal of Neurology & Neuromedicine*, *1*(4). https://www.jneurology.com/articles/the-essential-tremor-rating-assessment-scale.html

Vakil, E., & Herishanu-Naaman, S. (1998). Declarative and procedural learning in Parkinson's disease patients having tremor or bradykinesia as the predominant symptom. *Cortex; a Journal Devoted to the Study of the Nervous System and Behavior*, *34*(4), 611–620. https://doi.org/10.1016/s0010-9452(08)70518-5

Vescio, B., Quattrone, A., Nisticò, R., Crasà, M., & Quattrone, A. (2021). Wearable Devices for Assessment of Tremor. *Frontiers in Neurology*, *12*, 680011. https://doi.org/10.3389/fneur.2021.680011

Vuong, M. Q., Sreenivasan, V., Lee, S., Quinn, B., Keung, M. S., Grundy, M., Ayala Castañeda, J., Baek, H., & McKeown, M. J. (2026). Low-intensity transcranial ultrasound effects on the ventral intermediate nucleus and zona incerta in Parkinson's disease tremor. *Brain Stimulation*, *19*(1), 103025. https://doi.org/10.1016/j.brs.2026.103025

Wagner, M. J., & Smith, M. A. (2008). Shared Internal Models for Feedforward and Feedback Control. *Journal of Neuroscience*, *28*(42), 10663–10673. https://doi.org/10.1523/JNEUROSCI.5479-07.2008

Wanda, P. A., Li, G., & Thoroughman, K. A. (2013). State dependence of adaptation of force output following movement observation. *Journal of Neurophysiology*, *110*(5), 1246–1256. https://doi.org/10.1152/jn.00353.2012

Wang, S., Schwirtlich, T., McLaughlin, D., Beestrum, M., & Heinemann, A. W. (2025). Clinical Applications and Measurement Properties of the Digitized Archimedes Spiral Drawing Test: A Scoping Review. *Movement Disorders Clinical Practice*, *12*(11), 1742–1755. https://doi.org/10.1002/mdc3.70278

Wei, K., & Körding, K. (2009). Relevance of Error: What Drives Motor Adaptation? *Journal of Neurophysiology*, *101*(2), 655–664. https://doi.org/10.1152/jn.90545.2008

Yousif, N., & Diedrichsen, J. (2012). Structural learning in feedforward and feedback control. *Journal of Neurophysiology*, *108*(9), 2373–2382. https://doi.org/10.1152/jn.00315.2012

Zhou, W., Kruse, E. A., Brower, R., North, R., & Joiner, W. M. (2022). Motion state-dependent motor learning based on explicit visual feedback is quickly recalled, but is less stable than adaptation to physical perturbations. *Journal of Neurophysiology*, *128*(4), 854–871. https://doi org/10.1152/jn.00520.2021

Chapter 4: Parsing Error Source During Motor Adaptation in Parkinson's Disease

INTRODUCTION

The problem of untangling what drives changes in motor behavior is illustrated when shooting arrows at a target on a windy day. Imagin the case when even though you are aiming for the center, the arrow keeps landing on the outer rings. There are two possible reasons for this: the wind and your own ability. Eventually, through trial and error, you hit the bullseye. Motor adaptation is a type of trial-by-trial, error-based motor learning that adjusts motor output to reduce the mismatch between desired outcome and actual outcome (sensory prediction error) (Synofzik et al., 2006, 2008; Berniker and Körding, 2008; Shadmehr et al., 2010; Izawa and Shadmehr, 2011; Wolpert et al., 2011; Butcher et al., 2017). However, it is difficult to know what source of error was used to adjust motor behavior. There is strong evidence that when motor error occurs, such as missing the bullseye, the motor system can differentiate between how much of the error was caused by internal (ability to shoot straight) and external (the wind) variability when the errors are approximately the same magnitude (Ranjan & Smith, 2018; Kim et al., 2025).

In neurologically healthy adults, subjects can detect self-generated errors (SGEs) from externally-generated errors (EGEs) and their adaptive response when both are of the same magnitude is driven by the EGE (Ranjan & Smith, 2018). Thus, in the case above, with every shot you learn to account for how far the wind will carry the arrows and adjust your aim accordingly. You would not change your entire aiming strategy to account for a single arm twitch. This is most likely because motor noise, the source of SGE, is not only unpredictable (van Beers et al., 2009) but is also a constant property of the motor system and is internally compensated for (Faisal et al., 2008). Therefore, when the errors are approximately the same magnitude (i.e., small) only the magnitude of the EGE determines how much adaptation occurs.

However, there are individuals who produce a greater than average amount of motor variability due to neurological dysfunction. One such example is patients with Parkinson's Disease

(PD), who characteristically exhibit slowness of movement, rest tremor, stiffness, and impaired balance, which can impair movement control (Adamovich et al., 2001; Contreras-Vidal & Gold, 2004; Mongeon et al., 2015). The motor symptoms expressed in PD are the result of degeneration of dopaminergic neurons in the basal ganglia, resulting in impaired movement (Gironell et al., 2018). Rest and, later in disease progression, re-emergent postural tremor especially creates increased movement variability (Jankovic et al., 1999; Dirkx et al., 2018; Elble, 2013). While behavioral studies have demonstrated that a neurologically healthy motor system is able to compensate for motor noise during adaptation (Ranjan & Smith, 2018; Kim et al., 2025), it is currently unclear if this remains to be the case in a nervous system with increased motor noise. In this study, we aim to better understand how increased motor noise in patients with PD impacts the motor system's ability to parse and adapt to self- and externally-generated error.

METHODS

20 neurologically healthy controls (4M/16F, 69.5 ± 9.3 years) and 20 patients with diagnosed Parkinson's Disease (12M/8F, 65.5 ± 13.3 years) participated in the visuomotor rotation experiment. 10 neurologically healthy controls (3M/7F, 78.4 ± 4.6 years) and 10 patients with diagnosed Parkinson's Disease (7M/3F, 72.8 ± 8.3 years) participated in the force-field perturbation experiment. Participants provided written, informed consent in accordance with protocols approved by the Institutional Review Board at the University of California, Davis and were financially compensated for their part in the study. Clinical evaluations, such as motor scores, were performed by a neurologist at the University of California Movement Disorders Clinic. All participants used their right hand to complete the experiment, even if it was not their dominant hand (as determined by the Edinburgh Handedness Inventory). Table 1 outlines participant demographics for both the visuomotor rotation (Table 1A) and the force-field perturbation (Table 1B) experiment. Each participant performed the paradigm only once and was naive to the purpose of the experiment.

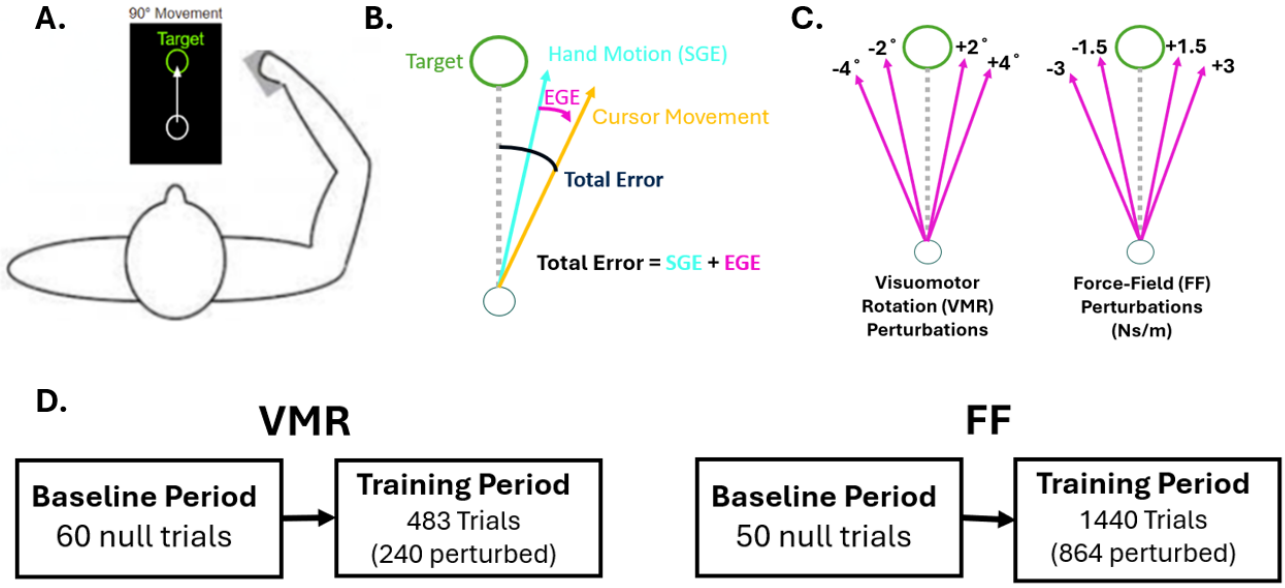

Figure 1. Experiment Set-up and Paradigm. A. In both experiments, Participants made straight arm reaching movements between two circular targets from midline. Forward reaching motion was completed in the 90° direction. The location of the hand was represented on the screen as a white filled circle. **B**. A schematic of how motor error is parsed. Self-Generated Error (SGE) is how much movement variability is inherent in each reaching action while Externally-Generated Error (EGE) is how much perturbation is applied to the reaching motion. Total error (where the cursor ends up) is the sum of SGE and the impact of EGE. **C.** Magnitude of perturbations applied in each experiment. In the visuomotor rotation (VMR) experiment, the cursor was rotated ±4˚ and ±2˚ from hand position. In the force-field (FF) perturbation experiment, hand position was laterally perturbed at ±3 and ±1.5 Ns/m. **D.** Paradigm structure for each experiment. In the VMR task, participants underwent a baseline period of 60 null trials to establish familiarity with the task. During the training period, every null movement trial was separated by a perturbed trial in which the cursor was rotated from the actual hand position. In the FF task, participants underwent a baseline period of 50 null trials followed by a training period in which every null trial was separated by a perturbation trial. The perturbations were lateral force-field perturbations perpendicular to hand position.

In both the visual and physical perturbation tasks, participants were asked to move a small, white cursor in a straight line between start and end targets, which were open red circles. A trial consisted of a single arm reach between the start target and end target. In the task, there were

two types of trials: null and perturbation. Null trials allowed participants to make straight arm reaching movements between the targets without any perturbations or restrictions to movement. During perturbation trials, participants received a perturbation lateral to their movement direction. For both experiments, we used a similar set up and experimental design as utilized by Ranjan and Smith (2018).

A.

VMR	Control	PD
N =	20	20
Age (Mean ± SD)	69.5 ± 9.3	65.5 ± 13.3
Sex at Birth	16F/4M	8F/12M
Handedness	19R/1L	16R/4L
UPDRS III (Mean ± SD)	NaN	30.9 ± 22.3
MoCA (Mean ± SD)	NaN	25.3 ± 3.03
MMSE (Mean ± SD)	NaN	28.7 ± 1.9
On DA Medication	NaN	17 ON

B.

FF	Control	PD
N =	10	10
Age (Mean ± SD)	78.4 ± 4.6	72.8 ± 8.3
Sex at Birth	7F/3M	3F/7M
Handedness	10R/0L	9R/1L
UPDRS III (Mean ± SD)	NaN	27.2 ± 10.2
MoCA (Mean ± SD)	NaN	22.5 ± 3.5
MMSE (Mean ± SD)	NaN	28 ± 2.3
On DA Medication	NaN	10 ON

Table 1. A. Participant demographics for VMR experiment **B.** Participant demographics for FF experiment

Visuomotor Rotation Experiment (VMR)

As shown in Figure 1, participants were seated in front of a horizontally-mounted monitor (120 Hz refresh rate). Underneath the monitor, participants grasped the handle of a stylus to control a 2.5 mm white cursor on the screen by making reaching movements on a digitizing tablet (Wacom Intuos 3), which recorded hand position at 200 Hz.

During a single trial, participants were asked to use the stylus to move the white cursor in a straight line between two circular targets (1cm open circles centered on the participant's midline, approximately 9cm apart). A single trial consisted of a single arm reach that began at the target closest to the participant's body and ended at the target furthest from the participant's body on the sagittal axis. A "successful" trial was one in which movement duration was less than or equal to 650 ms. If a trial was successful, participants received feedback; the end target turned green

accompanied with a short duration “beep” sound. If a trial was not successful, the end target turned red and did not make any sound. For the task, participants were instructed to obtain “as many green feedback trials as possible”.

Participants were first instructed on the task with a baseline period of 60 null movement trials, which also served as a familiarization period. After the baseline period, participants were exposed to the training period, during which they received 483 trials total, consisting of 240 visuomotor perturbation trials. During perturbation trials, the white cursor was rotated from the underlying hand position by ±2° or ±4° around the start position. The remaining trials were null movements with no visuomotor rotation, 0°.

Force-Field Perturbation Experiment (FF)

Participants were asked to grasp the handle of a robotic arm on a planar workspace that moved a cursor on a screen between presented targets. The robotic arm manipulandum (KINARM End-Point Lab, BKIN Technologies) sampled motor output, including position, force, velocity, and acceleration at 1,000 Hz. Participants could not directly view their hand position, as it was hidden from sight by a horizontal, upward-facing mirror that reflected a small white cursor, representing hand position, in addition to trial targets, which were open red circles. Participants were seated in front of this set-up in a chair adjusted to allow for comfortable viewing of the task displayed on the mirror.

During the task, participants were asked to use the robotic manipulandum to move the cursor (a white, filled circle 3mm in diameter) in a straight line between the start and end targets, which were approximately 0.5cm in diameter, spaced 10 cm apart on the screen, and 20-30cm away from the body on the sagittal axis. A trial consisted of a single arm reach between the start target and end target. A “successful” trial was one in which peak velocity was greater than 0.25 m/s but less than 0.55 m/s and the cursor came within 0.005m of the target center (ensuring it crossed target threshold). If a trial was successful, participants received feedback; the end target turned green accompanied with a short duration “beep” sound. If a trial was not successful, the

end target turned red and did not make any sound. While receiving instructions for the task, participants were told to obtain “as many green feedback trials as possible”.

Participants were first instructed on the task with 20 null movement trials, which served as a familiarization period. Once participants were familiar with the task, they were exposed to a baseline period, consisting of 50 null trials, 10 of which were randomly dispersed trials without any visual feedback. Following the baseline period, participants were exposed to the training period. During the training period, participants received 1440 trials total, consisting of 864 force-field (FF) perturbation trials. FF trials systematically perturbed reaching arm movements with forces proportional to movement velocity (k) and perpendicular to the direction of the hand motion on both the horizontal (F_x) and vertical (F_y) axis (Eq.1). Parameter k randomly varied across 4 different types of FF perturbations: ±1.5 and ±3 Ns/m.

$$\begin{bmatrix} F_x \\ F_y \end{bmatrix} = \begin{bmatrix} 0 & -k \\ k & 0 \end{bmatrix} \begin{bmatrix} \dot{x} \\ \dot{y} \end{bmatrix}$$ **(Equation 1)**

F_x: Forces applied in horizontal (x) direction

F_y: Forces applied in vertical (y) direction

k: ±1.5 and ±3 Ns/m perturbation force

$\dot{x}$: hand velocity in x direction

$\dot{y}$: hand velocity in y direction

Each FF trial was preceded and followed by a null trial (0 Ns/m FF) to capture trial-by-trial adaptation. 50% of null trials were without any visual feedback of the cursor and these trials were randomly dispersed throughout the training period. In all other trials, visual feedback of the cursor was present during both the forward and backwards reach between targets.

Movements Analyzed

Forward reaching motion was completed in the 90° direction while reaching back toward oneself was completed in the 270° direction. However, only arm movements completed in the 90° direction were perturbed and used to perform the analyses. No participants were excluded from

the dataset. Individual trials were excluded if movement duration was less than 750 ms. During the VMR experiment, this resulted in 1% of trials excluded in control subjects and 10% of trials excluded in patients with PD. During the FF experiment, this resulted in 11% of trials excluded in control subjects and 21% of trials excluded in patients with PD.

Measurements of Motor Error

As described in Ranjan and Smith (2018) total motor error was defined as the angle between the cursor movement direction relative to the target direction. Cursor movement direction was defined as the vector between the hand coordinates of movement onset and the hand coordinates of movement peak speed. Movement onset was defined as the x and y hand coordinates at which the movement speed first surpassed 5 cm/s. Target direction was defined as the vector between the movement onset coordinates and the coordinates for the center of the target. In a single trial, the total motor error was the sum of externally-generated perturbation (EGE) and self-generated motor noise (SGE). During unperturbed trials, EGE was zero. During perturbation trials, EGE was the effect of the perturbation. For VMR perturbation trials, this was the amount of visual rotation imposed on the cursor (±2° or ±4°). For FF perturbation trials, EGE was calculated as the size of the perturbation (±1.5 and ±3 Ns/m) multiplied by arm stiffness. Arm stiffness was determined for each individual participant by regressing the total motor error onto the perturbation for each trial. On all trials, SGE was the difference between total motor error minus EGE.

Estimation of Adaptive Response

We wanted to understand the sensitivity of the adaptive response to SGE and EGE. Each perturbation trial was preceded and followed by a null trial so that the adaptive response was calculated as the difference between the following null trial and the preceding null trial. This method of determining adaptive response allowed us to measure adaptation without any SGE conflation, which would be present if we used the typical method of calculating adaptation as the difference between the following null trial and the perturbation trial itself. For each participant, to

calculate adaptive sensitivity to EGE, we separated trials based on type of EGE and, within the 5 EGE types (e.g., 0, ±2° or ±4° for the VMR perturbations), binned the SGEs into 5 quintiles (25 bins total for each participant). Then, we regressed the average adaptive response of these bins onto both the EGE and SGE separately. To determine the r^2 values, we averaged the 25 adaptation bins versus EGE and SGE across participants in each group and regressed the average response onto the error signal.

Estimation of adaptive response sensitivity

To determine each participant's trial-by-trial sensitivity of adaptive response to SGE and EGE, we used a regression of the unbinned adaptive responses onto the calculated SGE and EGE of a single trial.

Statistical Analysis

Statistical analyses were performed in MATLAB (version R2023a) on trials that met the speed and duration criteria previously listed. To assess differences in baseline movement variability, we compared patients with PD and control subjects as well as participant performance across experiments with a two-way analysis of variance (ANOVA). For all ANOVAs, we corrected for multiple comparisons using Bonferroni's post hoc test. We then compared the relationship between SGE/EGE and the adaptive response by regressing the within-group average adaptive response to the SGE or EGE error signal. Goodness-of-fit for this regression was determined using the coefficient of determination (r^2). To assess the single-trial sensitivity of the adaptive response to both EGE and SGE in each participant, we performed a bivariate regression of unbinned adaptive responses in MATLAB, using EGE and SGE values as predictors in the model. To measure the difference between the regression coefficients for EGE versus SGE adaptive sensitivity, we utilized a paired t-test. For all tests, the significance level was 0.05 and data are presented by mean ± SEM.

RESULTS

As described in Ranjan and Smith (2018) and Kim et al. (2025), we measured the average adaptive response to the respective perturbation types. We accomplished this by binning all trials with the same EGE (5 bins) and, within each EGE bin, binned the trials into SGE quintiles for each participant (5x5 bins for 25 total bins for each participant). Then, we averaged EGE, SGE, and adaptive response in each bin across participants.

Baseline movement variability was similar between control subjects and patients with PD

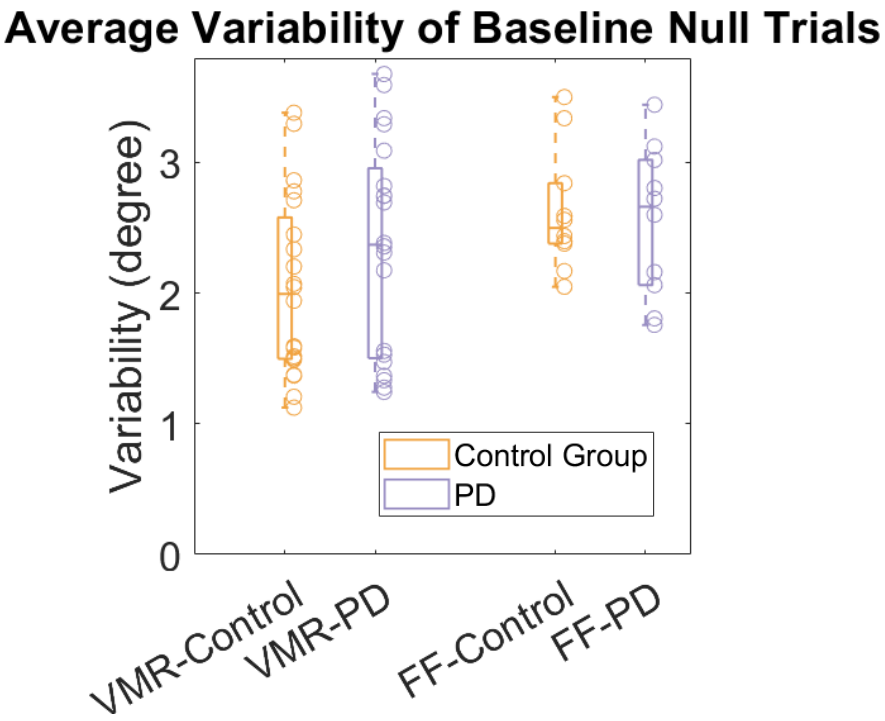

Figure 2. Comparison of baseline null performance. Comparison of baseline movement variability using null trials in each experiment, we found no significant differences between groups within experimental conditions. However, we did observe differences in participant baseline movement variability across experiments.

To determine how control subjects and patients with PD differed during baseline movements in each experiment, we examined movement variability standard deviation of reach heading angle across baseline null trials (Figure 2). Heading angle was calculated relative to target direction for each trial, such that variability reflected trial-to-trial differences in movement

direction. Patients with PD did not significantly differ in baseline movement variability from control subjects (two-way ANOVA; $F_{(1,59)}$ = 0.37; p= 0.54). However, participant performance significantly differed between experimental conditions (two-way ANOVA; $F_{(1,59)}$ = 4.26; p = 0.04; Table 2). There was no significant interaction effect between the two factors ($F_{(1,59)}$ = 1.03; p = 0.31). Thus, although there was greater baseline variability during the FF experiment, patients with PD and control subjects did not have differences in baseline movement variability within experimental conditions.

Condition	Control (Mean ± SEM)	PD (Mean ± SEM)
VMR	2.04 ± 0.15	2.3 ± 0.18
FF	2.62 ± 0.14	2.5 ± 0.18

Table 2. Average $\pm$ SEM of movement variability for each participant group and condition.

Patients with PD and Control subjects adapt similarly to different types of externally-generated error

In Figure 3, we compared the ability to adapt to externally-generated visual (Figure 3A) and physical (Figure 3B) perturbations in control subjects and patients. We found that patients with PD (mean slope: -0.06, 95% CI: [-0.12 0.0003], r^2 = 0.008, p = 0.05) adapted similarly to control subjects (mean slope: -0.08, 95% CI: [-0.17 0.07], r^2 = 0.03, p = 0.0005) in response to external visual perturbations (Figure 3a). We also observed similar performance between patients with PD and control subjects when participants were exposed to a lateral physical perturbation (Figure 3B). We found that patients with PD (mean slope: -0.42, 95% CI: [-0.26 -0.21], r^2 = 0.95, p < 0.0001) adapted similarly to control subjects (mean slope: -0.381, 95% CI: [-0.25 -0.17], r^2 = 0.815, p = 0.0007) in response to external visual perturbations.

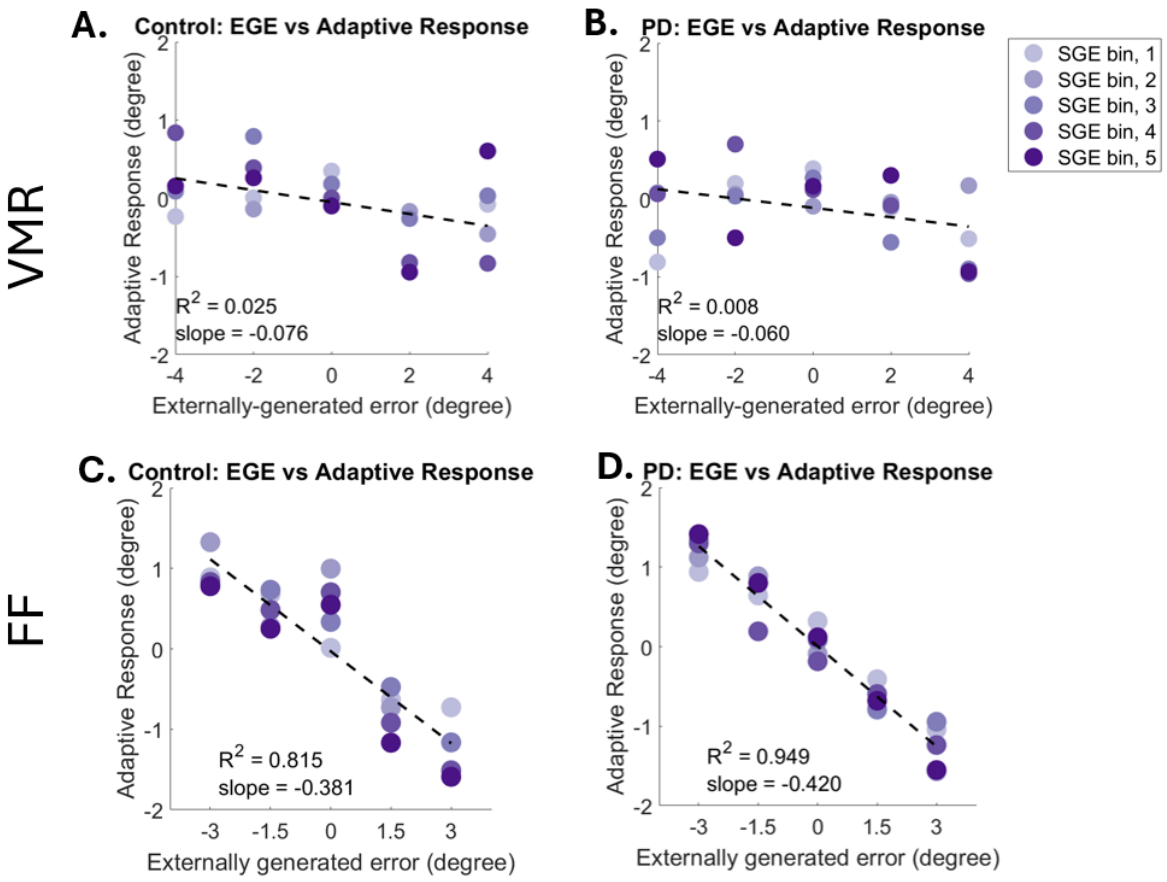

Figure 3. EGE versus Adaptive Response. A. Visuomotor Rotation (VMR) experiment: In control subjects, the magnitude of the EGE (visuomotor rotation) is determining the magnitude of the adaptive response similar to **B.** patients with Parkinson's Disease (PD). **C. Force-Field (FF) experiment**: In control subjects, the magnitude of the EGE (FF perturbation) determines the magnitude of the adaptive response similar to **D.** patients with PD.

Patients with PD and Control subjects adapt similarly to self-generated error

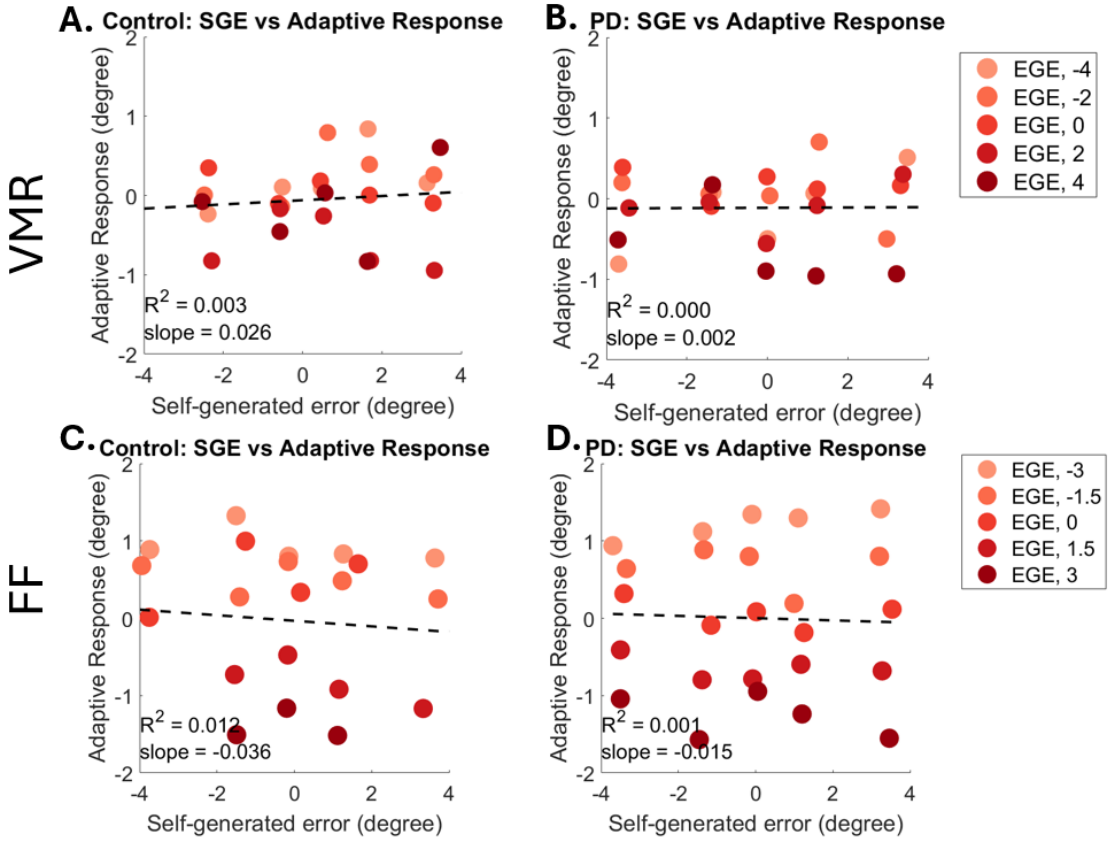

Figure 4. SGE vs Adaptive Response. A. Visuomotor rotation (VMR) experiment: While undergoing varying degrees of visuomotor rotation, control subjects do not significantly adapt to their own internally-generated motor noise (SGE) similar to **B**. patients with Parkinson's Disease (PD). This is consistent in the **Force-Field (FF) perturbation experiment** where in both **C.** control subjects and **D.** patients with PD SGE does not explain adaptive responses.

We then compared the relationship between self-generated error and the adaptive response to visual (Figure 4A,B) and physical (Figure 4C,D) perturbations in control subjects and patients. Our results demonstrate that patients with PD (mean slope: 0.002, 95% CI: [-0.05 0.06], r^2 = 0.00, p = 0.95) had a similar lack of adaptive response to self-generated error as controls (mean slope: 0.02, 95% CI: [-0.02 0.07], r^2 = 0.003, p = 0.26) during exposure to a visual perturbation. Similarly, during exposure to different levels of physical perturbation, we found that

the adaptive response of both PD patients (mean slope: 0.015, 95% CI: [-0.18 0.15], r^2 = 0.001, p = 0.86) and control subjects (mean slope: -0.036, 95% CI: [-0.17 0.1], r^2 = 0.012, p = 0.6) was unrelated to self-generated error. Therefore, during exposure to different levels of visual and physical perturbations, the adaptive response does not reflect modulation in response to self-generated error across groups.

Patients with PD are just as sensitive to EGE and SGE as Control Subject

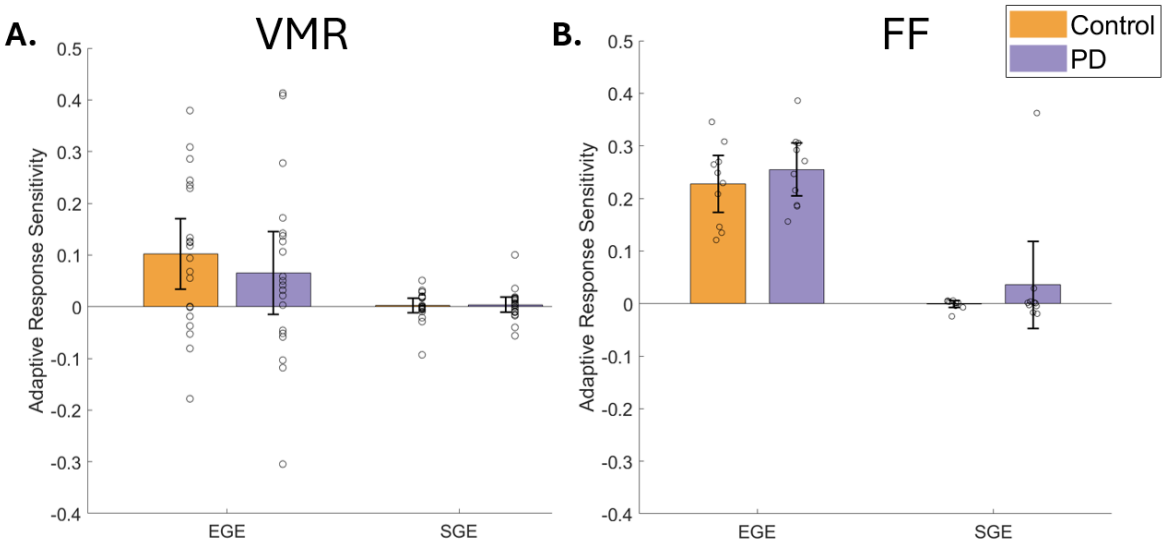

Figure 5. Adaptive Response Sensitivity. Response sensitivity to SGE and EGE reveals that during both **A.** visuomotor rotation (VMR) and **B.** force-field (FF) perturbation, adaptative response is most sensitive to EGE. Error bars are 95% confidence intervals.

We then assessed the single-trial sensitivity of the adaptive response to both EGE and SGE in each participant (Figure 5). When exposed to different levels of externally-generated visual perturbation, the adaptive response of patients with PD and control subjects is equally as sensitive to both EGE (t(38) = -0.7, p =0.5) and SGE (t(38) = 0.17, p = 0.86). Notably, both groups exhibited greater sensitivity to EGE than SGE.

While training with a visual perturbation (Figure 5A), control subjects and patients with PD had higher sensitivity to EGE (Mean ± 95% CI; Control: 0.1 ± 0.03, PD: 0.06 ± 0.01) than SGE

(Control: 0.002 ± 0.01, PD: 0.003 ± 0.01). Correspondingly, during exposure to physical perturbations (Figure 4B), patients with PD (0.25 ± 0.05) and control subjects (0.22 ± 0.05) have no significant difference in adaptive sensitivity to EGE ($t(18) = -0.85$, $p = 0.4$). Patients with PD (0.03 ± 0.08) and control subjects (-0.001 ± 0.0065) were also similar in their low sensitivity to SGE ($t(18) = -1.0$, $p= 0.32$). Thus, across both perturbation types, patients with PD and control subjects showed comparable sensitivity to both EGE and SGE. The consistently greater magnitude of the EGE sensitivity estimates relative to SGE sensitivity further suggests that adaptive responses were more strongly related to externally-generated than self-generated errors in both groups.

DISCUSSION

In this study, we investigated how increased motor noise in patients with Parkinson's Disease impacted their ability to differentiate between self-generated error (SGE) and externally-generated error (EGE). To study this, we utilized two similar motor adaptation paradigms: one which measured adaptation to small perturbations of movement visual feedback and the other which measured adaptation to small physical perturbations to movement. We compared the behavioral results between patients with PD and age-matched neurologically healthy controls and found that the two groups were equally able to adapt to EGEs while accounting for SGEs.

In Figure 4, we demonstrated that, regardless of perturbation type, patients with PD were just as able to identify and adapt to EGE as control subjects. These findings are consistent with previous research examining the role of internal and external sensory cues in movement monitoring and control (Gauvin et al., 2017; Fimm et al., 1994; Hseih et al. 1995). Patients with PD retain the ability to utilize external cues (outside sensory input) for behavioral error correction, as evidenced by improved motor performance in the presence of external cues (Fimm et al., 1994), preserved external monitoring of speech (Gauvin et al., 2017), and intact task switching with external cues (Hseih et al., 1995). Therefore, our study adds to this evidence by demonstrating that not only can patients with PD utilize external cues in their behavior, they are also able to accurately

differentiate and adapt to external errors while accounting for SGEs during movement (Figure 3 and 5).

When participants are unexpectedly exposed to a perturbation during reaching movement, they utilize feedback control to correct for online movement error (Shadmehr et al., 2010; Krakauer, 2019). However, once this perturbation and online correction occurs, internal model predictions update to expect the perturbation and accounts for this in future movements (Tseng et al., 2007; Shadmehr et al., 2010; Krakauer, 2019). In the present tasks, when the externally applied perturbation causes the hand to deviate from its expected trajectory, the resulting sensory prediction error provides a teaching signal that modifies the feedforward motor command for future movements. With repeated exposure to the perturbation, these updated predictions allow participants to compensate for the perturbation in subsequent reaches, reducing the discrepancy between the predicted and actual sensory outcome (Tseng et al., 2007; Krakauer, 2019). Patients with PD are constantly exposed to their own greater than average self-generated motor noise, especially in our study where patients have exhibited the motor symptoms of PD for more than a year. As patients with PD and control subjects had an equal baseline movement variability (Figure 2) and lack of adaptive sensitivity to SGE (Figure 3 and 5), this suggests that feedforward models can predict and account for the predictable consequences of self-generated motor errors, independent of disease status. If motor noise is a part of the predicted sensory outcome, then participants will not adapt to it as there is no gap between the predicted SGE and the movement outcome. This logic also explains why both patients and control subjects exclusively adapt to EGE (Figure 4 and 5) as the unexpected perturbation creates a difference in actual sensory outcome.

Limitations

We would like to acknowledge some limitations to our findings, which have influenced our results. Almost all our patients with PD were actively on dopaminergic medication (Carbidopa/Levodopa) throughout both experiments (VMR: 17 ON; FF: 10 ON), which could have impacted tremor presentation and movement. Additionally, as the two studies were conducted two years apart, we

had less participants in the FF experimental group due to difficulties in participant retention, which may have had an impact on the statistical power of our findings.

REFERENCES

Adamovich, S. V., Berkinblit, M. B., Hening, W., Sage, J., & Poizner, H. (2001). The interaction of visual and proprioceptive inputs in pointing to actual and remembered targets in Parkinson's disease. Neuroscience, 104(4), 1027–1041. https://doi.org/10.1016/s0306-4522(01)00099-9

Berniker, M., & Kording, K. (2008). Estimating the sources of motor errors for adaptation and generalization. Nature Neuroscience, 11(12), Article 12. https://doi.org/10.1038/nn.2229

Butcher, P. A., Ivry, R. B., Kuo, S.-H., Rydz, D., Krakauer, J. W., & Taylor, J. A. (2017). The cerebellum does more than sensory prediction error-based learning in sensorimotor adaptation tasks. Journal of Neurophysiology, 118(3), 1622–1636. https://doi.org/10.1152/jn.00451.2017

Contreras-Vidal, J. L., & Buch, E. R. (2003). Effects of Parkinson's disease on visuomotor adaptation. Experimental Brain Research, 150(1), 25–32. https://doi.org/10.1007/s00221-003-1403-y

Dirkx, M. F., Zach, H., Bloem, B. R., Hallett, M., & Helmich, R. C. (2018). The nature of postural tremor in Parkinson disease. Neurology, 90(13), e1095–e1103. https://doi.org/10.1212/WNL.0000000000005215

Elble, R. J. (2013). Tremor disorders. Current Opinion in Neurology, 26(4), 413. https://doi.org/10.1097/WCO.0b013e3283632f46

Faisal, A. A., Selen, L. P. J., & Wolpert, D. M. (2008). Noise in the nervous system. Nature Reviews Neuroscience, 9(4), Article 4. https://doi.org/10.1038/nrn2258

Fimm, B., Bartl, G., Zimmermann, P., & Wallesch, C. W. (1994). Different Mechanisms Underly Shifting Set on External and Internal Cues in Parkinson′s Disease. Brain and Cognition, 25(2), 287–304. https://doi.org/10.1006/brcg.1994.1037

Gauvin, H. S., Mertens, J., Mariën, P., Santens, P., Pickut, B. A., & Hartsuiker, R. J. (2017). Verbal monitoring in Parkinson's disease: A comparison between internal and external monitoring. PLOS ONE, 12(8), e0182159. https://doi.org/10.1371/journal.pone.0182159

Gironell, A., Pascual-Sedano, B., Aracil, I., Marín-Lahoz, J., Pagonabarraga, J., & Kulisevsky, J. (2018). Tremor Types in Parkinson Disease: A Descriptive Study Using a New Classification. Parkinson's Disease, 2018(1), 4327597. https://doi.org/10.1155/2018/4327597

Hsieh, S., Lee, C. Y., & Tai, C. T. (1995). Set-shifting aptitude in Parkinson's disease: External versus internal cues. Psychological Reports, 77(1), 339-349.

Izawa, J., & Shadmehr, R. (2011). Learning from Sensory and Reward Prediction Errors during Motor Adaptation. PLOS Computational Biology, 7(3), e1002012. https://doi.org/10.1371/journal.pcbi.1002012

Jankovic, J. (2005). Motor fluctuations and dyskinesias in Parkinson's disease: clinical manifestations. *Movement disorders: official journal of the Movement Disorder Society*, *20*(S11), S11-S16.

Kim, H. E., Chua, R., & Hu, D. (2025). Causal inference, prediction and state estimation in sensorimotor learning. Proceedings of the Royal Society B: Biological Sciences, 292(2052), 20251320. https://doi.org/10.1098/rspb.2025.1320

Krakauer, J. W., Hadjiosif, A. M., Xu, J., Wong, A. L., & Haith, A. M. (2019). Motor Learning. In R. Terjung (Ed.), Comprehensive Physiology (1st ed., pp. 613–663). Wiley. https://doi.org/10.1002/cphy.c170043

Mongeon, D., Blanchet, P., & Messier, J. (2013). Impact of Parkinson's disease and dopaminergic medication on adaptation to explicit and implicit visuomotor perturbations. Brain and Cognition, 81(2), 271–282. https://doi.org/10.1016/j.bandc.2012.12.001

Ranjan T, Smith MA. 2018 Cancellation of internally-generated errors from the signal driving motor adaptation. In Advances in motor learning and motor control (MLMC), San Diego, CA, 2 November 2018

Shadmehr, R., Smith, M. A., & Krakauer, J. W. (2010). Error Correction, Sensory Prediction, and Adaptation in Motor Control. Annual Review of Neuroscience, 33(1), 89–108. https://doi.org/10.1146/annurev-neuro-060909-153135

Synofzik, M., Lindner, A., & Thier, P. (2008). The Cerebellum Updates Predictions about the Visual Consequences of One's Behavior. Current Biology, 18(11), 814–818. https://doi.org/10.1016/j.cub.2008.04.071

Synofzik, M., Thier, P., & Lindner, A. (2006). Internalizing agency of self-action: Perception of one's own hand movements depends on an adaptable prediction about the sensory action outcome. Journal of Neurophysiology, 96(3), 1592–1601. https://doi.org/10.1152/jn.00104.2006

Tseng, Y.-W., Diedrichsen, J., Krakauer, J. W., Shadmehr, R., & Bastian, A. J. (2007). Sensory prediction errors drive cerebellum-dependent adaptation of reaching. Journal of Neurophysiology, 98(1), 54–62. https://doi.org/10.1152/jn.00266.2007

van Beers, R. J. (2009). Motor Learning Is Optimally Tuned to the Properties of Motor Noise. Neuron, 63(3), 406–417. https://doi.org/10.1016/j.neuron.2009.06.025

Wolpert, D. M., Diedrichsen, J., & Flanagan, J. R. (2011). Principles of sensorimotor learning. Nature Reviews Neuroscience, 12(12), Article 12. https://doi.org/10.1038/nrn3112

Chapter 5: Conclusion

Throughout this dissertation, we sought to understand how tremor impacts motor adaptation and control. We hypothesized that externally-generated tremor impairs the ability to adapt while internally-generated tremor (such as in Parkinson's Disease and Essential Tremor) does not impair adaptation. In the second chapter (first aim), we sought to understand how increasing externally-generated tremor magnitude impacted adaptation to a lateral force-field perturbation in neurologically healthy individuals. We found that increasing the magnitude of externally-generated tremor results in a decreasing ability to adapt. This impaired adaptation was due to externally-generated tremor magnitude interfering with the fast-learning process by adding extra noise to incoming sensory information. In the third chapter (second aim), we investigated how internally-generated tremor in patients with Parkinson's Disease (PD), patients with Essential Tremor (ET), and control subjects impacted adaptation to the same force-field perturbation. We discovered that there were no adaptation learning differences between groups. Increased tremor magnitude in patients with ET did not impair the reaching movement, during which adaptation occurs. However, increased tremor magnitude in patients with ET impaired the end of movement stabilization and end point error variability and increased tremor magnitude in patients with PD impaired postural hold. In the fourth chapter (third aim), we wanted to determine the extent tremor affects the ability to detect self-generated (SGE) and externally-generated (EGE) error during motor adaptation. During adaptation to both visual and physical perturbation, patients with PD were found to be just as sensitive to EGE and SGE as control subjects. In both groups, only the magnitude of the EGE determined the amount of motor adaptation.

Tremor only impairs adaptation if it interferes with the external perturbation driving the adaptive response

In the first aim, adding noise (externally-generated tremor) on top of external physical perturbations impaired adaptation while increasing noise to internally-generated movement

variability had no such effect on adaptation. This is consistent with the framework discussed in chapter four, which postulates that the magnitude of adaptation is only driven by externally-generated error, as the motor system's feedforward prediction already accounts for the sensory impacts of internally-generated motor noise (Ranjan and Smith, 2018). We found that tremor and other motor noise sources (SGEs) present in patients with PD did not appear to interfere with the parsing of SGE and EGE, therefore allowing patients with PD to adapt similarly to control subjects across perturbation types. By increasing the uncertainty of the EGE driving adaptation in aim one, we saw corresponding decreases in the adaptive response. Since adaptation is not driven by SGE, increasing the amount of motor noise via tremor would not impact the ability to adapt, as seen in the second and third aims.

Pathological tremor does not impact feedforward movement reach but does impact stages of movement that involve feedback control

Throughout each experiment, we investigated adaptation through two commonly used arm-reaching paradigms. In both, adaptative response occurred during the reaching phase of movement, defined as the period of movement between two targets. The initial phase of reaching relies heavily on feedforward motor commands, while feedback and impedance control contribute to stopping and stabilizing the arm at the target (Jayasinghe et al., 2022). Meanwhile, adaptation primarily relies upon sensory prediction errors to modify feedforward models for future movements when the actual sensory outcome does not match the predicted sensory outcome, such as hand position (Tseng et al., 2007; Krakauer, 2019). In the second aim, we found that increasing internally-generated tremor magnitude does not impact the reaching movement and, as a result, adaptative motor output. Additionally, in the third aim, we found that adaptation is not driven by internally-generated motor noise, even in patients with increased SGE. Together, this suggests that the feedforward controller for movement reach can predict and account for the consequences

of increased tremor in movement. As the motor system can predict the sensory consequences of pathological tremor, it does not drive nor interfere with reaching adaptation.

Prior literature suggests that postural holding relies on both feedforward and sensory feedback mechanisms, with feedback contributing to the ongoing correction and stabilization of the limb (Albert et al., 2020; Mathew & Crevecouer, 2021; Jayasinghe et al., 2022). Feedback-based motor control relies on online corrections that require constant estimation of the current sensory state of the limb, allowing the nervous system to detect and respond to deviations from the desired movement state (Shadmehr et al., 2010; Crevecoeur et al., 2018). Tremor creates greater sensory noise, which increases positional variance and oscillatory corrective movements, both of which affect positional stability. In aim two, we observed that increased tremor magnitude in patients with PD results in a greater amount of force needed to maintain postural hold, thereby impairing the ability maintain a stable postural hold. Thus, increased tremor magnitude appears to impair feedback control in this context.

We also investigated the transition from feedforward reaching movement to feedback controlled hold, a period of movement termed movement stabilization. As the reaching movement approaches the intended target, the motor system begins to utilize sensory feedback to determine that it has reached its intended location. In aim two, we found that, during this stabilization period, increased tremor magnitude in patients with ET was associated with increased endpoint variability. Therefore, it is possible that tremor magnitude may interfere with this “brake”, or stabilization, period of reaching movement (proposed by Hadjiosif et al., 2025) as the limb transitions from a moving to a steady state through utilization of feedback control.

Possible Neural Mechanisms Underlying Tremor-Impaired Stabilization and Postural Hold

After a sudden displacement of the limb, such as with a lateral force-field perturbation, an automatic muscle contraction called a long-latency stretch response (LLR) occurs between a spinal reflex and voluntary motion (Kurtzer et al., 2015). LLRs utilize feedback control to

coordinate information between joints (Kurtzer et al., 2015; Crevecouer et al, 2018) to maintain body stability. It maintains this stability to help achieve the goal of each movement (Pruszynski et al. 2011; Lee et al., 2019; Weiler et al., 2015), such as bringing a cursor to a target at the end of a movement. In this way, it acts as a feedback pathway for goal-directed movement. The cerebellum is suggested to modulate the magnitude of the LLR feedback response (Kurtzer et al., 2015). Stabilization places increased focus on feedback mechanisms, including long-latency stretch responses, whose gain and coordination are modulated by the cerebellum (which is impaired in ET). During movement stabilization, there is a difference in the desired endpoint (target) and the actual endpoint (cursor position) which is rapidly changing because of movement tremor. Under conditions without pathological tremor, the feedback response is normal and LLRs can help stabilize joints to bring the cursor position to the target (Kurtzer et al., 2015; Pruszynski et al. 2011; Lee et al., 2019; Weiler et al., 2015). However, LLRs that are delayed or enhanced could contribute to the tremor and have been suggested to underlie postural tremor (Mauritz et al., 1981; Richard et al., 1997). Stabilization combines maintaining a sensory state with rapid sensory feedback mechanisms. LLRs are one component of this feedback system, and the cerebellum may modulate their gain and coordination, which would explain how increased tremor magnitude in ET interferes with movement stabilization as we saw in aim two.

Postural hold is the maintenance of a sensory state (i.e. homeostasis), which requires continuous sensory feedback, most likely from a feedback controller. In aim two, our results suggest that increased tremor magnitude in patients with PD impairs the ability to maintain a postural hold. This may be due to PD leaving patients stuck in a maladaptive homeostatic state. Kelley and Kauffman (2024) created a computational model which positions tremor in PD as unstable feedback in an optimal feedback control system. They state that the basal ganglia–thalamus–motor cortex system could be contributing to inappropriate amplification of feedback (Kelley & Kauffman, 2024). Thus, the difficulty of postural hold in PD could be due to the motor system's altered feedback and difficulty suppressing an unwanted oscillatory state.

Just as patients with PD may be stuck in a maladaptive homeostatic state, patients with ET may have trouble transitioning into homeostasis. We found that increased tremor magnitude in patients with ET during movement stabilization corresponded to increased endpoint variability. This could suggest difficulty transitioning from a dynamic motor state to a stable postural hold, which possibly reflects impaired cerebellar-dependent feedback control. The lack of tremor in our ET patient population during postural hold would therefore not interfere with the feedback control during this movement phase once the transition had taken place.

To gain greater insight into the underlying neural mechanisms of how tremor in PD and ET impact different stages of movement, future studies could utilize cerebellar brain inhibition (CBI), which is measured using transcranial magnetic stimulation (TMS). CBI is the neural signal where the cerebellum inhibits activity from the motor cortex, which allows for muscle control, balance, and motor adaptation (Fernandez et al., 2018). A stronger CBI is associated with increased movement precision during movement reach (Caligiore et al., 2016) and CBI changes in direct proportion to the amount of motor adaptation that occurs (Jayaram et al., 2011; Celnik, 2015). In neurologically health individuals during movement stabilization, we would expect to see an increase in CBI modulation because the cerebellum drives much of the sensory feedback processes underlying joint stabilization. In ET, we might expect to see normal CBI modulation during movement reach and postural hold but abnormal CBI modulation during movement stabilization. In PD, we would expect to see normal CBI modulation during movement reach and stabilization, but abnormal CBI modulation during postural hold. This would be in line with previous studies, which found that CBI was reduced in patients with PD (Ni et al., 2010; Carrillo et al., 2013).

REFERENCES

Albert, S. T., Hadjiosif, A. M., Jang, J., Zimnik, A. J., Soteropoulos, D. S., Baker, S. N., Churchland, M. M., Krakauer, J. W., & Shadmehr, R. (2020). Postural control of arm and fingers through integration of movement commands. eLife, 9, e52507. https://doi.org/10.7554/eLife.52507

Caligiore, D., Pezzulo, G., Baldassarre, G., Bostan, A. C., Strick, P. L., Doya, K., Helmich, R. C., Dirkx, M., Houk, J., Jörntell, H., Lago-Rodriguez, A., Galea, J. M., Miall, R. C., Popa, T., Kishore, A., Verschure, P. F. M. J., Zucca, R., & Herreros, I. (2017). Consensus Paper: Towards a Systems-Level View of Cerebellar Function: the Interplay Between Cerebellum, Basal Ganglia, and Cortex. Cerebellum, 16(1), 203–229. https://doi.org/10.1007/s12311-016-0763-3

Carrillo, F., Palomar, F. J., Conde, V., Diaz-Corrales, F. J., Porcacchia, P., Fernández-Del-Olmo, M., Koch, G., & Mir, P. (2013). Study of cerebello-thalamocortical pathway by transcranial magnetic stimulation in Parkinson's disease. Brain Stimulation, 6(4), 582–589. https://doi.org/10.1016/j.brs.2012.12.004

Carrillo, F., Palomar, F. J., Conde, V., Diaz-Corrales, F. J., Porcacchia, P., Fernández-Del-Olmo, M., Koch, G., & Mir, P. (2013b). Study of cerebello-thalamocortical pathway by transcranial magnetic stimulation in Parkinson's disease. Brain Stimulation, 6(4), 582–589. https://doi.org/10.1016/j.brs.2012.12.004

Celnik, P. (2015). Understanding and modulating motor learning with Cerebellar stimulation. Cerebellum (London, England), 14(2), 171–174. https://doi.org/10.1007/s12311-014-0607-y

Crevecoeur, F., & Kurtzer, I. (2018). Long-latency reflexes for inter-effector coordination reflect a continuous state feedback controller. Journal of Neurophysiology, 120(5), 2466–2483. https://doi.org/10.1152/jn.00205.2018

Desmurget, M., & Grafton, S. (2000). Forward modeling allows feedback control for fast reaching movements. Trends in Cognitive Sciences, 4(11), 423–431. https://doi.org/10.1016/s1364-6613(00)01537-0

Fernandez, L., Major, B. P., Teo, W.-P., Byrne, L. K., & Enticott, P. G. (2018). Assessing cerebellar brain inhibition (CBI) via transcranial magnetic stimulation (TMS): A systematic review. Neuroscience and Biobehavioral Reviews, 86, 176–206. https://doi.org/10.1016/j.neubiorev.2017.11.018

Hadjiosif, A. M., Kita, K., Albert, S. T., Scheidt, R. A., Shadmehr, R., & Krakauer, J. W. (2025). Separating the control of moving and holding in human post-stroke arm paresis. eLife, 12, RP90780. https://doi.org/10.7554/eLife.90780

Jayaram, G., Galea, J. M., Bastian, A. J., & Celnik, P. (2011). Human locomotor adaptive learning is proportional to depression of cerebellar excitability. Cerebral Cortex, 21(8), 1901–1909. https://doi.org/10.1093/cercor/bhq263

Jayasinghe, S. A. L., Scheidt, R. A., & Sainburg, R. L. (2022). Neural Control of Stopping and Stabilizing the Arm. Frontiers in Integrative Neuroscience, 16, 835852. https://doi.org/10.3389/fnint.2022.835852

Kelley, C. R., & Kauffman, J. L. (2024). Parkinsonian Tremor as Unstable Feedback in a Physiologically Consistent Control Framework. IEEE Transactions on Neural Systems and Rehabilitation Engineering: A Publication of the IEEE Engineering in Medicine and Biology Society, 32, 2665–2675. https://doi.org/10.1109/TNSRE.2024.3430116

Krakauer, J. W., Hadjiosif, A. M., Xu, J., Wong, A. L., & Haith, A. M. (2019). Motor Learning. In R. Terjung (Ed.), Comprehensive Physiology (1st ed., pp. 613–663). Wiley. https://doi.org/10.1002/cphy.c170043

Kurtzer, I. L. (2015). Long-latency reflexes account for limb biomechanics through several supraspinal pathways. Frontiers in Integrative Neuroscience, 8, 99. https://doi.org/10.3389/fnint.2014.00099

Lee, H., & Perreault, E. J. (2019). Stabilizing stretch reflexes are modulated independently from the rapid release of perturbation-triggered motor plans. Scientific Reports, 9(1), 13926. https://doi.org/10.1038/s41598-019-50460-1

Mathew, J., & Crevecoeur, F. (2021). Adaptive Feedback Control in Human Reaching Adaptation to Force Fields. Frontiers in Human Neuroscience, 15, 742608. https://doi.org/10.3389/fnhum.2021.742608

Mauritz, K. H., Schmitt, C., & Dichgans, J. (1981). Delayed and enhanced long latency reflexes as the possible cause of postural tremor in late cerebellar atrophy. Brain: A Journal of Neurology, 104(Pt 1), 97–116. https://doi.org/10.1093/brain/104.1.97

Ni, Z., Pinto, A. D., Lang, A. E., & Chen, R. (2010a). Involvement of the cerebellothalamocortical pathway in Parkinson disease. Annals of Neurology, 68(6), 816–824. https://doi.org/10.1002/ana.22221

Ni, Z., Pinto, A. D., Lang, A. E., & Chen, R. (2010b). Involvement of the cerebellothalamocortical pathway in Parkinson disease. Annals of Neurology, 68(6), 816–824. https://doi.org/10.1002/ana.22221

Pruszynski, J. A., Kurtzer, I., & Scott, S. H. (2011). The long-latency reflex is composed of at least two functionally independent processes. Journal of Neurophysiology, 106(1), 449–459. https://doi.org/10.1152/jn.01052.2010

Ranjan T, Smith MA. 2018 Cancellation of internally-generated errors from the signal driving motor adaptation. In Advances in motor learning and motor control (MLMC), San Diego, CA, 2 November 2018

Richard, I., Guglielmi, M., Boisliveau, R., Perrouin-Verbe, B., Mauduyt de la Grève, I., Bioulac, B., Guiheneuc, P., & Mathé, J. F. (1997). Load compensation tasks evoke tremor in cerebellar patients: The possible role of long latency stretch reflexes. Neuroscience Letters, 234(2–3), 99–102. https://doi.org/10.1016/s0304-3940(97)00681-2

Shadmehr, R., Smith, M. A., & Krakauer, J. W. (2010). Error Correction, Sensory Prediction, and Adaptation in Motor Control. Annual Review of Neuroscience, 33(1), 89–108. https://doi.org/10.1146/annurev-neuro-060909-153135

Tseng, Y.-W., Diedrichsen, J., Krakauer, J. W., Shadmehr, R., & Bastian, A. J. (2007). Sensory prediction errors drive cerebellum-dependent adaptation of reaching. Journal of Neurophysiology, 98(1), 54–62. https://doi.org/10.1152/jn.00266.2007

Weiler, J., Gribble, P. L., & Pruszynski, J. A. (2015). Goal-dependent modulation of the long-latency stretch response at the shoulder, elbow, and wrist. Journal of Neurophysiology, 114(6), 3242–3254. https://doi.org/10.1152/jn.00702.2015